JPRS-JST-89-013
11 JULY 1989

JPRS Report

Science & Technology

Japan

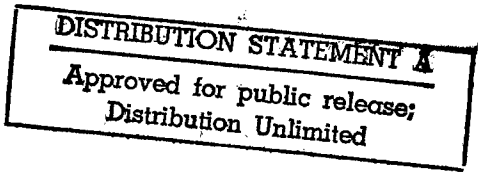

JPRS-JST-89-013
11 JULY 1989

SCIENCE & TECHNOLOGY
JAPAN

CONTENTS

AEROSPACE, CIVIL AVIATION

Organic Thin Films for Information Conversion

43067501a Tokyo THE 28TH ELECTROCHEMICAL SEMINAR in Japanese Jul 88 pp 37-44

[Article by Shogo Saito, Synthetic Science and Engineering Research Department, Kyushu University]

[Text] 1. Introduction

The development of high functional organic materials is eagerly awaited, and these expectations are becoming stronger than ever. The main subject of the CHEMRAWN (Chemical Research Applied for World Needs) international conference held in May 1987 was "Advanced Materials for Innovation in Energy, Transportation and Communication." There were also discussions under the heading of "Advanced Materials for Energy, Electronics and Biotechnology" at the Chemistry Summit that was held in October 1987; its participants included 1,800 engineers and researchers from Japan and foreign countries. The research and development project to create a basis for the next generation of industrial technology guided by the Ministry of International Trade and Industry has emphasized research on new materials. In particular, many research subjects involved organic materials and organic devices.

Future electronic devices will involve the application or utilization of the functions of organic molecules. In particular, optical functions are fascinating and attractive. The new concept of molecular electronic devices has had a major impact on the world. As this concept has changed over time, it has evolved into the concept of superelectronic devices. As a result, it is emerging as a new research theme that brings together chemistry, physics and electronic engineering.

With the movement noted above as the background, the author conducted a specific research program entitled "Organic Thin Films for Information Conversion" from 1984 through 1986, sponsored by the Ministry of Education, and announced the results of this research in 1987. An outline of the information conversion studied in this research program is shown in Figure 1. The line of thinking that served as the basis for this research is as follows.

1) To establish a guideline for designing molecules that includes the possibility of the advent of information conversion functions as shown in Figure 1.

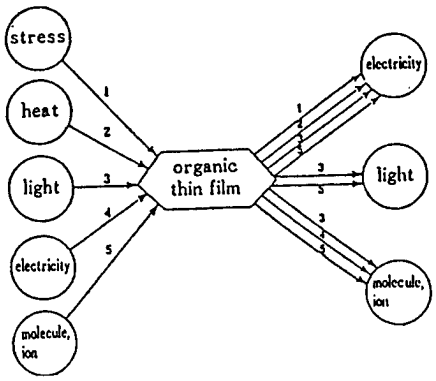

Figure 1. Organic Thin Films Having Information Conversion Functions

2) To clarify quantitatively the correlation between the functions and the cohesive structure of molecules in a thin film.

3) To seek the attainment of functions with a higher degree of efficiency by controlling molecular orientation in a thin film.

In this paper, several topics that are fundamentally related to optical functions and electronic functions have been selected from the research conducted by the author and his colleagues, and the outline of the results and problems associated with these topics are discussed (see Figure 2).

2. Electronic Conductive Polymeric Thin Film and Its Nonlinear Optical Effect

The π-conjugated chain formed by the regular repetition of single and double chemical couplings among carbon atoms that are composed of polymers is the basic guideline for designing electric conductive polymers. Polyacetylene is the principal material in this field. However, in order to obtain a fine thin film that does not contain macro defects, considerable attention has been devoted to poly-p-phenylenevinylene (PPV). A PPV thin film can be obtained through the procedures by which a former polymer that is soluble in water is synthesized and processed to become a thin film. Then, through heat treatment, the thin film is finally manufactured.

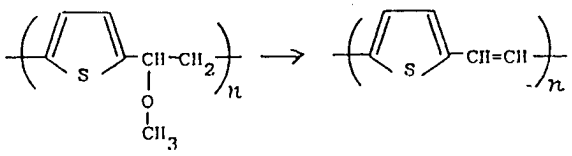

This method can be applied to PPV derivatives and poly (thienylenevinylene) (PTV). In addition, it becomes possible to improve molecular orientation in a thin film, or thin film manufacturing, by using the former polymers of the different type as shown below.

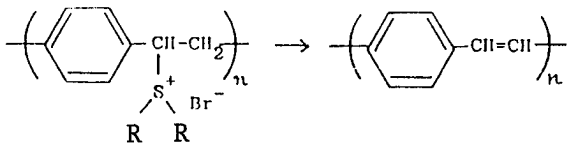

Thin films of poly (allylenevinylene) polymers have different electronic properties that originate in differences in molecular structures (ionization potential). Table 1 shows some examples of electric conductivity in thin films. It is possible to produce a stable thin film having an electric conductivity of more than 10^3 s/cm by adding adequate electron-receptive molecules to a drawn film as a dopant.

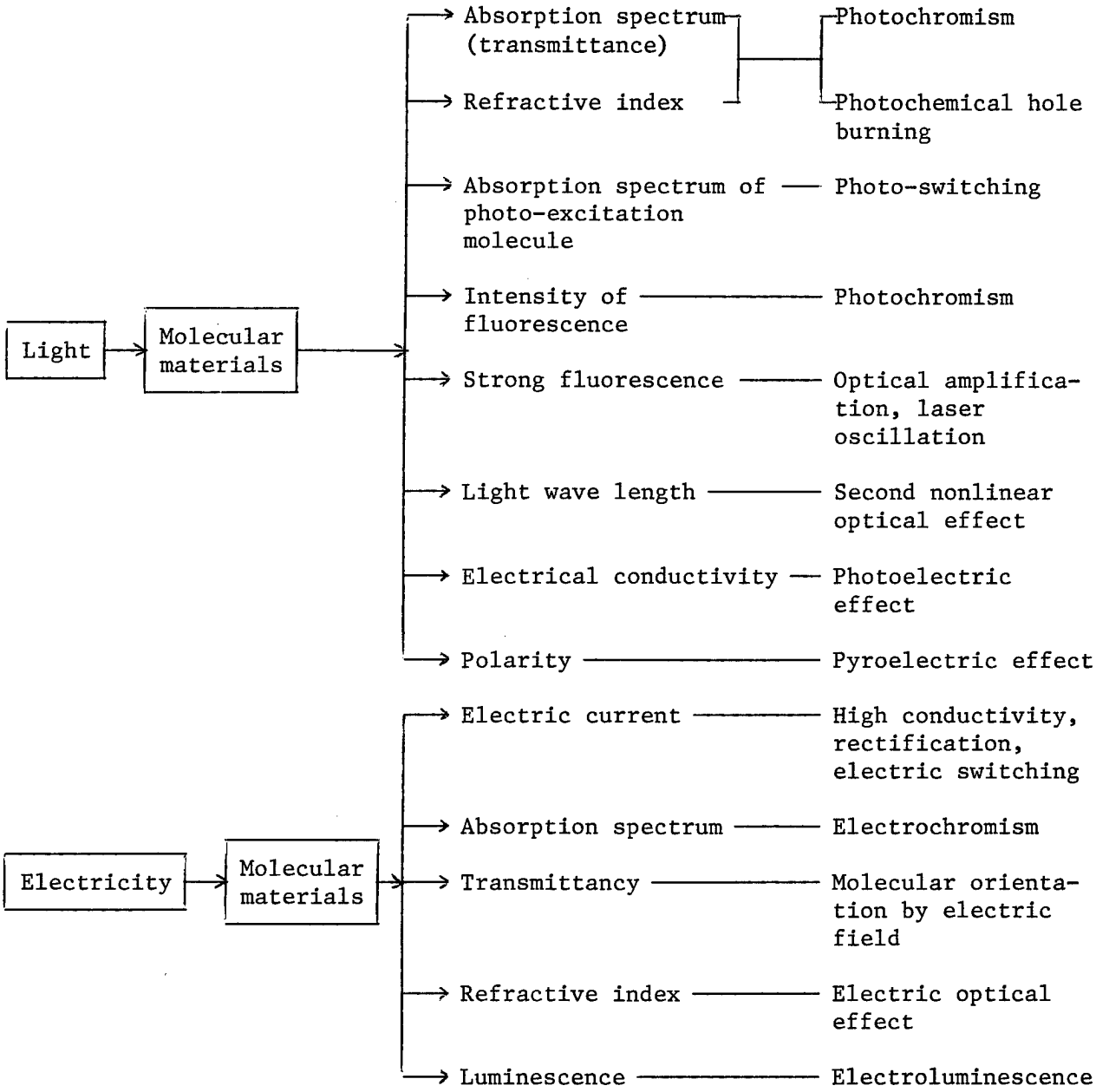

Figure 2. Optical Function and Electronic Function of Organic Molecular Functional Materials

Table 1. Electric Conductivity of Poly (Allylenevinylene) Thin Films

Polymer	σ_{RT}(in vac) undoped	σ_{RT}(in air) O_2 doped	σ_{RT}(in air) I_2 doped
PPV	10^{-19}S/cm	10^{-12}S/cm	10^{-4}S/cm
CH_3O-PPV 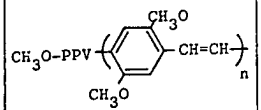	$10^{\div 14}$	10^{-11}	10
PTV 	10^{-13}	10^{-9}	60

Poly (allylenevinylene) thin films also display photoconductivity. The absorption ends of the photoabsorption spectrum of these materials are in the order of a benzene ring, a methoxy benzene ring and a thiophene ring. They move to the field of long waves and reach the semi-infrared region as changes occur in the molecular structure. These films are sensitive to sunrays and semiconductor lasers with a wavelength of about 0.8 μm. A large amount of photo-current is measured when exposed to these sources as compared to that measured in a dark place. The applicational study of these kinds of films for photoelectric conversion devices is a research subject of great interest.

It is noteworthy that poly (allylenevinylene) polymeric thin films show remarkable nonlinear optical effects. The thin film that contains a π-conjugate well developed in a one-dimensional direction is expected to show a three-dimensional nonlinear optical effect. Nevertheless, the author and his colleagues confirmed third harmonic generation (THG) by using PPV thin films in the first place. Figure 3 shows the pattern of the third nonlinear sensitivity coefficient χ in the case of basic wavelengths from 1.85-2.15 μm. An interesting point is that the value of χ could be drastically improved by controlling molecular chain orientation in the PPV thin films and by changing the chemical structure of the PPV. In fact, the value of χ for PTV is confirmed to be about 10 times larger than that of PPV, which is shown in Figure 3. It is thought that π-conjugate polymeric thin films could become not only third harmonic generation devices but also important elements in constructing future photoelectronic devices such as photo-twin stable elements and photo-switches. Judging from experiments on a photo-switch, the response time of PPV and PTV thin film elements can be estimated to be less than 10^{-11} seconds. In the future, it is likely that they will show a super-high-speed response of about 10^{-14} seconds. Such high speeds cannot be realized through the use of inorganic crystalline devices.

3. Photo-Conductive Organic Thin Film

Photo-conductive organic thin films are already practically applied in electronic copy machines as a photo-sensitive body. Thin films having such functions can be applied to a laser printer and a new type of information accumulation device. Accordingly, active research and development activities

are presently underway. The details will be discussed in the corresponding chapter. When their application to future photoelectron energy conversion devices is considered, designing large-area organic thin films that show a high degree of carrier migration created by photoexcitation becomes a universal and important research subject.

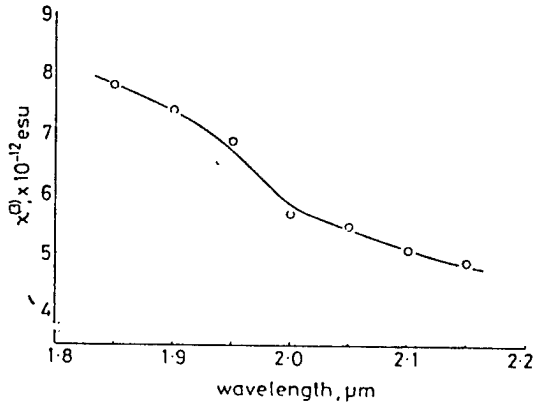

Figure 3. Light Incidence Wavelength Dependence of Third Harmonic Strength of PPV Thin Films

In this paper, it needs to be noted that the degree of carrier migration in the thin film where coloring molecules having semiconductor functions are dispersed in a high-density polymer medium (molecularly doped polymer) is dependent upon the kind of a polymer medium involved. Tafu et al. studied this effect using carbazole coloring elements as the functioning substance. They showed that as the glass transition temperature Tg of the medium polymer became lower, the degree of migration increased. By contrast, our study showed that the opposite result was obtained when triphenylamine coloring elements were used. Examples of the measurement results are shown in Figure 4. Here, μ is the degree of migration and E is electric intensity. PPO, PC and PMMA mean poly (phenyleneoxide), poly-carbonate and poly-methacrylicacidmethyl, respectively. Accordingly, a study on the use of several kinds of poly-carbonate was conducted. As a result, it was concluded that such a medium effect was not derived from polymer's Tg and molecular motion. Instead, it was more reasonable to consider that the effect was reflective of the number of phenyl radicals in the polymer structure and/or a difference in the degree of migration of a medium polymer.

4. Organic Thin Films With Electric Field Luminescence Functions

It is well known that when voltage is impressed on an organic substance that generates strong fluorescence when placed between different kinds of electric charge injected electrodes, electroluminescence (EL) corresponding to the fluorescence spectrum of the organic substance is observed. In the late 1960's, a research group from the Densoken-Riken-Osaka University observed the EL of anthracene. Later, Roberts et al. of Durham University found

that it is possible to obtain an EL element driven by low voltage if a Langmuir-Blodgett (LB) film is made from amphipatic molecules containing anthracene and perylene.

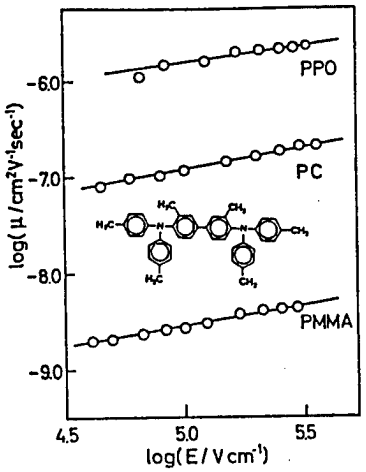

Figure 4. Degree of Migration in Coloring Element Dispersed Polymeric Thin Films

We studied the possibility of EL for cast films, LB films and evaporation films with organic coloring elements. Recently, an EL device that can be operated for a relatively long time by using a three-layer organic thin film produced by the evaporation method with high brightness has been proposed. Figure 5 shows the organic device and the model of the coloring elements applied to it.

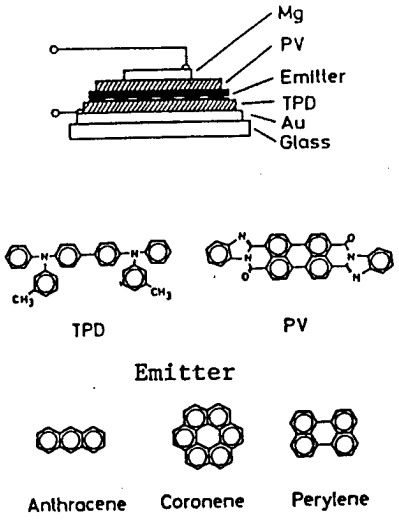

Figure 5. Examples of Organic EL Devices and Their Coloring Molecules

The TPD shown in Figure 5 is the layer to transfer only hole carriers, and PV is the electron migration layer. When anthracene, coronene and perylene are used, the EL of corresponding colors--such as blue, green and orange--can be observed, respectively. The EL spectrum corresponds almost exactly to the form of the fluorescent spectrum. Due to ordered bias impression, clear luminescence can be observed under larger voltage that causes a double injection of electrons and holes on the EL layer. Both the TPD and PV layers are non-crystalline films. These layers are effective for stabilizing the operational properties of the element and for conducting carrier injection into the luminescence layer.

The luminescence layer that gives an EL of the highest brightness is the evaporation film of 12-phthaloperynone derivative as shown below.

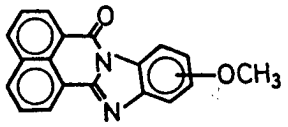

The property in which EL intensity is almost proportional to the injection current can be obtained by this layer. EL intensity exceeds 1 $\mu W/cm^2$ in the presence of an injection current of 1 mA/cm^2. The largest EL wavelength is 580 nm.

5. Asymmetric LB Film and Its Functions

If an asymmetric structured polarized thin film characterized by distinguished anisotropy in the orientation of a strong permanent dipole can be made in the form of a solid thin film, it is expected that such a thin film would broadly display optical conversion functions such as the pyroelectric and second nonlinear optical effects. The purpose of our current study is to establish conditions for manufacturing stable asymmetric polarized thin films by applying the LB method and to achieve the functions expected of them.

First, we synthesized several kinds of amphipatic molecules containing azobenzene units, and we tried to form the permanent dipole in the direction of the molecular apse line by selecting hydrophilic radicals. Next, the stable Y film was produced by using the model molecule expressed as mAn (where m is the number of carbon atoms in the hydrophobic tail, A is azobenzene and n is the number of carbon atoms in the space between A and hydrophilic end radicals) and then the configuration of the molecules in the film was determined. The result is shown in Table 2. In this table, the tilt angle means the angle between the axial direction of the film composition molecules and the vertical direction of the basis.

In constructing polarized LB films, the Y typed film with a head-head accumulative structure is unsuitable. As shown in Figure 6, polarized molecules of the X-, Z- or hetero Y type need to accumulate. Thus, we made the LB film using the amphipatic molecules indicated below by applying the accumulation method of the Y-, Z- and hetero Y types.

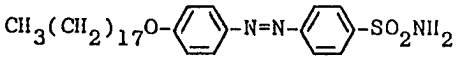

Table 2. Structure of Film Composition Molecules Including Azobenzene Unit and Their Arrangement in LB Films

$CH_3(CH_2)_{m-1}$-[A]-O-(CH_2)COOH

molecule m	molecule n	tilt angle (degree)
8	3	47
8	5	42
12	5	38

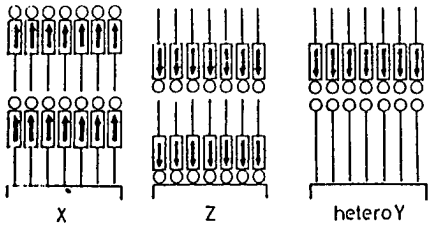

Figure 6. Asymmetric LB Accumulation Films

The orientation of the permanent dipole in the film was evaluated by measuring the Stark effect. The second component is arachic acid in the case of hetero Y typed accumulation.

Figure 7 shows the measurement result of the primary Stark effect. In this figure, $\Delta T/T$ is a variational ratio of phototransmissivity by electric field impression. The electric intensity applied to the films is 3.2×10^5 Vcm^{-1} in either case. When molecules having a permanent dipole in a direction parallel to the axis of molecular length are oriented one-dimensionally in the LB film, the primary Stark effect is given as

$$\frac{\Delta T}{T} = \frac{2.303\ \lambda^2}{hc} \frac{dD}{d\lambda} |\Delta\mu||F|\langle\cos\theta\rangle$$

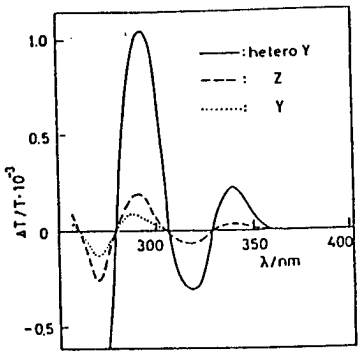

Figure 7. Stark Effect on LB Films Based on Different Accumulation Methods

The result shown in Figure 7 indicates that asymmetric orientation was realized in the LB film of the hetero Y type as expected. The order parameter <Cos θ> related to the orientation of the azobenzene unit in the hetero Y film was evaluated to be 0.57. It is a matter of course that the Stark effect is weak in the Y-typed film. In the case of the film with Z typed accumulation, a similar result was obtained. This fact may indicate that the film with 2-typed accumulation is unstable and causes the stable symmetric film to be similar to the Y-typed film. This conclusion can be supported by data from the layer's period in the LB film measured by X-ray diffraction. In addition, when the pyroelectric effect was measured by irradiating three different kinds of LB films with rays with a long wavelength, only the hetero Y-typed film generated the pyroelectric response signal positively.

In order to apply asymmetric LB films to second nonlinear optical materials, it is necessary to create asymmetric LB films from the molecules having a greater degree of polarization (particularly under the exposure of rays). The result of the study of such molecular designing is shown in Figure 8a. In order to emphasize the polarity of molecular ends rather than their hydrophile property, molecule 3 in this figure introduced NO_2 radicals. The absorption spectrum of the LB film composed of this molecule is completely different from that of the LB film composed of molecule 2, which emphasizes the hydrophile property. It is almost identical to the spectrum of a solution of molecule 3. In other words, in the LB film composed of molecule 3, an azobenzene unit does not show an H-association and molecule 3 does not stand vertically relative to the base surface. However, the result shown in Figure 8a indicates that molecule 3, with its strong polarity, which is considered to be difficult to orient in a direction perpendicular to the film surface, can be successfully oriented by mixture with the strong hydrophile molecule 2.

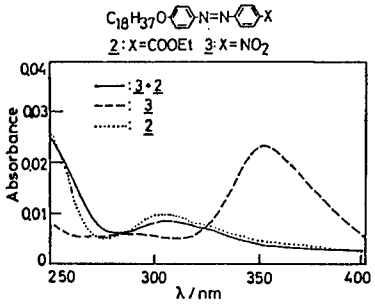

Figure 8a. Absorption Spectrum of Single and Mixtured Films

6. Photo-Information Memory Film

Since photo-information memory films that utilize the photochromism of organic molecules, as shown in Figure 8b, use a reversible optical reaction based upon a molecular unit, there is a good possibility of applying them in super-high-density and large capacity photo-information accumulation media. Figure 8b presents four important factors to be controlled for such applications.

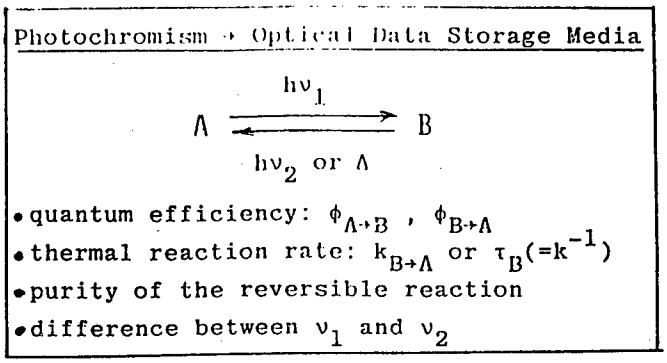

Figure 8b. Important Control Factors Related to Photochromism

It is important to investigate reactions that involve durability. Figure 9 shows one of our conclusions at this stage. In this figure, (a) is the model reaction, and our conclusion is that an electron ring reaction that utilizes the molecular inner binding formation of cis-stilbene can stand repeated stress. Meanwhile, (b), (c) and (d) are the examples actually tested: (b) is the system finally proposed by Irie et al. of Osaka University; and (c) is that obtained by the author and his colleagues (Kyusyu University). In both cases, a molecular design to rapidly carry out the electron ring reaction by avoiding the cis-transisomerization reaction was adopted. Finally, (d), which is called fulgide, was proposed by Heller et al. of Wales University.

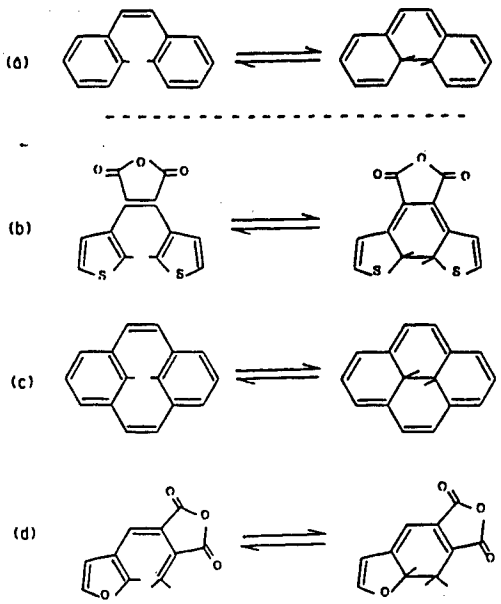

Figure 9. Photochromic Reaction Offers Repeated Durability
(a) Cis-stilbene, (b) Cis-stilbene derivative,
(c) Di-hydropylene, (d) Fulgide

A study to establish guidelines for molecular designing to increase the quantum yield efficiency of regular and inverse optical reactions was conducted on (c) di-hydropylene. Changes in the chemical structure were observed through three different methods. These are (1) change of the substitution radicals (R^1, R^2) at the positions of 10b and 10c, which are the reaction components, (2) whether or not there exists a t-butyl radical in the 2, 7 position, and (3) introduction of the electron aspiration radical X to expand the ring π-conjugate system (see the chemical structure formula below).

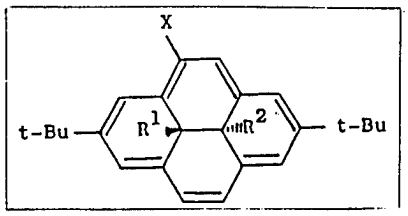

The guideline for increasing the optical reaction quantum yield coefficiency was concluded to be $R^1 = R^2 = Me$, the molecule contains no t-butyl radical, $X = NO_2$, and the molecules are asymmetric.

Among the candidate photochromic materials that were obtained through such extensive study and research, there are many that have a high dark thermal reaction speed K (in brief, information accumulation time $\tau = K^{-1}$) from an unstable condition to a stable one. Our study showed that the dark thermal reaction was strongly affected by the media surrounding the photochromic molecules. Thus, a study designed to control K or τ by utilizing the effect of the media (molecular environment effect) was conducted. As shown in Figure 10, salicyldenaniline derivative was selected as the photochromic molecule. Its dark thermal reaction speed was measured under various conditions including in solution, in an amorphous polymeric medium, and in the form of an LB film or crystalline structure.

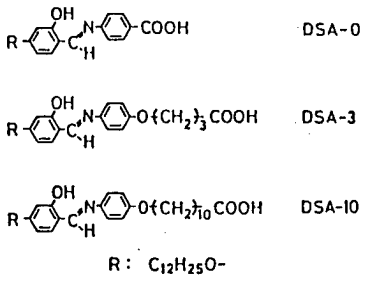

Figure 10. Amphipatic Molecules Including Salicyldenaniline

Figure 11 presents some typical conclusions drawn by this study. A summary of these conclusions is as follows:

--A thermal color erasing reaction takes place in accordance with the primary reaction, except when in an amorphous polymeric medium. Dispersive behavior of which K has distribution appears under amorphous polymeric media.

--The medium had a strong effect on the thermal coloring reaction speed K.

$$K_{soln} >> K_{rubber} >> K_{glass} > K_{LB} \geq K_{xtal}$$

Since K_{rubber} and K_{glass} are not defined for only one meaning, their value is an average (Figure 11).

--As shown in Figure 11, the following relationship is observed at room temperature

$$\tau_{LB}/\tau_{soln} = \tau_{xtal}/\tau_{soln} = 10^6$$

--Relative to τ_{LB}, depending upon the length of the spacing portion, in the amphipatic molecules including salicyldenaniline, it is possible to control it to a certain extent.

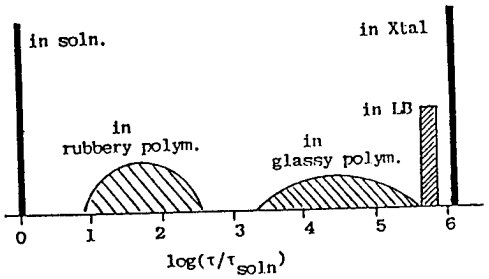

Figure 11. The Effect of the Media on Thermal Color Erasing Reaction of Coloring Molecules (Salicyldenaniline derivative)

From the above conclusion, it can be stated that to incorporate photochromic molecules into LB films it is considered most suitable to control the thermal reaction speed and photo-information accumulation time by the effect of the media.

Electrically Conducting Organic Thin Films

43067501b Tokyo THE 28TH ELECTROCHEMICAL SEMINAR in Japanese Jul 88 pp 63-71

[Article by Toshihiro Onishi, Polymer Basic Technology Research Association]

[Excerpts] [Passage omitted]

3. Electrically Conductive Organic Thin Films by Soluble Intermediate Body Method [passage omitted]

(c) Poly-allylenevinylene (PAV) Polymer

It has been reported that PAV polymers such as poly-p-phenylenevinylene (PPV) can be produced as powders through the application of the Wittig reaction and the dehalogenation hydrogen method.[7] PAV is judged to be a copolymer between acetylene and aromatic chemical compounds. The electric conductivity of PPV is reported to be 3 S/cm. This figure is lower than that of PA and PPP. The reason for this low electric conductivity is the low degree of conjugation in the molecules (narrow width of valence band). The author et al. have focused on the fact that PPV with a large molecular weight could be obtained through a soluble intermediate body that possessed sulfonium salt on its side chains,[8,9] and have tried to develop a sulfonium salt decomposition method.

Figure 3 shows an outline of the sulfonium salt decomposition method using PPV as an example. Polymeric sulfonium salt can be obtained by polymerizing di-sulfonium salt (monomer) in the presence of an alkali. After dialysis and refining, it is formed into films and thin membrances. The allylenevinylene structure is generated through thermal processing. When doping is applied to this material, electric conductivity will appear. In order to obtain a high degree of electric conductivity, it is necessary to orient the molecules through a stretching process. At this moment, the highest electric conductivity to be obtained is 10^4 S/cm (H_2SO_4).

i. Poly-p-phenylvinylene[10]

PPV can be produced by thermal processing polymeric sulfonium salt that is obtained from polymerization of p-xylilene-bis (diethyl-sulfoniumbromido). Its infrared absorption spectrum indicates that a vinylene radical of the PPV

produced by this processing has a trans structure. As shown in Figure 4, the disconnecting reaction of sulfonium salt side chains starts when the temperature exceeds 80°C, and the reaction terminates around 200°C. However, a reduction of weight gradually takes place even at temperatures higher than 200°C. When the gas generated during disconnecting was analyzed by a quadrupole mass analyzer, the signals attributed not only to di-ethylsulfide but also to ethylbromido were measured. In addition, as shown in Table 2, by considering the fact that S is still existent, which is observed through the elementary analysis of PPV produced by thermal processing at low temperature, the author et al. proposed the scheme shown in Figure 5 as the disconnecting reaction for polymeric sulfonium salt.

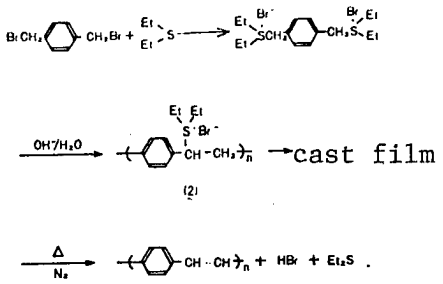

Figure 3. Formation of Poly-allylenevinylene by the Sulfonium Salt Decomposition Method

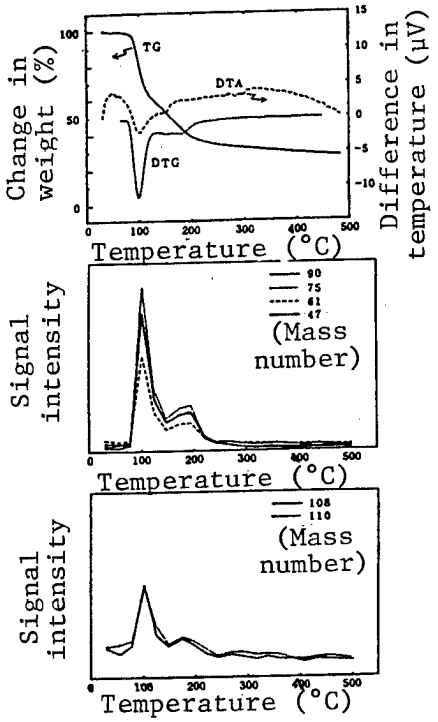

Figure 4. Thermal Analysis and Generated Gas Analysis of PPV Intermediate Body

Table 2. Elementary Analysis of Thermally Processed PPV Intermediate Body

Processing temperature (°C)	Elementary analysis (%)		
	C	H	S
200	91.0	6.1	3.1
300	93.7	6.1	<0.5
Calcd. for PPV	94.1	5.9	0

Processing time: 30 minutes

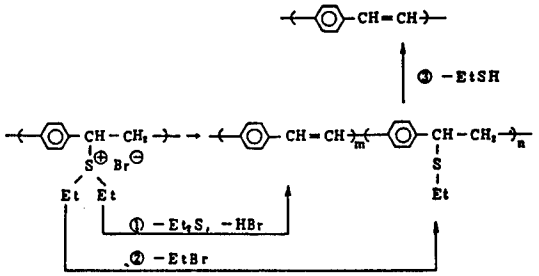

Figure 5. Disconnecting Scheme for PPV Intermediate Body

As shown in Figure 6, electric conduction increases as the processing temperature rises. However, it tends to become saturated above 200°C. PPV obtained at a processing temperature of 200°C contains 2-3 percent S as shown in Table 2. If thioethyl has the side chains, the number of repetitions of conjugated chains is calculated to be 10. As seen from this, although the length of the conjugated chains is short, the PPV shows a relatively high degree of electric conduction. This fact suggests that very long conjugated chains are not necessary to describe electric conductivity.

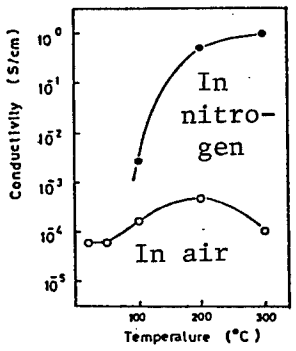

Figure 6. Relationship Between Thermal Processing Temperature and Electric Conduction of Intermediate Body in PPV

Electric conduction can be greatly improved by stretching or drawing. Stretched PPV shows strong dichroism, as can be seen from the polarized infrared absorption spectrum shown in Figure 7. It also shows the orientation patterns of X-ray diffraction. From these analyses, it was concluded that PPV molecules were oriented in a direction parallel to the stretched direction. The relationship between molecular orientation and electric conduction can be investigated from vibrational dichroism using a phenylene ring of 1520 cm^{-1} as the scale to indicate the orientation of the molecules. In this study, various kinds of stretching methods were applied. Since the intermediate body was softened at the disconnecting temperature range, it was heated to a temperature between 100 and 200°C. Then, the three different methods for stretching the body were applied. The first method is to stretch the body in a one-dimensional direction (one-axis thermal stretching method). The second is the swelling thermal stretching method. In this method, the intermediate body is swollen in a solution of water and acetone. The body is stretched when it is swollen, and then thermal desulfonium salt processing is applied. The third is the anisotropic successive two-axis stretching method in which the body is drawn first in the vertical direction and then is drawn again in the lateral direction with a different stretching ratio. Figure 8 shows the results and the outline of these methods. In the case of the one-axis thermal stretching method, it was found that along with one-axis orientation electric conduction could be increased drastically from several tens to 5,000 S/cm by H_2SO_4 doping. Anisotropy in electric conduction was observed to be a difference of 100 times at its maximum. The relationship between dichroism and electric conduction differs depending on the stretching method used. By using the anisotropic successive two-axis stretching method, a value of 10^4 S/cm was almost achieved. The values of electric conduction obtained by these methods are a match for those reported for conventional Shirakawa polyacetylene. The reason for the high electric conductivity of stretched PPV is thought to lie in the easy migration of carriers among molecules, which pass through tight molecules in a tassel-shaped micelle structure. Although PPV is estimated to have less electric conductivity than polyacetylene and poly-p-phenylene when its conduction at the inside of molecules is taken into consideration,[11] it can be said that the conduction of carriers is faster among molecular chains than inside molecular chains judging from the fact that PPV showed a degree of electric conductivity equivalent to that of polyacetylene. In addition, the relationship between dichroism and electric conduction, which indicates that molecular orientation differs depending on the stretching method used, can be interpreted as the effect of differences in structure of a high order created by the stretching together with differences in carrier migration processing among molecules.

ii. Substituent poly-p-phenylenevinylene[12]

Two important characteristics of PPV are aromatic rings that occur on the inside of the molecules and easy chemical ornament by the use of substituents. The author et al. were interested in the effect of the substituents on electric conductivity, and tried to substitute alkoxy radicals that release electrons for phenylene radicals. As a result, it was possible to synthesize PPV (RO-PPV) possessing the substituted alkoxy radicals at 2.5 position in a

manner similar to that used for nonsubstituted PPV, and flexible red films were obtained. In this case, however, since the polymeric sulfonium salt was unstable, a disconnecting reaction occurred during the film synthesizing process. Accordingly, it was not possible to produce highly stretched films. As shown in Table 3, it was found that CH_3O-PPV displayed an electric conductivity of 200 S/cm. This figure was not affected by the types of dopants, i.e., a strong dopant such as SO_3 or a dopant such as iodine that has relatively a weak electron affinity. According to molecular orbit calculation, the result of degradation in ionized electric potential (Ip) of PPV was seen to be due to the substitution of methoxy radicals. Therefore, it was concluded that the high electric conductivity of methoxy substituted PPV with iodine doping was due to the presence of sufficient electron migration for the generation of carriers because of the decrease of Ip even with weak dopants.

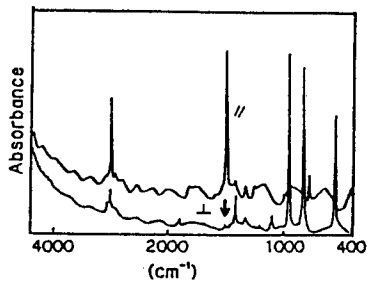

Figure 7. Polarized Infrared Absorption Spectrum of Drawn PPV

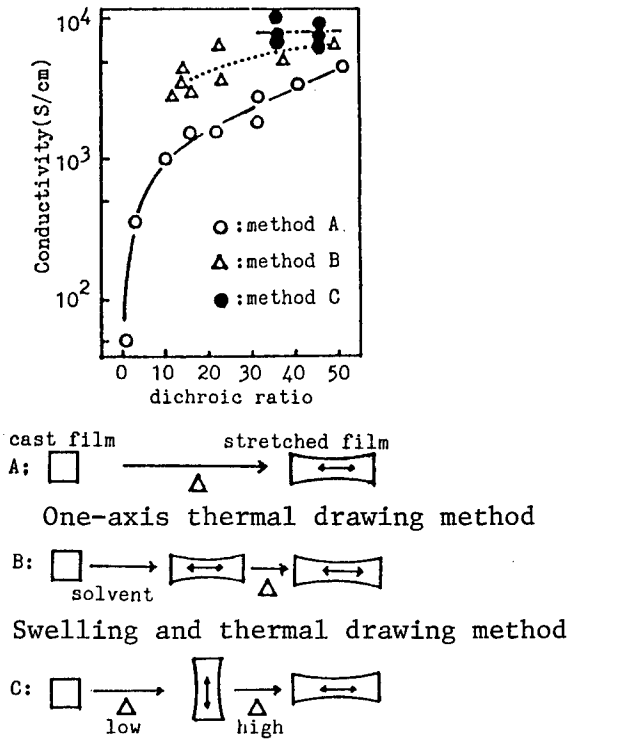

Figure 8. Dichroism and Electric Conduction of Drawn PPV

Table 3. Electric Conductivity of Alkoxy Radical Substituted PPV

Substituent	Electric conduction (S/cm)							
	I_2		SO_3		AsF_5		H_2SO_4	
CH_3O-	203	(1.85)	159	(2.00)	68	(-)	411	(-)
C_2H_5O-	257	(1.17)	43	(0.80)	14	(-)	-	
H-	2.5×10^{-3}	(0.1)	7.7	(0.41)	38	(-)	27	(-)
CH_3-	2.1×10^{-4}	(0.13)	10^{-4}	(-)	-		-	

Values in parentheses are the amount of dopant (Mol/monomer unit)

Another interesting phenomenon was that nonsubstituted PPV was degraded by optical oxidation when it was exposed to the air. However, RO-PPV received only minor degradation due to optical oxidation.

Many studies on attempts to make electric conductive polymers soluble by applying long-chain substituents have been reported. The author et al. tried to compose long-chain substituted PPV among RO-PPV. A comparison of poly-2,5-long-chain alkoxy-p-phenylenevinylene made from the two different methods, which are the sulfonium salt decomposition method and the dehalogenation hydrogen method, is shown in Figure 9. In the case of the sulfonium salt decomposition method, the conventional technique for polymerization was used except for the use of a methanol/water mixture solvent in order to dissolve monomers. The soluble intermediate body obtained by the above method was processed to obtain cast films. Then, they were thermally processed and synthesized at more than 100°C in a nitrogen gas environment. When the dehalogenation hydrogen method was used, the product was synthesized directly from de-HBr on 2,5-long-chain alkoxy-p-xylilenedibromido by using an alkali. Heptyloxy and lauryloxy radicals were adopted as the long-chain alkoxy radicals. Because of the introduction of long-chain radicals, thin film formation can be achieved through the use of alkoxy substituted PPV.

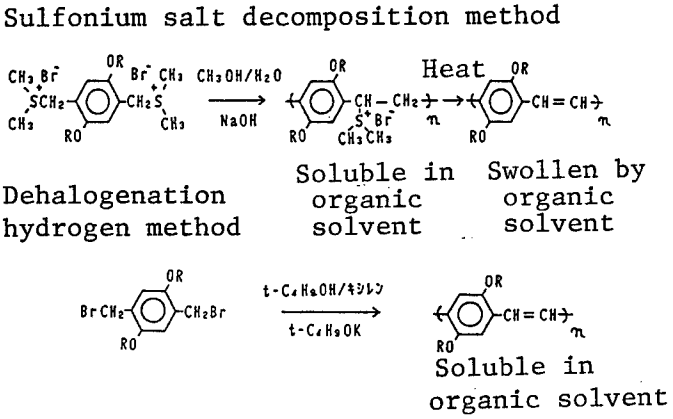

Figure 9. Composition Method for Long-Chain Alkoxy Radical Substituted PPV

As shown in Tables 4 and 5, the solubility of polymers is drastically influenced by the introduction of long-chain alkoxy radicals. The intermediate body obtained by the sulfonium salt decomposition method and RO-PPV obtained by the dehalogenation hydrogen method were soluble in organic solvents. However, RO-PPV obtained by the sulfonium salt decomposition method differed from the characteristics of the intermediate body. It was swollen by organic solvents after desulfonium chloridation took place, but was not soluble in organic solvents. The chain length of alkoxy radicals influenced the molecular weight. This is thought to correspond to the solubility of polymers. Although molecular weight increased depending upon the chain length of the alkoxy radicals under the dehalogenation hydrogen method, there was almost no change in absorption wavelength ends. This could be because conjugated chains were cut by residual halogen. In the case of the sulfonium salt decomposition method, the electric conductivity of $C_7H_{15}O$-PPV became 110 S/cm when stretched five times, and that of $C_{12}H_{25}O$-PPV reached 12.6 S/cm when stretched four times.

Table 4. Long-Chain Alkoxy Radical Substituted PPV Obtained by the Sulfonium Salt Decomposition Method

Alkoxy radical	Solubility (solvent)	Molecular weight (intermediate body)	Absorbed wavelength (nm)	Electric conduction (I_2) (S/cm)
CH_3O	Water	-	606	1.5×10^{2}
$C_7H_{15}O$	$CHCl_3$	5×10^{5}	609	1.1×10^{1}
$C_{12}H_{25}O$	$CHCl_3$	8×10^{4}	608	8.4×10^{-1}

Table 5. Long-Chain Alkoxy Radical Substituted PPV Obtained by the Dehalogenation Hydrogen Method

Alkoxy radical	Solubility (solvent)	Molecular weight	Absorbed wavelength (nm)	Electric conduction (I_2) (S/cm)
CH_3O	Not soluble	-	617	9.6×10^{-3}
$C_7H_{15}O$	$CHCl_3$	5×10^{4}	593	6.9×10^{-2}
$C_{12}H_{25}O$	$CHCl_3$	1×10^{5}	591	2.5×10^{-1}

iii. Poly-2,5-thienylenevinylene (PTV)[13]

It is said that a complex five-ring polymer has a low ionized electric potential and interacts with a dopant. It is also thought to be relatively stable. This led to an attempt to introduce a thienylene ring into the allylenevinylene structure. It proved possible to synthesize PTV using the sulfonium salt decomposition method. Its electric conductivity was 15 S/cm. It was reported, however, that the intermediate body was unstable.[14] The author et al. studied independently the synthesis of PTV using the sulfonium salt decomposition method and found a procedure that went through the intermediate body with a new structure (Figure 10). In the case of PPV, it was

found that stable sulfonium salt side chains became the intermediate body. By contrast, in the case of PTV, a soluble intermediate body having alkoxy radicals on side chains was generated for the substitution of alcohol with the use of alcohol as a polymerization solvent. The structure of the new intermediate body was confirmed through the measurement of IR, ^{13}C- and H-NMR. The intermediate body is soluble in organic solvents and stable. Thin film formation from this material is possible using a spin technique. It is also possible to carry out stretching processes on these films. Alkoxy radicals placed on side chains are disconnected by thermal treatment, and a 2,5-thienylenevinylene structure is generated. PTV films made by this process have a metallic luster and are highly stable when exposed to the air. PTV showed an electric conductivity of 200-400 S/cm in a nonstretched condition after iodine doping. Moreover, as shown in Table 6, electric conduction is improved by one-dimensional stretching, reaching a maximum of 5.9×10^3. The result of the study for anisotropy of the electric condition of stretched PTV indicated there was a difference in anisotropy of 35 times for the extreme case. Measurement of the polarized infrared absorption spectrum showed dichroism, and it was confirmed that molecules were oriented in the direction of stretching. The band gap estimated from the absorption spectrum was 1.65 eV. This agrees with calculations (1.6 eV) done by Bredas.[15] [passage omitted]

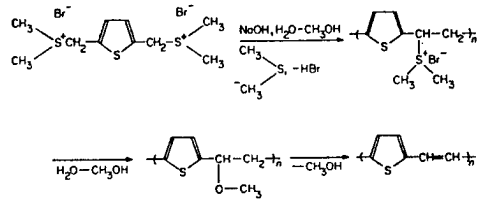

Figure 10. Synthesizing Scheme for PTV

Table 6. Infrared Dichroic Ratio and Electric Conduction of Drawn PTV

Drawn ratio	Dichroism (3010 cm^{-1})	Electric conduction (S/cm)	Anisotropy
6	-	5.9×10^3	-
6	7.7	2.1×10^3	35
4	9.8	2.5×10^3	32
3	7.1	1.7×10^3	-
1	1.1	3.7×10^2	-

References

[Passage omitted]

7. H,-H, Horhold and J. Opfermann, Makromol. Chem., 131, 105 (1970).

8. M. Kanbe and M. Okaware, J. Polym. Sci., A-1, 6, 1058 (1968).

9. R. A. Wessling and R. G. Zimmermann, U.S. Pat., 3, 401, 152 (1968).

10. I. Murase, T. Ohnishi, T. Noguchi and M. Hirooka, Polym. Commun., 25, 327 (1984). Mol. Cryst. Liq. Cryst., 118, 333 (1985).

11. J. L. Bredas, R. R. Chance and R. H. Baughman, J. Chem. Phys., 76, 3673 (1985).

12. I. Murase, T. Ohnishi, T. Noguchi and M. Hirooka, Polym. Commun., 26, 362 (1985).

13. I. Murase, T. Ohnishi, T. Noguchi and M. Hirooka, ibid., 28, 229 (1987).

14. K. Harper and W. J. W. Watson, Patent Information Bulletin 1986-148231.

15. J. L. Bredas, R. L. Elsenboumer, R. R. Chance and R. Silbey, J. Chem. Phys., 78, 5656 (1983).

[Passage omitted]

20th National Conference on Crystal Growth

Effects of Melt Composition in LE-VB Process

43067504 Tokyo JOURNAL OF THE JAPANESE ASSOCIATION OF CRYSTAL GROWTH in Japanese 10 Jul 88 p 8

[Article by Hideo Nakanishi, Hiroki Koda, and Keigo Senkawa, LSI Research Institute of NTT Corp.: "Effects of Melt Composition on GaAs Single-Crystal Growing by LE-VB Method"]

[Text] 1. Introduction

Crystal growing at a small temperature gradient is easier with the LE-VB method than with the LEC method, so that the former method has an appeal as a prospective technique for growing large, low-dislocation GaAs crystal. While the composition of melt to be used for crystal growing and the electrical properties of the crystal grown from the melt are closely correlated,[1] the range of melt composition permissible for single-crystal growth has not been determined. We studied the effects of melt compositions on the growth of single crystal using melts of different compositions prepared by us. As a result, starting melts with an As ratio (As mole fraction) of 0.496-0.503 were observed to enable the growing of an ingot entirely consisting of a single crystal.

2. Experiment

We prepared starting melts with controlled composition by the direct synthesis method in which, as shown in Figure 1, a seed crystal and Ga and As, as raw materials, were loaded in a crucible with bulk GaAs inserted between them so as to protect the seed crystal. We prepared melts with varied As fractions, ranging from 0.491 to 0.505. The crucible was one made of pBN and it measured 30 mm in diameter. The orientation was set at <001>.

3. Results and Discussion

Figure 2 (a) shows an etched longitudinal section of a crystal grown from a melt with an initial As mole fraction of 0.503. It is seen from this photo that the ingot, not to mention its directly seeded portion, was entirely comprised of a single crystal grown with high reproducibility. The crystal

shown in Figure 2 (b) is one grown from a melt with a higher initial AS mole fraction, 0.505. In this latter case, the melt and seed crystal did not merge very well and subgrain formation resulted immediately after the start of crystal pulling, allowing polycrystal formation to take place easily. A similar condition was observed when melts containing an excessive amount of Ga were used. In fact, crystal pulling from a melt with an initial mole fraction of 0.496 or smaller resulted in the formation of no single crystal. When a melt containing an excessive ratio of As or Ga is used, the liquidus line and solidus line that appear in the Ga-As phase equilibrium diagram diverge widely, increasing the possibility of overcooling of the crystal composition. This is considered to have been the case when subgrain formation took place in our experiment as mentioned above.

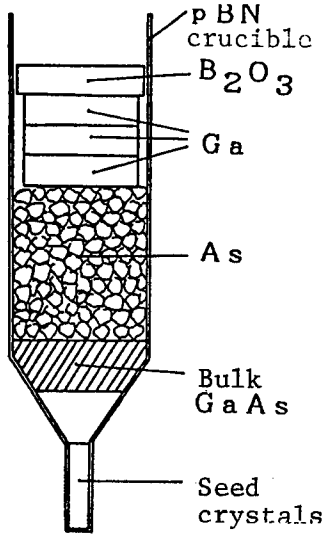

Figure 1. Schematic diagram of raw material loading in crucible

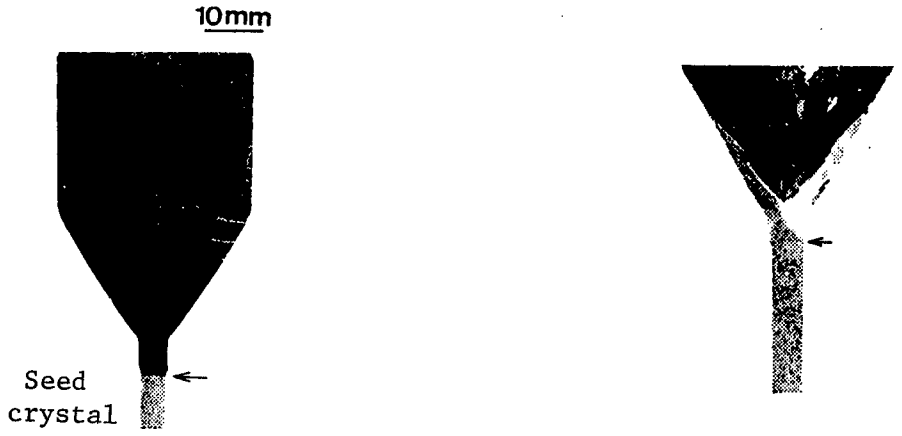

(a) Grown using melt with As mole fraction of 0.503

(b) Grown using melt with As mole fraction of 0.505

Figure 2. Photos of KOH-etched longitudinal wafer sections (arrow indicates seeded location)

References

1. Nakanishi, et al., Proceedings of Autumn Meeting of the Japan Society of Applied Physics, 1988, p 227.

Influence of Hydrogen on Carbon Behavior

43067504 Tokyo JOURNAL OF THE JAPANESE ASSOCIATION OF CRYSTAL GROWTH in Japanese 10 Jul 88 p 10

[Article by Joji Nishio, General Research Institute of Toshiba Corp.: "Study of Transportation and Reaction of Carbon Contained in LEC GaAs Single Crystal"]

[Text] 1. Introduction

The mechanisms of impurity mixing and purification during the growth of GaAs single crystals by the LEC method are very complex due to the effects of B_2O_3 placed, as a liquid sealant, directly over the starting melt.[1] In studying how impurities are mixed into crystals being grown, the influence of the ambient gas cannot be ignored. In an attempt to clarify the mechanisms of carbon mixing and purification during GaAs single-crystal growing, we studied the behavior of carbon as to its transportation and reaction by sampling and analyzing the ambient gas.

2. Experiment

Ambient gas samples were collected at right above B_2O_3 under three types of conditions. They were analyzed by gas chromatography. To quantitatively analyze H_2, a TCD (thermal conductivity type detector) was used, whereas a FID (hydrogen flame ionization detector) was used for CO as well as CO_2.

1) Under the conditions for ordinary single-crystal pulling, but with no raw material loaded in the crucible (unloaded experiment).

2) Under the conditions for ordinary single-crystal pulling.

3) Under the conditions for ordinary single-crystal pulling, except that the PBN crucible was covered with a lid.

We also pulled single crystals under conditions 2) and 3), and measured the carbon concentrations in their portions with a solidification rate of about 0.1 by the FTIR method.

3. Results and Discussion

The results of gas chromatography conducted under the above three types of conditions and the carbon concentrations measured on single crystals pulled under conditions 2) and 3) are summarized in Table 1.

Table 1. Results of Gas Chromatography

Time of gas sampling	Unloaded experiment H_2	Unloaded experiment CO	Under ordinary conditions H_2	Under ordinary conditions CO	With crucible covered H_2	With crucible covered CO
Before heating	<10	<7	<10	<7	<10	<7
Immediately after raw material melting	23	32	21	43	41	58
Before pressurization subsequent to pressure reduction	86	136	42	28	324	254
Immediately before start of pulling	44	48	139	52	101	49
Immediately after end of pulling	65	89	251	75	310	163
Carbon concentration in crystal			4.3×10^{15} atoms/cm^3		1.4×10^{17} atoms/cm^3	

*Gas concentrations: in volume ppm

The CO_2 concentration was lower than 7 ppm (maximum measurable concentration) in every gas sample. In Table 1, the differences in H_2 concentration between samples collected under different conditions at different times draw attention. It is evident that the samples collected under condition 1) contained higher concentrations of CO_2 than did those collected under condition 2). The hydrogen detected in these sample gases is considered to have been generated through the decomposition of water contained in B_2O_3. For the water to be decomposed, the following reaction must be promoted:

$$H_2O_{(\text{in } B_2O_3)} + C_{(\text{in melt})} \rightarrow CO_{(\text{in } B_2O_3)} + H_{2(\text{in } B_2O_3)}$$

The above reaction requires that hydrogen leave the melt-B_2O_3 interface where the reaction is assumed to take place. It is assumed that, under condition 3), the covered crucible blocks the leaving of H_2 as shown in Figure 1, inhibiting the purification reaction of carbon in the melt and resulting in a higher carbon concentration in the crystal subsequently obtained.

The above results of our experiment and analysis suggest that oxygen exercises a great influence on the mechanisms of carbon mixing and purification during GaAs single-crystal growing.

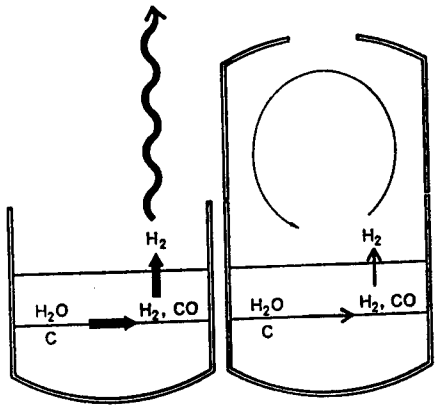

Figure 1. Influence of hydrogen on carbon purification mechanism

References

1. Nishio, et al., NCCG19 28aA4 (1987).

Influence of Growing Conditions on TiC Crystallinity

43067504 Tokyo JOURNAL OF THE JAPANESE ASSOCIATION OF CRYSTAL GROWTH in Japanese 10 Jul 88 p 16

[Article by Shigeki Otani, Takaho Tanaka, and Yoshio Ishizawa, National Institute of Resources in Inorganic Materials: "Conditions for Growing TiC Single Crystals by FZ Method and Crystallinity Achieved"]

[Text] 1. Introduction

The TiC single crystal has been drawing attention as a material for field-emission type cathodes with extremely small noise and drift.[1] To be used as the cathode material, the TiC single crystal must be of a very high purity. The powdery raw materials used to grow TiC single crystals contain tungsten as impurities. Even when the FZ (floating zone) method in which crystals are grown at very high temperature (2900°C) is used, tungsten impurities cannot be removed. In fact, tungsten impurities have been a source of trouble in the growing of TiC single crystals. As a means of removing tungsten impurities, we employed the self-combustion method in synthesizing TiC and producing sintered rods. As a result, problems due to tungsten impurities were eliminated and it has become possible to grow TiC single crystals under a wide range of conditions.[2] Subsequently, we studied the influence of crystal-growing conditions on the crystallinity of the grown crystals.

2. Experiment

Ti powder and degassed carbon black were mixed at a certain ratio (C/Ti = 0.99) and the mixture was pressed into a cylindrical green compact. The green compact was then set in a graphite susceptor and one end of it was placed in a

vacuum heater at 1300°C, letting the green compact start a self-combustion reaction. A sintered rod produced through the above steps was set in a high-frequency FZ furnace and a crystal of the <100> orientation was grown using the furnace in an 8-atm helium ambience.

TiC has a wide indefinite-ratio range (C/Ti = 0.55 to 0.97). We grew TiC single crystal with a composition of a nearly fixed ratio. In growing the TiC single crystal, the starting-melt composition was controlled to bring it close to the eutectic composition (C/Ti = 1.3) as done in the conventional method of TiC single crystal growth.[3] The composition of the sintered rod was controlled such that composition changes due to evaporation do not occur (C/Ti = 0.98). Based on these arrangements, TiC single crystals with a uniform composition ratio (C/Ti = 0.96) were grown utilizing zone leveling.

3. Experiment and Discussion

Among various factors involved in the growth of TiC single crystals, the growth speed and crystal diameter, in particular, had a strong influence on the crystallinity of the grown crystal.

A longitudinal crystal section shown in Figure 1 shows changes caused in the crystal due to a decrease in growth speed from 2 cm/h to 0.5 cm/h effected while the crystal was being grown. The crystal shown in Figure 1 had a large diameter, making the crystal notably dependent on the growth speed. It is seen from this figure that the crystal quality started becoming poorer as early as several mm before the portion corresponding to the time when the growth speed was lowered from 2 cm/h to 0.5 cm/h. This phenomenon is considered attributable to the facts that the crystal portions having been grown are subjected to great thermal stress while being moved through a steep temperature gradient (150°C/mm max) and that the crystal being grown at a lower speed is subjected to thermal stress for a longer time.

Figure 2 shows the etching patterns on central portions of transversal sections of two TiC single crystals with different diameters. It is seen that the thinner crystal is notably superior in crystallinity to the thicker one.

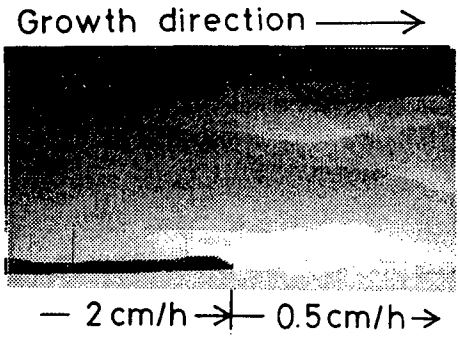

Figure 1. Longitudinal section of TiC single crystal

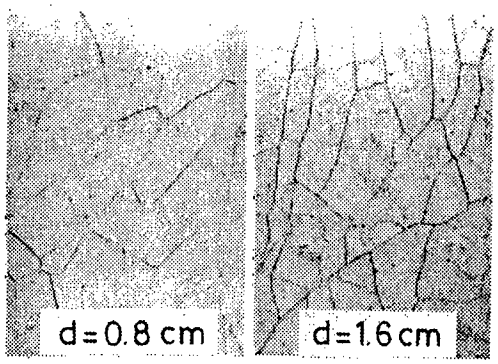

Figure 2. Etching patterns on transversal sections of TiC single crystals
(⟵⟶ 0.5 mm)

References

1. Y. Ishizawa, et al., J. Vacuum Soc. Japan, 29 (1986), 578.

2. S. Otani, et al., J. Crystal Growth, 83 (1987), 481.

3. S. Otani, et al., J. Crystal Growth, 61 (1983), 1.

RHEED Oscillations at Capturing of As by Ga or Al

43067504 Tokyo JOURNAL OF THE JAPANESE ASSOCIATION OF CRYSTAL GROWTH in Japanese 10 Jul 88 p 52

[Article by Takeshi Kojima, Itaru Nakagawa, and Kimihiro Ota, Electro-Technical Laboratory: "RHEED Oscillations and Surface Melting Accompanying the Capturing of As"]

[Text] Introduction

It is known that when excess Ga or Al on the surface of a GaAs or AlAs crystal is crystallized into GaAs or AlAs by capturing As, the intensity of RHEED (reflected high-energy electron diffraction) oscillates.[1,2]

To study the relationship between the above phenomenon and surface melting, we conducted experiments to see whether the capturing of As by Al on the surface of an AlAs crystal causes the RHEED intensity to oscillate both with and without excess Ga being present there. The results are reported in the following.

Experiment and Discussion

To conduct experiments on sample surfaces with the identical initial surface conditions, we prepared samples for use in each experiment by growing an AlAs crystal by 500Å or more and annealing it at 700°C. Figure 1 shows the waveforms of RHEED oscillations observed to take place when As was captured by Al on the surface of an AlAs crystal over which Al had been deposited in an amount equivalent to 4 MLs, at varied temperatures. When the substrate was irradiated with As at 600°C, RHEED oscillations were observed to take place four times, leading to luminance recovery on each occasion. At a substrate temperature of 550°C, RHEED oscillations observed at the fourth layer were incomplete. However, even such incomplete RHEED oscillations were followed by a gradual recovery of luminance. At 200°C, RHEED intensity drops were not followed by recovery. When a substrate in that state with weakened RHEED was irradiated with As, two or three oscillations were observed. These oscillations may have represented changes in the RHEED pattern or may have indicated the presence of a melted layer on the sample surface where only the atoms in the topmost layer were able to move.

Figure 2 shows the dependence of RHEED oscillations on the amount of aluminum deposit and substrate temperature. In Figure 2, closed circles denote regions where RHEED oscillations were observed to take place accompanying the

capturing of As. As seen from Figure 2, RHEED oscillations were observed in the first ML at a temperature of 300°C or higher, in the third and fourth MLs at 600°C or higher and in the fifth ML at 720°C or higher (higher than the melting point of Al). Incomplete oscillations which did not match the amount of Al deposition but which were followed by luminance recovery were observed at temperatures higher than 200°C. Luminance recovery did not occur at temperatures not higher than 200°C.

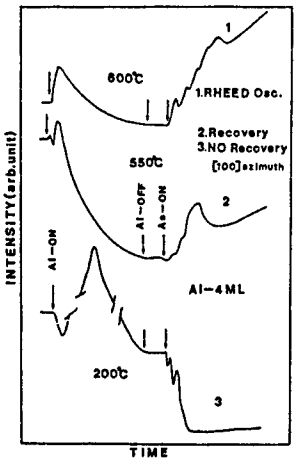

Figure 1. RHEED oscillation waveforms

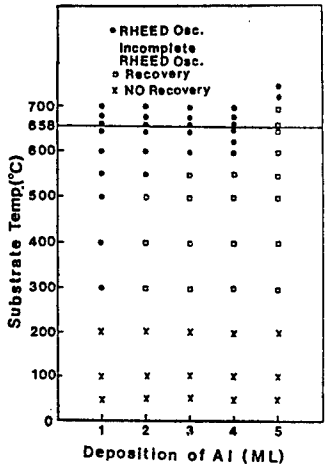

Figure 2. Dependence of RHEED oscillations on Al amount and substrate temperature

Figure 3 shows a phase diagram plotted by observing RHEED oscillations which accompanied the capturing of As on an AlAs crystal surface deposited with Al_xGa_{1-x} in an amount equivalent to 3 MLs. Also shown in Figure 3 is a phase curve of an Al-Ga alloy. It seems that there are some correlations between the two curves shown in Figure 3.

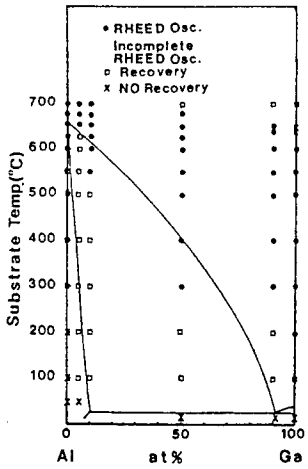

Figure 3. Dependence of RHEED oscillations on Al-Ga amount and substrate temperature

References

1. B. F. Lewis, R. Fernandeg [as published], A. Madhukar, and J. Grunthaner, J. Vac. Sci. Technol. B4, 560 (1986).

2. Takashi Kojima, Kimihiro Ota, and Itaru Nakagawa: HYOMEN KAGAKU, Vol 8, No 3, 179 (1987).

Amorphous GaAs Buffer Layer To Reduce Dislocations

43067504 Tokyo JOURNAL OF THE JAPANESE ASSOCIATION OF CRYSTAL GROWTH in Japanese 10 Jul 88 p 54

[Article by Yoshinori Ujiie, Takashi Suzuki, and Nobu Nishinaga, Electronics Department of Tokyo University: "GaAs Growth on Si Substrate Utilizing Amorphous GaAs Buffer Layer Formed by MBE"]

[Text] 1. Introduction

Research on the epitaxial growth of GaAs on Si substrates has been actively promoted in recent years. A focal point of this research is how to reduce the misfit dislocations caused by lattice mismatch between Si and GaAs. Various methods have been proposed, but none of them appears to be effectively applicable to the manufacture of optical devices. In studying a measure against APD, we experimented in forming an amorphous GaAs buffer layer over a Si (111) substrate and letting it block the propagation of misfit dislocations generated in a GaAs epitaxial layer. As a result, this approach proved to be remarkably effective in reducing misfit dislocations as reported in the following.

2. Experiment

For our experiment, we prepared exactly (111)-oriented Si substrates. The wafers were processed using the wet technique. For cleaning, Ishizaka's method was used. MBE [molecular bean epitaxy] was carried out at a flux ratio (As_4/Ga) of 8 and a growth velocity of 0.3 μm/h. In the growth process, first, an Si substrate is processed at 800-900°C. It is then irradiated with an As_4 beam to form a single atomic layer of As. Next, at Ts = 100°C, an amorphous GaAs buffer layer is deposited in a thickness of 100 Å. The substrate is then heated to 600°C for recrystallization. This substrate recrystallization is followed by an ordinary epitaxial-growth process. The epitaxial thickness was controlled to be 1.2 μm.

3. Results and Discussion

Through the observation of RHEED conducted during the GaAs epitaxial growth process performed utilizing an amorphous GaAs buffer layer formed on the Si (111) substrate, surface restructuring was observed to take place over areas of $\sqrt{1.9} \times \sqrt{1.9}$ and 2 x 2, respectively, during the early stage and the middle-to-latter stage of growing (Figures 1 and 2 [not reproduced]). From

these observations, it is thought that a GaAs (111) B layer was grown.[1] This result can be taken as indicating that the first surface layer of the Si substrate resulted in being replaced by As.[2] The GaAs layer etched for crystallinity evaluation showed dislocation densities on the order of 10^3 cm^{-2} (Figure 3 [not reproduced]), suggesting that the process performed by us was notably effective in reducing dislocations. This may be explained as follows: The recrystallization of the amorphous GaAs buffer layer is considered attributable to the growth of steps achieved without generating nuclei. When the recrystallization takes place, dislocations generated at the interface are forcedly arranged to run in parallel to the interface, allowing remarkably fewer dislocations to run through to the epitaxially grown layer.

References

1. A. Y. Cho, J. Appl. Phys. 41, 2780 (1970).

2. R. I. G. Uhrberg, Phys. Rev. B35, 3945 (1987).

GaAs MOVPE Growth Using Diethyl Arsine

43067504 Tokyo JOURNAL OF THE JAPANESE ASSOCIATION OF CRYSTAL GROWTH in Japanese 10 Jul 88 p 55

[Article by Koji Boku, et al., Toyohashi Gijutu Kagaku Daigaku: "GaAs MOVPE Growth Using Diethyl Arsine"]

[Text] 1. Introduction

As the arsenic source for GaAs MOVPE growth, AsH_3 has been in use, enabling the growing of quality GaAs layers. However, since AsH_3 is very highly toxic and is kept in a high-pressure cylinder, it requires very careful handling. Diethyl arsine [DEAs: $(C_2H_5)_2AsH$] is liquid at ordinary temperature, as well as being less toxic than AsH_3. In addition, its vapor pressure is relatively high[1] ranging around several tens of Torr at room temperature so that it is comparatively easy to handle. For these reasons, expectations are being placed on diethyl arsine as a prospective arsenic source to replace AsH_3. We recently experimented in growing GaAs using TMG and DEAs. The results were reported in the following.

2. Crystal Growth

For crystal growing, we used a MOVPE system incorporating a horizontal reaction tube and Si- and Cr-doped GaAs (100) 2° off substrates. The substrates were set on the reaction tube after being etched by the use of a sulfuric acid-based etchant ($H_2SO_4:H_2O_2:H_2O$ = 4:1:1, 50°C). The V/III ratio was varied from 4.0 to 20 by changing the DEAs supply rate from 4.5 to 22.6 x 10^{-5} mol/min while keeping the supply of TMG constant at 1.13 x 10^{-5} mol/min. Crystals were grown at 450-750°C under ordinary pressure.

3. Results

Figure 1 shows the temperature dependence of the growth rate observed in our experiment. When the growth temperature was 550°C or higher, the growth rate was supply-dependent. At temperatures below 550°C with the growth rate being reaction-dependent, the activation energy was ~0.8 eV. This value approximately agrees with the corresponding values reported on cases where TMG-AsH_3 was used.[2] From these experiment results, it is assumed that DEAs was decomposed at low temperature, permitting arsenic to reach the substrate surface in the form of As_4. The growth rate did not show any dependence on the V/III ratio.

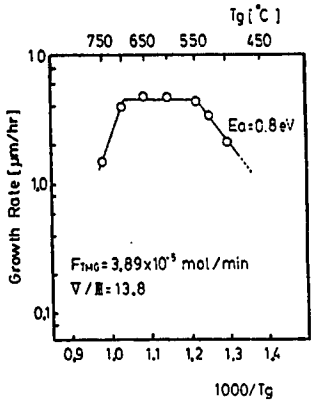

Figure 1. Growth temperature dependence of growth rate

The surface-morphological view of a sample grown at 650°C and V/III = 8 is shown in Figure 2 [not reproduced]. A mirror-like surface was obtained at a growth temperature ranging from 550 to 750°C and a relatively low V/III ratio (>6).

Hall measurement was conducted on the grown layer to assess its electrical properties. The highest values of n and μ recorded so far at a growth temperature of 650°C and a V/III ratio of 8 are 6.0 x 10^{15} cm^{-3} and 11,050 cm^2/Vs (77K), respectively. With a growth temperature of 550°C or lower and a V/III ratio of up to 6, an inversion of the p-n conduction type was observed as in the cases where TMG-AsH_3 is used. The donor-acceptor compensation ratio (N_A/N_D) calculated based on the results of Hall measurement conducted at room temperature decreased with increasing temperature from 0.7 (at 600°C) to 0.3 (at 750°C).

4. Acknowledgement

The author would like to thank Tori Chemical Research Corp. for providing us with DEAs.

References

1. Nagakubo, et al., Proceedings of Meeting of the Japan Society of Applied Physics, Autumn 1988, p 311, 31p-Z-6.

2. D. H. Reep and S. K. Ghandhi, J. Electrochem. Soc., p 130 (1983) 675.

GaAs Growth on GaP Substrate by MBE Method

43067504 Tokyo JOURNAL OF THE JAPANESE ASSOCIATION OF CRYSTAL GROWTH in Japanese 10 Jul 88 p 56

[Article by Koji Boku, et al., Toyohashi Gijutu Kagaku Daigaku: "GaAs Growth on GaP Substrate by MBE Method"]

[Text] Introduction

Growing GaAs on a Si substrate involves such problems as 1) lattice mismatching, 2) difference in thermal expansion coefficient between two materials, and 3) anti-phase domain, so that the process of its growth in the initial phase has not been made entirely clear.[1]

To study problem 1) above, we experimented in growing GaAs on GaP substrates. The GaP substrates were adopted instead of Si substrates to reduce the effects of problems 2) and 3). The initial growth process was examined by RHEED.

Experiment

After a GaP(100) substrate was degreased and chemically etched using an aqua regia-based etchant (HNO_3:HCl:H_2O = 1:2:2, at 50°C), it was introduced into a chamber. GaAs growth was started after the substrate was irradiated with an As molecular beam for heat-cleaning. In this experiment, the beam flux ratio (γ) was changed from 0.5 to 4 while the growth temperature and speed were kept constant at 580°C and 0.7 μm/h, respectively. GaP(100)5°-off substrates were also used to obtain data on GaAs growth on Si off-substrates.

Results

It has been confirmed that, at an optimum beam flux ratio (γ = 2), GaAs grew two-dimensionally (2-D) beginning with the initial phase of growth. As shown in Figure 1 [not reproduced], when γ = 2, the GaAs epitaxial layer was confirmed to grow while maintaining a (2 x 4) streaky RHEED pattern. The surface of GaAs grown under these conditions was so highly flat that almost anything was observed when it was inspected using a Nomarski interference microscope. However, with γ = 4 in an As-rich state, a spotted RHEED pattern appeared when the GaAs film reached about 30 Å in thickness. Streaks were restored when the film thickness reached about 1,000 Å. In this case, GaAs was found to have grown three-dimensionally during the initial phase of growth. The surface of the GaAs film grown showed slight ruggedness when inspected by

surface morphology. With $\gamma = 0.5$ in a Ga-rich state, the RHEED pattern of the GaAs epitaxial layer became spotted after the GaAs film thickness surpassed about 100 Å. Subsequently, the GaAs film did not restore a streaky pattern. In this case, the GaAs film surface was observed to be rough.

When GaP off-substrates were used, the RHEED pattern gradually became spotted.

These experiment results confirm that GaAs is grown two-dimensionally on a GaP substrate beginning with the initial phase of growth, even though there is a difference of 4 percent between the lattice constants of the two materials. This fact indicates that the difference in lattice constant between the materials involved is not the main factor in causing the three-dimensional growth of GaAs on a Si substrate. It has also been suggested that off substrates may serve to inhibit two-dimensional GaAs growth.

References

1. M. Kawabe, et al., Jpn. J. App. Phys., 26 (1987) L114.

Fast Diamond Film Synthesis by Arc Discharge

43067504 Tokyo JOURNAL OF THE JAPANESE ASSOCIATION OF CRYSTAL GROWTH in Japanese 10 Jul 88 p 60

[Article by Fumio Akatsuka and Yoichi Hirose, Nihon Kogyo Daigaku: "High-Speed Synthesis of Diamond Thin Film by Arc Discharge"]

[Text] 1. Introduction

The synthesis of diamond thin film by the vapor phase method has recently become possible and has been attracting attention. While the detailed mechanism of diamond synthesis by the vapor phase method has not been made clear, it is assumed that active species (for example, excited carbon or hydrocarbon radicals, or atomic hydrogen) play an important role in the synthesis process. We assumed that the use of a hot (5000°C or higher) plasma generated by the arc discharge method instead of the conventional method in which heated filaments are used would make it possible to generate more radical species more quickly, enabling faster formation of a diamond thin film.

In this article, high-speed synthesis of a diamond thin film by the d.c. arc-discharge plasma CVD method, evaluation of the synthesized diamond thin film and the mechanism of diamond synthesis will be discussed.

2. Experiment Method

The system used in our experiment is schematically shown in Figure 1. The reaction gas is introduced into the pre-exhausted reaction chamber until the prescribed pressure is reached. An arc discharge plasma is generated by separating two electrodes which have been in contact. Hydrogen (H_2) was

used as the reaction gas, ethanol (C_2H_5OH) as the carbon source and argon (Ar) as a discharge stabilizer. Silicon (Si) substrates as well as those made of other materials were used in the experiment. To prevent substrates from being excessively heated by the plasma, the substrate holder was cooled by water.

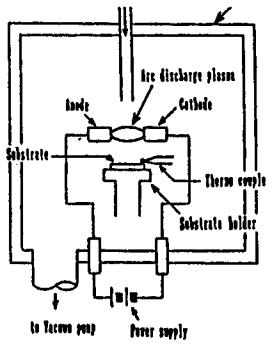

Figure 1. Schematic of experiment system

3. Experiment Results and Discussion

In the experiment, a thin film was formed at a speed of about 200-250 μm/h. In Table 1, the spacing of lattice planes observed by analyzing the synthesized thin film by the X-ray diffraction microscopy method is compared with that of a natural diamond (ASTM6-675). With the two closely agreeing with each other in lattice plane spacing, the synthesized thin film was identified as a diamond. In diamond film analysis, whether the diamond film contains non-diamond carbon such as graphite is checked. Raman spectroscopy is an effective method of detecting non-diamond carbon. Figure 2 shows a Raman spectrum obtained from the synthesized diamond thin film. As Figure 2 shows, the spectrum has the only sharp peak at a shift point of 1333 cm^{-1} the same as with natural diamond. The broad peak to be seen at around 1550 cm^{-1} if amorphous carbon is present is not shown. The reason for this may be explained as follows: Since the arc-discharge plasma is very hot (5000°C or higher), most hydrogen (H_2) passing through the plasma is dissolved into atomic hydrogen (H). The atomic hydrogen then etches non-diamond carbon bonded less tightly than diamond, resulting in the generation of diamond thin film of improved quality. When plasma emission spectrochemical analysis was conducted on the synthesized diamond, a strong emission of atomic hydrogen was observed.

4. Conclusion

The growing of diamond thin film by the arc-discharge CVD method has been confirmed by X-ray diffraction. The growth speed was 200-250 μm/h. Raman spectroscopy conducted on the grown diamond thin film indicated that the film was of a good quality containing little non-diamond carbon such as graphite or amorphous carbon.

Table 1. Interplanar Spacing Measured by X-ray Diffraction on Synthesized Diamond and That Measured on Natural Diamond

Natural diamond (ASTM-6-675)		Synthetic diamond
hkl	d (A)	d (A)
111	2.06	2.055
220	1.261	1.258
311	1.0754	1.073
222	---	---
400	0.8916	0.89

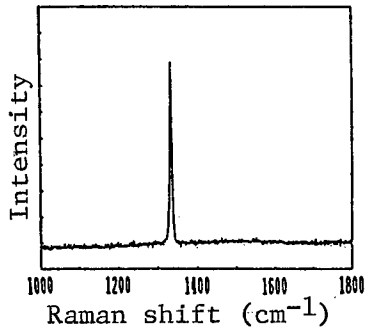

Figure 2. Raman spectrum of diamond thin film

Lateral Growth of GaAs and GaP by LPE

43067504 Tokyo JOURNAL OF THE JAPANESE ASSOCIATION OF CRYSTAL GROWTH in Japanese 10 Jul 88 p 66

[Article by Zuian Cho and Nobu Nishinaga, Department of Technology, Tokyo University: "Lateral Growth of GaAs and GaP"]

[Text] 1. Introduction

The technique for lateral growth (ELO) that utilizes the anisotropy of the speed of crystal growth has great potential for application to semiconductor device fabrication. It is known that the development and subsequent propagation of defects such as dislocations in the crystal being epitaxially grown during a semiconductor device fabrication process result in seriously impaired functions of the finished devices. Therefore, reducing the development of defects is a major task to be tackled. Keeping in mind the possible applications to OEIC's, we have experimented in laterally growing GaAs, GaP and GaAsP, which is a mixed crystal, by the LPE method that is most effective in fabricating semiconductor lasers and other optoelectronic devices. In this article, the characteristics of GaAs/GaAs ELO as well as GaP/GaP ELO carried out in our experiment and the dislocation reducing effect of the process will be discussed.

2. Experiments

SiO_2 films of about 200 nm in thickness were formed on (111), (110), (100) and (211) GaAs and (111) GaP substrates by RF sputtering. Next, several types of patterns were created on the substrates by photolithography. Lateral growth was then conducted by the LPE method using these patterns as seeds. The crystallinity of the grown films were examined by RC etching as well as AB etching.

3. Results

(1) Epitaxial layers with mirror-like surfaces were obtained by growing GaAs on (111) and (100) GaAs substrates at a growth temperature of 750°C, a supersaturation of 3°C and a cooling speed of 0.2°C/min. The growth time ranged from 16 to 60 min. The lateral growth front in many cases ended up in a (111) plane. GaAs grown on (110) or (211) GaAs substrates did not have flat surfaces. GaP grew laterally in the same manner as in the case of GaAs.
(2) Striped species oriented in the $\langle 1\bar{1}0 \rangle$ direction on (111) GaP and GaAs substrates resulted in a large difference in growth rate between two lateral directions $\langle 11\bar{2} \rangle$ and $\langle \bar{1}\bar{1}2 \rangle$. This phenomenon is shown in Figure 1 [not reproduced]. This phenomenon is assumed to be caused when one end face of the crystal being grown forms plane A (Ga plane) while the other end face makes up plane B (P or As plane). Since plane A is prone to get rough, many kinks and steps are assumed to be generated in it. Figure 2 [not reproduced] is a photo of an AB-etched surface of GaP. In the photo, many etch-pits are shown along stripes whereas the laterally grown epitaxial layer is free of such etch-pits. This is because dislocations in the substrate did not propagate to the layer laterally grown on the SiO_2 film. Similar results were observed also with GaAs. It was relatively easy to laterally grow layers of either GaP or GaAs to a thickness of about 100 μm.

4. Conclusion

Layers measuring about 100 μm in thickness of both GaP and GaAs have been laterally grown utilizing the anisotropy of crystal growth. These laterally grown layers have been found almost free of dislocations.

Acknowledgement: The authors are grateful to Mr Washiyama for his contribution to the above study.

Silicon Vapor-Phase Epitaxy in Excited Hydrogen

43067504 Tokyo JOURNAL OF THE JAPANESE ASSOCIATION OF CRYSTAL GROWTH in Japanese 10 Jul 88 p 92

[Article by M. K. Mazumder, Yuji Takakuwa, and Nobuo Miyamoto, Research Institute of Electrical Communications at Tohoku University: "Silicon Vapor-Phase Epitaxy in Hydrogen Excited by Ultraviolet Rays"]

[Text] It is regarded increasingly necessary to use low-temperature silicon epitaxy processes in order to enable the fabrication of semiconductor devices with higher integration density. We experimented in silicon vapor-phase

epitaxy using hydrogen excited by ultraviolet rays as the carrier gas to reduce the generation of crystal defects during the low-temperature process. As a result, it has been confirmed that the new method tested in our experiment enables a notable reduction in the generation of defects on the Si (111) 0° off surface.[1]

Figure 1 shows the results of the silicon vapor-phase epitaxy experiment we conducted at a growth temperature of 1000°C and a line velocity of 6.0 cm/sec. As seen from Figure 1, the new method resulted in a reduction of as much as 52 percent in defect generation. To verify that the reduction in defect generation was attributable to the use of excited hydrogen, we conducted the following two experiments: The piping for hydrogen (99.99999 percent pure) included in the experiment system was partly made of special synthetic quartz with the quartz portion being surrounded by four low-pressure mercury lamps. The system housing was filled with dry nitrogen to prevent the absorption of ultraviolet rays from oxygen contained in the air. This arrangement resulted in a reduction of about 50 percent in the generation of defects as seen from Figure 1 and Table 1. To see whether hydrogen would absorb the same ultraviolet rays (185 nm and 254 nm), we also made experiments with the system filled with hydrogen and oxygen instead of nitrogen. As a result, as shown in Table 1, pyramidal hillock density variations were eliminated, indicating that hydrogen as well as oxygen absorbed ultraviolet rays. Furthermore, to verify the presence of excited hydrogen having absorbed light, a Pt-mesh was inserted in the carrier hydrogen gas. As a result, as shown in Figure 2, variations entirely disappeared. This result is thought to indicate that the excited hydrogen was consumed as though it were a catalyst due to the presence of the Pt-mesh.

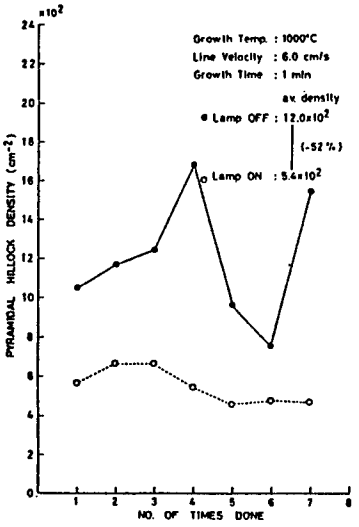

Figure 1

Table 1

	Variation of Pyramidal Hillock Density
N_2	- 55.0 %
	- 54.1 %
Air	+ 1.2 %
	+ 9.4 %
H_2	+ 12.5 %
	+ 5.9 %

Growth Temperature :1000°C
Growth Period :1min.
Line Velocity : 6.0 cm/sec

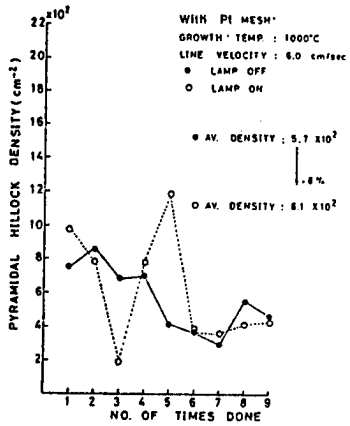

Figure 2

It has been evidenced that the reduction in the generation of defects achieved in silicon vapor-phase epitaxy made using hydrogen excited by ultraviolet rays as the carrier gas was due to the effect of excited hydrogen having absorbed ultraviolet rays of 185 and 254 nm wavelengths emitted from low-pressure mercury lamps.

References

1. 48th Meeting of the Japan Society of Applied Physics (1987) 19a-Q-7/II.

Growth of Optical Crystal D.LAP

43067504 Tokyo JOURNAL OF THE JAPANESE ASSOCIATION OF CRYSTAL GROWTH in Japanese 10 Jul 88 p 94

[Article by Kana Fujioka, Atsushi Yokotani, Takatomo Sasaki, Tatsuhiko Yamanaka, Sadao Nakai, and Chiyoe Yamanaka of the Laser Research Section, Osaka University and the Laser Research Institute: "Growth and Evaluation of Organic Nonlinear Optical Crystal D.LAP"]

[Text] 1. Introduction

LAP (L-arginine phosphate monohydrate) has been attracting attention as an organic, nonlinear optical crystal with superior properties. To obtain further improved properties, we experimented in growing D.LAP crystal--a deuterium compound. In this article, the D.LAP crystal-growing method used in our experiment and the results of evaluating the crystal grown by the method will be described.

2. Crystal Growth

To prepare the starting solution, D_3PO_4 was produced by hydrolyzing P_2O_5 with 99.8 percent D_2O. The D_3PO_4 was then mixed with L-arginine at a mole ratio of 1:1. This process was performed inside an N_2-substituted glove box so as not to lower the D substitution rate. The solution prepared was transferred

to a hermetically sealed crystal-growing tub whose interior is isolated from the outside air. In the tub, D.LAP was grown by the temperature drop method. As a result, a D.LAP crystal about 3 cm square was obtained. The crystal grew at the growth rate at a rate of about 1.4 mm growth in the + b-axis direction per day (Figure 1 [not reproduced]).

3. D-Substitution Rate in Crystal

The D-substitution rate was calculated by measuring the amount of H by the IR method and then substituting the measurement into the following equation: (D/D + H) x 100 (%). As a result 91±5 percent of H contained in hydrophilic groups in molecules was found to have been substituted. We are thinking of making further measurement by the NMR and MS methods to obtain more information.

4. Crystal Evaluation

For the D.LAP crystal grown by us, we measured the transmittance in the ultraviolet and infrared regions, temperature rise due to laser irradiation, laser damage threshold value, refractive index as data to determine the matching angle for the generation of the double higher harmonic of a 1.06-μm YAG laser, and the angle tuning curve. The measurements obtained are compared with the corresponding data on LAP and KDP in Table 1. In the infrared region, the transmittance rose by the effect of D-substitution, resulting in reduced loss at around 1.06 μm--fundamental wavelength of the YAG laser (see Figure 2). With regard to other properties, too, D.LAP appeared generally superior to KDP. Thus, it has been confirmed that D.LAP is superior to KDP as an optical crystal for higher harmonic generation and that it can also be used as a high-power laser.

Table 1. Wavelength Conversion Characteristics of D.LAP, LAP and KDP

		D·LAP	LAP	KDP
Absorbance at 1.06μm (cm^{-1})		0.02	0.09	0.05
UV Cut-off 95% for 5mm (μm)		0.26	0.26	0.20
*Acceptance Angle of 2ω (mrad-cm)		0.52 (1°50')	——	1.1 (3°50')
		1.1 (3'40")	0.84 (2°50')	2.2 (6°30')
*Temperature Acceptance Angle of 2ω(°C)	Type I	——	6.8	8.8
	Type II	——	13.9	17.6
$*d_{eff}/d_{eff}^{KDP,Type\,I}$	Type I	1.5	——	0.75
	Type II	1.8	1.3	1
Damage Threshold ($J\text{-}cm^{-3}$)		9~13	9~13	10

* These data were not optimized.

5. Afterword

To make larger D.LAP crystal available, we will try to improve the growth rate and enlarge the crystal cross-section. We have also been considering a new synthesis method to achieve a higher substitution rate.

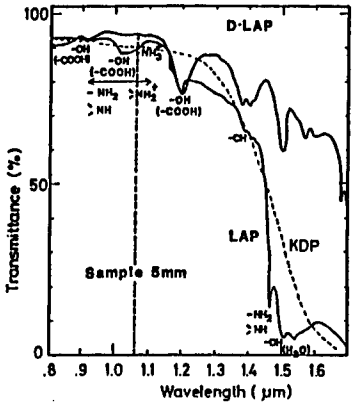

Figure 2. Near infrared transmittance characteristic

Optical Absorption of Ti:Al_2O_3 Single Crystal

43067504 Tokyo JOURNAL OF THE JAPANESE ASSOCIATION OF CRYSTAL GROWTH in Japanese 10 Jul 88 p 96

[Article by Shigeyuki Kimura, Nobuhiro Kodama, Kenji Kitamura, and Tsutomu Sawada, inorganic material research, Tosoh Corp.: "Optical Absorption Characteristic of Ti:Al_2O_3 Single Crystal"]

[Text] Introduction

Ti^{3+}:Al_2O_3 has been drawing attention as a laser crystal tunable in the near infrared region. A problem with this tunable laser crystal is that it has a parasitic absorption band extending over the laser oscillation wavelength range. The effect of this absorption band has become more noticeable as a result of the introduction of high-density Ti^{3+}.[1] The cause of the presence of its absorption band is not known yet, but it is assumed to be attributable to some crystal defects. Ti^{3+} is sensitive to oxidation reduction and its optical absorption changes when it is annealed under various partial pressures of oxygen (P_{O2}). We studied this phenomenon[2] and came to assume that (Ti^{3+} + Ti^{4+}) in an oxidation atmosphere or (Ti^{2+} + Ti^{3+} + oxygen vacant lattices) in a reduction atmosphere plays a role in causing the above phenomenon. To probe for a way of inhibiting the parasitic absorption of this laser crystal, we conducted more experiments at varied annealing conditions and studied the cluster behavior.

Experiments

Ti^{3+}:Al_2O_3 single crystal was synthesized by the condenser-type FZ method in which a xenon arc was used for heating. Next, 2-8 mm thick, flat plates containing a and c axes were sliced out from the synthesized crystal and both sides of each slice were polished to a mirror-like finish. The samples were comprised of two types of crystal: one with x = 0.001 for the Ti content and $Al_{(1-x)}Ti_xO_{1.5}$ and the other with x = 0.003. For absorption measurement, the transmitted light from a tungsten halogen lamp was measured using a 800 nm filter. For this measurement, a non-doped Al_2O_3 was used as a

reference sample. For annealing, samples were introduced into a Mo furnace in a (H_2 + CO_2) atmosphere (log P_{O2} = -7) and were kept there for 40 hours. Next, their absorption was measured. Subsequently, they were annealed again for 24 hours in a H_2 atmosphere. They then underwent absorption measurement and were subsequently annealed for another 36 hours in the same atmosphere. (Annealing temperature: 1750°C)

Results and Discussion

The changes in absorption coefficient (α_{800}) observed during annealing are shown in Figure 1. Based on the assumption that the two types of clusters are responsible for optical absorption, the results of our experiment can be explained as follows: After the samples were treated with H_2 + CO_2, (Ti^{3+} + Ti^{4+}) was generated in a large quantity, causing the value of α_{800} to increase. At this time, Al vacant lattice points were generated to accommodate Ti^{4+}. Next, their treatment in an H_2 atmosphere caused two types of reaction to progress simultaneously: one reaction in which oxygen vacant lattice points were generated and the other in which Al vacant lattice points disappeared. At the same time, a cluster of (Ti^{2+} + Ti^{3+} + oxygen vacant lattices)--another factor affecting (α_{800})--was generated, promoting the disappearance of (Ti^{3+} + Ti^{4+}). Since the reaction in which oxygen vacant lattice points were generated was slower than that in which Al vacant lattice points disappeared, the number of oxygen vacant lattice points did not grow significantly until most (Ti^{3+} + Ti^{4+}) disappeared, allowing the occurrence of a temporary state in which (Ti^{3+} + Ti^{4+}) and (Ti^{2+} + Ti^{3+} + oxygen vacant lattices) were present only in an extremely small number and during which the lowest value of (α_{800}) was recorded. Subsequently, as annealing was continued, oxygen vacant lattice points kept on increasing, eventually causing the number of (Ti^{2+} + Ti^{3+} + oxygen vacant lattices) to increase and the value of α_{800} to rise.

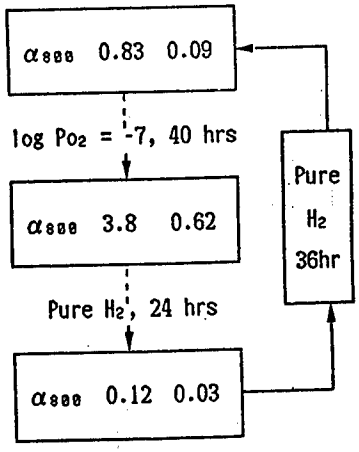

Figure 1. Effects of incomplete annealing (Figures represent absorption coefficient in cm^{-1})

The above explanation may be correct, considering that the oxygen diffusion coefficient in alumina single crystal is smaller than Al diffusion coefficient by about two orders of magnitude. If the above explanation is mostly correct, it should be possible to keep the value of α_{800} low by inhibiting the generation of clusters responsible for optical absorption.

References

1. P. Lacovara, et al., IEEE J. Quantum Electron. QE-21 1614 (1985).

2. Kimura, Kitamura, Kodama, and Sawada, Proceedings of 32nd Artificial Mineral Symposium, A01 (1986).

Growth of Superconductor $RBa_2Cu_3O_{7-\delta}$ (R = Y,Er)

43067504 Tokyo JOURNAL OF THE JAPANESE ASSOCIATION OF CRYSTAL GROWTH in Japanese 10 Jul 88 p 104

[Article by Takashi Ono, Nariyuki Hayashi, Kaori Sasaki, Tetsuo Inoue, and Akira Komatsu, metal laboratory of Tohoku University: "Growth and Evaluation of Oxide Superconductor $RBa_2Cu_3O_{7-\delta}$ (R = Y,Er) Single Crystal"]

[Text] This study is aimed at growing oxide superconductor $RBa_2Cu_3O_{7-\delta}$ (R = Y,Er) single crystal out of a CuO excess solution by the gradual cooling method, studying the characteristics of the single-crystal growth and confirming the relations between the crystal quality and superconducting properties.

R_2O_3 (R = Y,Er), $BaCO_3$ and CuO were prepared as raw materials in quantities for a relationship of $RBa_2Cu_3O_{7-\delta}$:CuO = 1:3 in mole ratio. They were mixed and ground in a mortar, formed into pellets, and were provisionally sintered at 900°C for 24 hours. The sintered bodies were put in an aluminum crucible (Figure 1). They were then melted in a crystal-growing furnace at 1150-1250°C. The molten material was gradually cooled down to 900-1000°C at a rate of 2-6°C/hour. After it was cooled to the above temperature, the furnace was turned off and the molten material was let to stand until it was cooled down to room temperature. The solidified material was cut into slices together with the crucible. The slices were annealed at 900°C for 24 hours, then mechanically pulverized. From the pulverized samples, $RBa_2Cu_3O_{7-\delta}$ single crystals on the order of millimeters in size were picked up. These operations were all performed in the air.

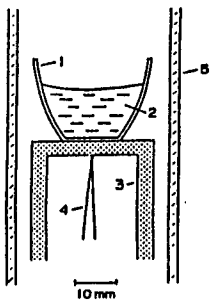

Figure 1. Furnace structure

$RBa_2Cu_3O_{7-\delta}$ single crystals obtained as described above were in plate form with wide crystal planes. Steps were observed on their crystal planes, suggesting that surface growth had taken place. Y- and Er-based crystals had steps characteristic of themselves, as shown in Figures 2 and 3, respectively. Many steps observed on Er-based samples were high with deep grooves between terraces. Er-based samples included those with crystal planes as large as about 4 mm square. The steps observed on many Y-based samples were lower than those on Er-based samples and many terraces observed on them approximately looked like squares, clearly reflecting the anisotropy between planes a and b. Spiral growth patterns like the one shown in Figure 4 were often observed on both Y- and Er-based samples. Through very careful observation, it was possible to notice many twinning plane stripes on the single crystal samples. Many of these crystals exhibited a sharp drop in electrical resistance at a temperature of about 90K. Figure 5 shows the results of resistance measurements on Y-based samples. Even among the samples verified as constituting $RBa_2Cu_3O_{7-\delta}$ single crystals based on the results of EDX analysis or analysis by the Laue method, those which did not show twinning stripes when examined with an optical microscope did not transfer into a superconductive state at 77K or higher temperature.

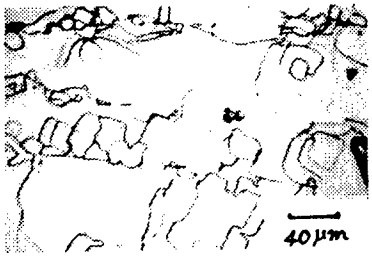

Figure 2

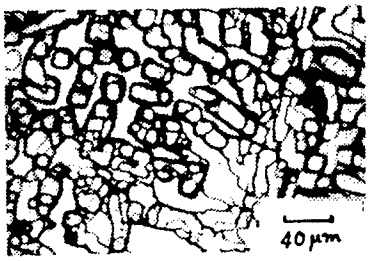

Figure 3

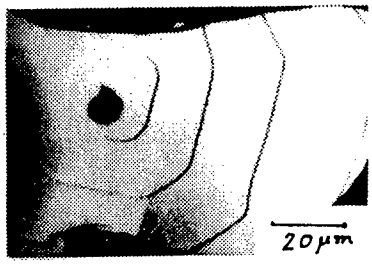

Figure 4

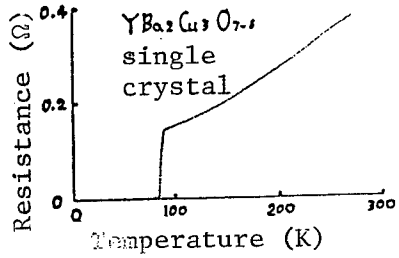

Figure 5

Our observations of the crystal growth mechanism and the properties of oxygen-annealed samples will be reported in more detail at the forthcoming meeting.

Growth of Superconductor $GdBa_2Cu_3O_{7-\delta}$

43067504 Tokyo JOURNAL OF THE JAPANESE ASSOCIATION OF CRYSTAL GROWTH in Japanese 10 Jul 88 p 105

[Article by Nariyuki Hayashi, Kazufumi Yoshida, Takashi Ono, Tetsuo Inoue, and Akira Komatsu, metal laboratory of Tohoku University: "Growth and Evaluation of Superconductor $GdBa_2Cu_3O_{7-\delta}$ Single Crystal"]

[Text] The sintered bodies of $RBa_2Cu_3O_{7-\delta}$ (R = Y, rare earth) are known to exhibit high Tc values. For this single crystal in plate form with a 1-2-3 composition grown out of a CuO excess solution by the gradual cooling method, oxygen control is very complex. Therefore, its properties are notably dependent on the raw material and heat treatment. For Er- or Y-based material, for example, a considerable amount of oxygen can be supplied by means of heat treatment, making quality superconductive crystal available, but things are not so easy for Gd-based material. The present study is aimed at experimentally growing large, quality single crystals of $GdBa_2Cu_3O_{7-\delta}$, confirming the mechanism of the crystal growth and determining appropriate conditions for heat treatment to be performed to improve the properties of the superconductor.

Gd_2O_3, $BaCO_3$ and CuO were prepared as raw materials in quantities for a relationship of $GdBa_2Cu_3O_{7-\delta}$:CuO = 1:3 in mole ratio. They were mixed and formed into disks and were provisionally sintered at 900°C for 24 hours. For crystal growing, the Bridgman method in which the solution solidification speed can be controlled with relative ease was used (see Figure 1). The solid-liquid interface was slightly projecting into the liquid-phase side with solidification progressing in one direction, from the aluminum crucible bottom upward. The solidification speed was varied in the range of 1.0 to 60 mm/h. Single crystals in plate form measuring 3 x 3 mm^2 were grown at a speed of R to 35 mm/h. From a cavity formed in a solidified material, we scraped off single crystals in plate form and examined their surfaces with a differential interference microscope. Their surfaces had, as shown in Figure 2, many steps, including spiral steps, which had developed from sub-boundaries, suggesting that surface growth had taken place. They also had collective single crystals comprising small laminar crystals stacked each in an appropriately adjusted orientation as shown in Figure 3. These single crystals, as grown, were semiconductors as seen from Figure 4 plotted by measuring their electrical resistance. Whether heat-treated in the air or in an oxygen atmosphere, they did not exhibit superconductivity. No evidence of twin formation was observed on any sample.

We will conduct similar experiments with single crystals in plate form collected from inside the above solidified materials and will study observation results in comparison with those obtained on the above samples.

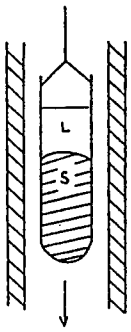

Figure 1. Crystal growing furnace
Crucible diameter: 25 mm
Heater: Siliconitto
Ambience: Air

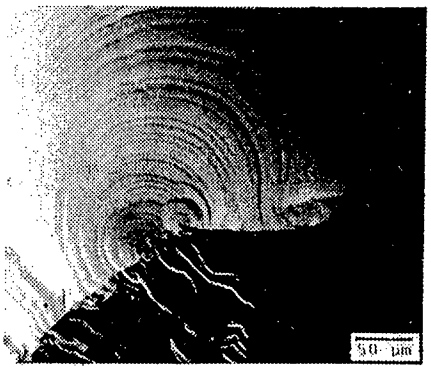

Figure 2. Steps on surface of $GdBa_2Cu_3O_{7-\delta}$ (Step sources are located along sub-boundaries)

Figure 3. Stacked laminar crystals

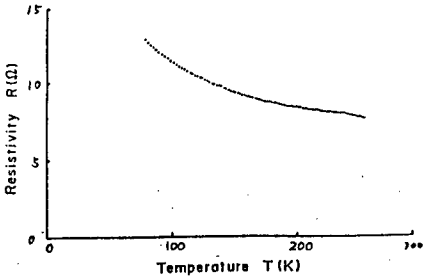

Figure 4. Electrical resistance of single crystals in plate form, as grown

$DyBa_2Cu_3Oy$ Single-Crystal Growth

43067504 Tokyo JOURNAL OF THE JAPANESE ASSOCIATION OF CRYSTAL GROWTH in Japanese 10 Jul 88 p 106

[Article by Tetsuo Inoue, Nariyuki Hayashi, Akira Komatsu, Takashi Ono, and Masato Shimizu, metal laboratory of Tohoku University: "Growth and Evaluation of $DyBa_2Cu_3Oy$ Single Crystal"]

[Text] Among the sintered-body superconductors, those on the order of Tc = 90K exhibit relatively high reproducibility. In the growth of single crystals by the flux method, reproducibility cannot be determined easily. The products resulting from the use of this method range widely from those which are like semiconductors to those on the 90K order.

$DyBa_2Cu_3O_y$ crystal undergoes phase transformation from a tetragonal system into an orthorhombic system (superconductor phase) at about 600°C or lower. To enable this phase transformation to be completed, the crystal must be supplied with adequate oxygen. This phase transformation also involves the formation of fine twin structures. According to a recent report,[1] whether a crystal will exhibit a high Tc value can be predicted to a certain extent by examining the degree of twin structure development in it.

The present study is aimed at growing $DyBa_2Cu_3O_y$ single crystals under the conditions listed in Table 1 and studying the relations between the conditions applied to crystal growing and the formation of twin structures in the grown crystals. According to the results of our differential thermal analysis, the constant-ratio (123) compounds decomposed and melted at about 1020°C. Samples 1-4 indicated peak heat absorption at about 940°C. This temperature is assumed to be a partial melting starting temperature.

Table 1

Sample No.	Composition of the mixture (mol. ratio)	Temperature	Cooling rate
1	(123):CuO=1:2	1050°C for 12h	17°C/h
2	(123):CuO=1:3	1050°C for 12h	ibid.
3	(123):CuO:BaO=1:6:1.3	970°C for 12h	ibid.
4	ibid.	1157°C for 12h	ibid

The results of our experiment are summarized in the following:

(1) Samples 1-3 were found to have been divided into a partially melted portion and a completely melted portion. A sample in such a divided state is shown in Figure 1. A relatively large crystal in plate form (3 x 3 mm^2) was found to have grown on the surface of the completely melted portion (a pool of melt) of the sample. Sample 4 was found to have been completely melted.

(2) The crystals grown in the partially melted portions of samples had notable twin structures without exception. Such twin structures were not observed on the crystals grown on the melt surfaces even after they were oxygen-annealed (at 540°C for 50 hours) (examined with a polarizing microscope).

(3) The crystals grown in the partially melted portions of samples exhibited high Tc values (see Figure 2 (a)) even in their as-grown state. The large crystals in plate form grown on the melt surfaces did not exhibit superconductivity at 77K or higher temperature even after they were oxygen-annealed (at 540°C for 50 hours) (see Figure 2 (b)).

(4) Even among the thin crystals in plate form (1 x 1 mm^2) grown in samples, not on melt surfaces, under the same conditions as for sample 4, there were those which, after being heat-treated at 900°C for 24 hours (in the air) and then oxygen-annealed (at 540°C for 50 hours), developed twin structures and exhibited high Tc values (middle point = 89K).

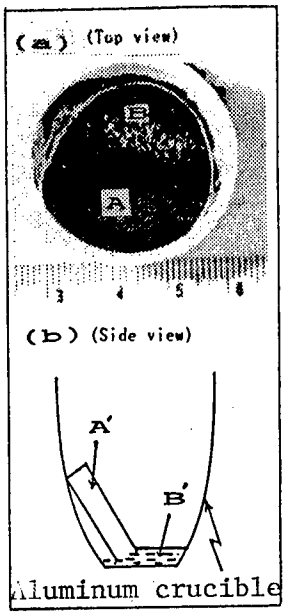

Figure 1. Sample 1
A,A': Partially melted portion of pressed pellet
B,B': Melt

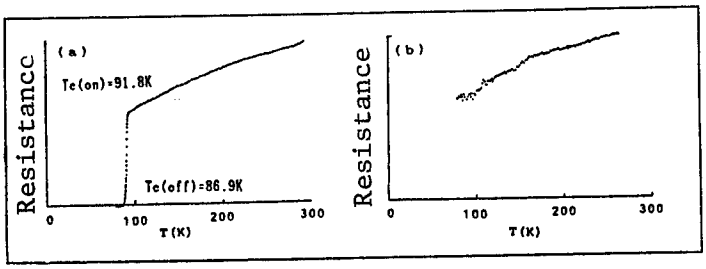

(a) Polycrystal grown in partially melted portion (as grown) (Fig. 1, A,A')

(b) Crystal in plate form grown on melt (oxygen-annealed) Fig. 1, B,B')

Figure 2

References

1. Shigeyuki Tsurumi, "Chemistry of Oxide Superconductors" (Fueki, Kitazawa editions, Kodansha, SCIENTIFIC, 1988) p 139.

$Er_2Ba_2(Cu,Pt)_2O_8$ Single Crystal Growth

43067504 Tokyo JOURNAL OF THE JAPANESE ASSOCIATION OF CRYSTAL GROWTH in Japanese 10 Jul 88 p 108

[Article by Tsunaetu Shishido, Yoko Saito, Tsuginari Fukuda, Kazutoshi Ukei, Naoki Toyota, and Takahiko Sasaki, metal laboratory of Tohoku University:
"Growth and Evaluation of $Er_2Ba_2(Cu,Pt)_2O_8$ Single Crystal"]

[Text] 1. Introduction

We obtained a pillar-shaped single crystal of a new composite oxide, $Er_2Ba_2(Cu,Pt)_2O_8$, through the process of synthesizing $ErBa_2Cu_3O_{7-\delta}$ single crystal using a Pt crucible.[1-4]

2. Experiment

Er_2O_3,$Ba(OH)_2 \cdot 8H_2O$,CuO prepared in a specified mole ratio was put in an aluminum crucible and preliminarily sintered at 950-1000°C in the air. CuO was added to the sintered body and the mixture was transferred into a Pt crucible. It was then heated to 1100°C and kept at this temperature for 1 hour. Next, it was cooled to 900°C at a rate of $10°Ch^{-1}$ and subsequently let to stand in the furnace. The same experiment was also conducted using PbO as flux instead of CuO.

3. Results and Discussion

3-1. Experiment Conducted Using CuO as Flux

Through this experiment conducted by the self-component flux method, we obtained a plate-shaped crystal of $ErBa_2Cu_3O_{7-\delta}$ compound (~3 x 3 x 0.1 mm^3). In addition, a pillar-shaped crystal of a composite oxide, $Er_2Ba_2(Cu,Pt)_2O_8$, was also found to have been formed (~0.7 x 0.1 x 0.1 mm^3) at the bottom of the Pt crucible). Table 1 shows crystallographic data on this pillar-shaped crystal. Figures 1 and 2 show the crystal structure and an electron-microscopic view. As seen from the perspective drawing in Figure 1, the structure of this compound is unique in that a /Cu\O/Pt\O/ zigzag chain runs through along axis b of the structure. The axis b coincides with the crystal growth orientation. Considering that the valences of Ba and Er stay constant while the solute and flux are heated in the Pt crucible, it is assumed that Pt is attacked and taken into the solution by the work of Cu involving changes in valence.

3-2. Experiment Conducted Using PbO as Flux

We repeated the above experiment, but using PbO as flux which was expected to cause valence changes at high temperature. As a result, a pillar-shaped single crystal of a composite oxide $Er_2Ba_2(Cu,Pt)_2O_8$ of approximately the same size as that obtained in the above experiment was again obtained. This single crystal was chemically analyzed and its lattice constant was measured. As a result, it was confirmed that few lead ions had found their way into

the compound during the experiment, i.e., the crystal was almost free of contamination due to the flux.

Table 1. Crystallographical Data

Formula	$Er_2Ba_2Cu_{1.1}Pt_{0.9}O_8$
C.S.	orthorombic
S.G.	Pcmn
a/A	10.287(3)
b/A	5.659(1)
c/A	13.157(3)
V/A^3	765.9
Z	4
R	0.060

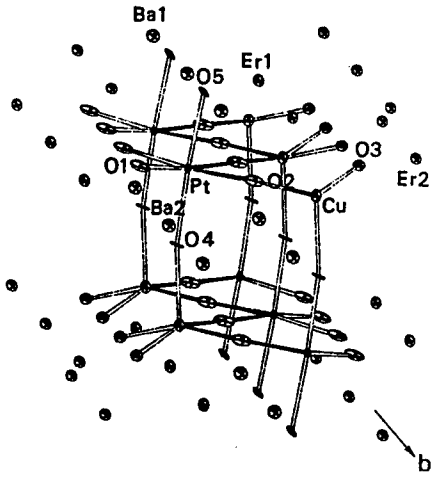

Figure 1. Crystal structure

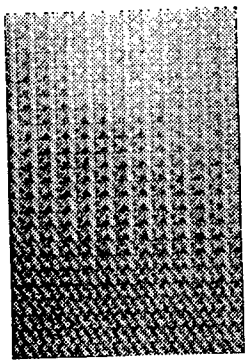

Figure 2. Electron microscopy

3-3. Physical Properties

The single crystals we obtained were not large enough to enable their physical properties to be measured appropriately. We are now in the process of devising a way to obtain larger samples. When a sample synthesized by the sintering method was tested, it underwent a magnetic transition from paramagnetism to ferromagnetism at 10K.

Acknowledgement: We wish to express our thanks to Messrs Shindo, Kajiya, Aoyagi, Kikuchi, Shono, Hirabayashi, and Muto for their kind assistance extended to us in carrying out electron diffraction tests.

References

1. T. Shishido, T. Fukuda, N. Toyota, K. Ukei, and T. Sasaki, J. Cryst. Growth, 85 599 (1987).

2. K. Ukei, T. Shishido, and T. Fukuda, Acta. Cryst. C (in press).

3. N. Shishido, T. Fukuda, N. Toyota, K. Ukei, and T. Sasaki, Journal of The Japanese Association of Crystal Engineers, 14, No 3 & 4, 25 (1987).

4. N. Shishido and T. Fukuda, "Chemistry of Oxide Superconductors," Fueki, Kitazawa editions, Kodansha, pp 50-51 (1988).

Bi-Ca-Sr-Cu-O Film Formation by Liquid Phase Epitaxy

43067504 Tokyo JOURNAL OF THE JAPANESE ASSOCIATION OF CRYSTAL GROWTH in Japanese 10 Jul 88 p 109

[Article by Hiroyuki Takeya and Fumihiko Takei, Material Property Laboratory, Tokyo University: "Formation of Bi-Ca-Sr-Cu-O System Superconductor Film by Liquid Phase Epitaxial Method"]

[Text] 1. Introduction

The technique for forming a single-crystal thin film of high-temperature oxide superconductor is a key to superconductor applications, so that it has been studied by many researchers. The thin film formation techniques are divided into the vapor phase epitaxial method (including sputtering, evaporation, and MBE) and liquid phase epitaxial method (LPE, etc.). While a considerable number of researcher groups belonging to semiconductor manufacturers or various research institutes are studying the gas phase epitaxial method, not so many research results have been reported concerning the liquid phase epitaxial method. Under these circumstances, we experimented in forming films of the Bi-Ca-Sr-Cu-O system--a high-temperature superconductor discovered this year [1988].

2. Experiment

We first mixed Bi_2O_3, $CaCO_3$, $SrCO_3$ and CuO and produced sintered bodies of the mixture. The sintered bodies were mixed with various kinds of flux and melted in a Pt crucible by RF heating. A substrate, MgO, was dipped in the melt and epitaxial growth was conducted. The fluxes were comprised of those appropriately selected from among the following three types: 1) self-flux (Bi_2O_3, CuO), 2) oxide flux, and 3) salt flux.

3. Results

As an experiment result obtained so far, crystal film deposition on the substrate was observed at relatively high temperature, i.e., around 900°C. An SEM of such a film deposited over an MgO(001) substrate is shown in Figure 1. According to the results of EPMA analysis made for this sample, the black areas in Figure 1 represent the substrate, while the brighter portions are composed of materials such as Bi_2, $_4Ca_0$, $_\tau Sr_2$ and $_3Cu_2Ox$. Figure 2 shows an X-ray diffraction pattern plotted by making measurement on an as-grown film attached to a diffractometer together with the substrate. As clearly seen from Figure 2, only 00ℓ diffraction lines were observed, indicating that

epitaxial film growth was achieved. From the film composition analyzed by EPMA and the X-diffraction pattern shown in Figure 2, it is observed that the main phase of $Bi_2CaSr_2Cu_2Ox$ contains about 10 percent of Bi_2Sr_2CuOx mixed as a subphase during the growth process. We plan to conduct more experiments while varying such conditions as the starting composition, flux mixing ratio, substrate and flux types, and temperature.

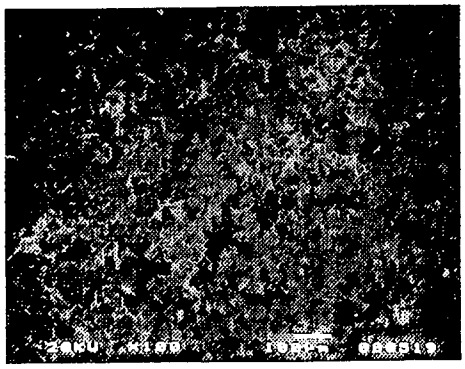

Figure 1. Scanning electron microscopy of film deposited on MgO substrate

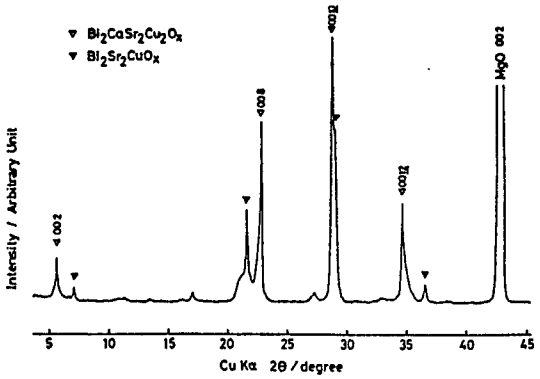

Figure 2. X-ray diffraction pattern

Oxide Superconductor Phase Equilibrium Diagrams

43067504 Tokyo JOURNAL OF THE JAPANESE ASSOCIATION OF CRYSTAL GROWTH in Japanese 10 Jul 88 p 110

[Article by Kunihiko Oka and Hiromi Uki of Electro-Technical Laboratory, Masatoshi Saito and Masahiro Ito of Sumitomo Metal Mining Co., and Kenji Nakane of Sumitomo Chemical Co.: "Phase Equilibrium Diagram of Oxide Superconductor"]

[Text] Introduction

To study the physical properties of $RBa_2Cu_3O_{7-y}$ (R: rare earth) system and develop its applications, it is essential to make quality, large single crystals of the system available. In growing single crystals of this system, relevant phase equilibrium diagrams should provide useful guiding information. We plotted four composition-temperature phase equilibrium diagrams with respect to as many directions based on the phase equilibrium diagram of the Y_2O_3-BaO-CuO system (Figure 1), i.e., directions of $YBa_2Cu_3O_{7-y}$ to CuO, $Ba_3Cu_{12}O_{15}$, $Ba_3Cu_7O_{10}$ and $Ba_3Cu_5O_8$, respectively, by carrying out differential thermal analysis, experimenting in crystal growth by the heating-quenching method and conducting X-ray diffraction analysis on produced samples. We then studied the potential for growing crystals of the above system based on the plotted diagrams.

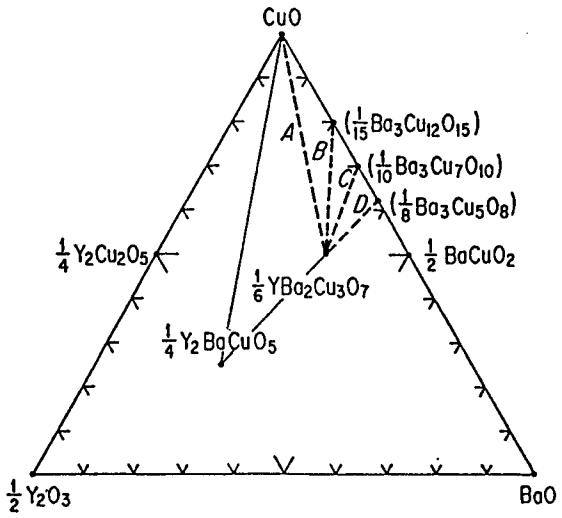

Figure 1. Phase equilibrium diagram of Y_2O_3-BaO-CuO system

Experiment

Sample mixtures of CuO, $Ba_3Cu_{12}O_{15}$, $Ba_3Cu_7O_{10}$ and $Ba_3Cu_5O_8$, which are the materials coming at the rightmost positions with respect to $YBa_2Cu_3O_{7-y}$ in the directions A, B, C and D, respectively, indicated on Figure 1, were prepared in different compositions with differentials between components varied in the range of 5-10 percent. Differential thermal analysis was then conducted on them and their approximate eutectic lines, peritectic lines, and melting points were analyzed. Subsequently, repeated experiments in single crystal growth by the heating-quenching method were carried out, focusing on compositions and temperatures around those roughly determined as mentioned above. The samples produced were pulverized and X-ray diffraction analysis was conducted on them. The overall results of all the experiments conducted were analyzed and phase equilibrium diagrams were eventually plotted. Based on the plotted diagrams, crystal growth experiments were conducted by the flux method as well as the solution-pulling method in which seeds of $SrTiO_3$ single crystal were used.

Results

Figure 2 shows a three-dimensional phase equilibrium diagram combining the four phase equilibrium diagrams plotted with regard to the directions of 1/6 $YBa_2Cu_3O_{7-y}$ to (CuO, 1/15 $Ba_3Cu_{12}O_{15}$, 1/10 $Ba_3Cu_7O_{10}$ and 1/8 $Ba_3Cu_5O_8$), respectively. It has been found that, in all the four phase equilibrium diagrams, the liquid phase starts appearing at 900°C and that Y_2BaCuO_5 and a liquid phase appear over wide ranges of temperature and composition. It has also been known that the liquidus for the composition in which $YBa_2Cu_3O_{7-y}$ needed in growing $YBa_2Cu_3O_{7-y}$ single crystal and a liquid phase are included rises very sharply and that the composition is confined in a very narrow range. Hence, it has been concluded that it is very difficult to grow $YBa_2Cu_3O_{7-y}$ single crystal. We experimented in growing single crystal by the flux method based on the phase equilibrium diagram for the $YBa_2Cu_3O_{7-y}$ - $Ba_3Cu_7O_{10}$ system and obtained single crystals measuring 1-2 mm in thickness.

We selected this system as the experiment target because its liquidus indicating the existence of $YBa_2Cu_3O_{7-y}$ and a liquid phase appeared over a relatively wide range of area. We were unable to grow crystal by the solution-pulling method partly because the phenomenon of solution climbing the crucible wall was more notable than in the case of the La_2CuO_1 system.[1]

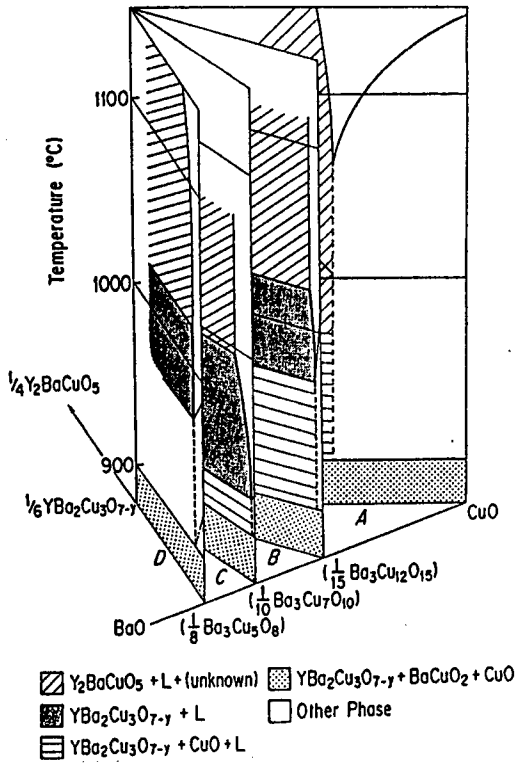

Figure 2. Phase equilibrium diagram of 1/6 $YBa_2Cu_3O_{7-y}$ to (CuO, 1/15 $Ba_3Cu_{12}O_{15}$, 1/10 $Ba_3Cu_7O_{10}$ and 1/8 $Ba_3Cu_5O_8$)

References

1. Oka and Uki, Bulletin of the Japanese Association of Crystal Growth, 14 (1987) 183.

Growth of Bi-Sr-Ca-Cu Oxide Single Crystal

43067504 Tokyo JOURNAL OF THE JAPANESE ASSOCIATION OF CRYSTAL GROWTH in Japanese 10 Jul 88 p 111

[Article by Toshisada Nomura, Tomohisa Yamashita, Hisashi Yoshino, and Takeshi Ando, general laboratory, Toshiba Corp.: "Growth of Bi-Sr-Ca-Cu Oxide Single Crystal and Its Superconductive Properties"]

[Text] 1. Introduction

A new oxide superconductor of a Bi-Sr-Ca-Cu-O system was discovered by Maeda, et al. of National Research Institute for Metals in January this year [1988].[1]

Since then, the new oxide superconductor has been energetically studied at various institutes. The superconductors comprised of this system include two types of phases: one type with a Tc of up to 110K and the other with a Tc of up to 80K. Vigorous research has been made, particularly, on the chemical composition of high-temperature phases and the method of extracting single phases. Therefore, in these areas, more and more information has become available. In promoting the study on the superconductive properties or anisotropy of this system, it is essential to evaluate the superconductor in the form of single crystal. There have been some study reports on 80K-phase single crystals.[2-4] However, the reported results of measurement made using samples which were not large enough cannot be said satisfactory. With the aim of producing relatively large single crystals and confirming their superconductive properties, anisotropy in particular, we experimented in growing single crystals of a system containing Bi_2O_3 and CuO as fluxes and measured the anisotropy of the produced single crystals.

2. Experiment

Powders of Bi_2O_3, $SrCO_3$, $CaCO_3$, and CuO with a minimum purity of 4N were mixed to a specified composition. The powdery mixture was placed in an aluminum crucible. It was then heated to and kept at 1000°C in the air. Subsequently, it was gradually cooled to obtain single crystals. The produced crystal phase was identified by the powder X-ray diffraction method. Its chemical composition was determined by EDX. The electrical resistance was measured by the d.c. four-terminal method using electrodes made of indium-based solder. For magnetization measurement, a SQUID was used.

3. Results and Discussion

Single crystals with various compositions coming on the triangle formed, on the phase diagram, by linking three end members, $1/2Bi_2O_3$, (Sr,Ca)O, and CuO were grown and the produced crystal phases were identified. Relatively large single crystals (7 x 5 x 1 mm^3 maximum) of $Bi_2(Sr,Ca)_3Cu_2Ox$, which is a superconductor on the 80K order, were obtained from starting materials with a composition ratio in the range of Bi:Sr:Ca:Cu = 2:1:1:2~3. These relatively large single crystals had cleavage on plane C as in the case of $Bi_2(Sr,Ca)_2CuOx$ or $(Sr,Ca)BiO_3$. The curve shown below represents the temperature dependence of the electrical resistance of the single crystals. The chemical composition of these single crystals was $Bi_{2.2}(Sr,Ca)_{2.6}Cu_2Ox$. As clear from the curve, the temperature dependence of their electrical resistance was found to be characteristic of metal both inside plane C and in the direction of axis C. The values of Tc (onset) and Tc (zero) were also identical whether in plane C or along axis C. They measured 84K and 81.5K, respectively. These Tc values coincide with those determined based on the temperature dependence of magnetization. The electrical resistivity showed a x35 anisotropy at 84K, measuring 0.4 mΩcm in plane C and 14 mΩcm along axis C, respectively. This anisotropy is considered attributable to that of the crystal structure.

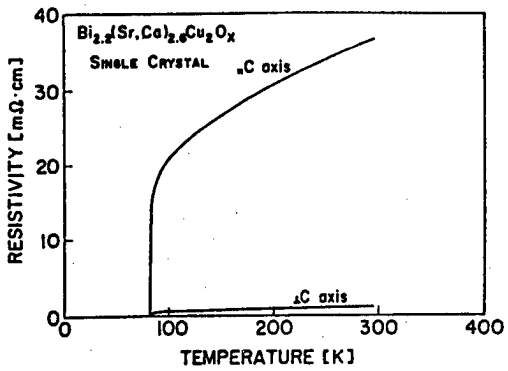

Temperature dependence of electric resistivity

References

1. H. Maeda, et al., Jpn. J. Appl. Phys., 27 (1988).

2. J. Z. Liu, et al., Phys. Lett. (1988).

3. H. Takagi, et al., NATURE, 332, 17 March (1988).

4. L. F. Schneemeyer, et al., NATURE, 332, 31 March (1988).

Bi-Sr-Ca-Cu-O Single Crystal Growth Using Alkali Chloride

43067504 Tokyo JOURNAL OF THE JAPANESE ASSOCIATION OF CRYSTAL GROWTH in Japanese 10 Jul 88 p 112

[Article by Akinori Katsui, Optical Energy Laboratory, NTT, and Hideaki Otsuka, Electronic Applications Laboratory, NTT: "Growth of Bi-Sr-Ca-Cu-O Single Crystal Using Alkali Chloride Solvent"]

[Text] In growing an oxide superconductor of an incongruent melting type from a solution, using a non-stoichiometric starting composition is effective in achieving higher crystal purity.[1]

In this regard, CuO-rich compositions should be appropriate for starting solutions to be used in growing a series of superconductors containing Cu which have been discovered so far. Successful results of the growth of $(La,Sr)_2CuO_y$ crystals carried out based on this idea have been reported.[2,3] However, this method does not exhibit its desired effect in the growth of $Ba_2YCu_3O_y$ crystals. A problem is that the decomposing temperature of $Ba_2YCu_3O_y$ is considerably lower than that of $(La,Sr)_2CuO_y$. Other problems include that the melting point of CuO used as a solvent is higher than desirable and that the crystal grown and the solvent used cannot be separated with ease. These conditions are also involved in the growth of Bi-Sr-Ca-Cu-O compounds. We experimented in growing Bi-Sr-Ca-Cu-O crystal from a solution using an alkali chloride such as KCl as a solvent.[4] This method was previously used successfully in growing $Ba(Pb,Bi)O_3$.

The starting material was prepared by melting a powdered oxide mixture such as $Bi_4Sr_3Ca_3Cu_4O_v$ in the air and quenching it to room temperature. About 5 grams of the starting material prepared as above was placed in a platinum crucible together with about 140 grams of KCl or KCl:NaCl = 50:50. With a lid put on the platinum crucible, the starting material was heated to and kept at 920-960°C for about 15 hours. Next, it was gradually cooled to about 700°C, then let to stand in the furnace until being cooled to room temperature. The solvent loss during the crystal growth process amounted to 1-4 grams at the above temperature range.

In all cases of experimental crystal growth, a thin crystal plate measuring about 50 microns in thickness and 1-2 grams in weight formed over the solidified solvent surface. It was separated from the solvent by being dipped in flowing hot water. It consisted of a stack of thin film layers each measuring up to 1 micron in thickness. Its surface was in parallel with plane C. Therefore, cleaving it in the direction of plane C made it possible to obtain smooth-surfaced single-crystal thin films in desired size. The thin plate grown from a starting composition of $Bi_4Sr_3Ca_3Cu_4O_v$ was comprised of a single phase ($Bi_2(Sr,Ca)CuO_v$[5]) with c = 24.3A. Similar results were obtained also with starting compositions of $Bi_4Sr_3Ca_3Cu_6O_v$ and $Bi_2Sr_2CaCu_2O_v$. The use of a starting composition of $BiSrCaCu_2O_v$ resulted in the growth of a thin crystal plate comprising a ($Bi_2Sr_2CaCu_2O_v$[5,6]) with a c = 30.8A. In this case, needle-like crystals of CuO were found to have formed on the back side (the side that had been in contact with the solvent) of the thin crystal plate.

We measured the temperature dependence of the electrical resistance of sample crystals. The electrical resistance of samples with c = 24.3A exhibited temperature dependence like that of semiconductors. The resistance of a phase with c = 30.8A measured 0 at about 80K. Such contents as Na, K, and Cl of crystals grown in these experiments were analyzed by the use of an EPMA [electron probe microanalyzer]. From the analysis results and the above experiment results, it is assumed that the amount of impurities taken in from the solvent was extremely small.

References

1. A. Katsui, Y. Hidaka, and H. Takagi, J. Crystal Growth, 66 (1984) 228.

2. V. Hidaka, Y. Enomoto, M. Suzuki, M. Oda, and T. Murakami, J. Crystal Growth, 85 (1987) 581.

3. K. Oka and H. Unoki, Jpn. J. Appl. Phys., 26 (1987) L1590.

4. A. Katsui and M. Suzuki, Jpn. J. Appl. Phys., 21 (1982) L157.

5. E. Takekawa-Muromachi, Y. Uchida, A. Ono, F. Izumi, M. Onoda, Y. Matsui, K. Kosuda, S. Takekawa, and K. Kato, Jpn. J. Appl. Phys., 27 (1988) L365.

6. R. M. Hazen, C. T. Prewitt, R. J. Angel, N. L. Ross, L. W. Finger, C. G. Hadidiacos, D. R. Veblen, P. J. Heaney, P. H. Hor, R. L. Meng, Y. Y. Sun, Y. Q. Wang, Y. Y. Xue, Z. J. Huang, L. Gao, J. Bechtold, and C. W. Chu, Phys. Rev. Lett., 60 (1988) 1174.

Structural Analysis of Large Satellites

43067502a Tokyo PROCEEDINGS OF THE JSASS/JASME STRUCTURES CONFERENCE in Japanese 14-16 Jul 88 pp 10-13

[Article by Shoichi Nasu and Takashi Sakurai, Mitsubishi Space Software Co., Ltd.: "Structural Analysis of Large Satellites by Partial Structure Synthesis"]

[Text] 1. Introduction

Artificial satellites for such purposes as communications, broadcasting, and observation have been increasing in size and complexity in recent years. Hence, the growing importance of their structural analysis and the mounting complexity of the work involved. Furthermore, division of work at the component level is making progress and, accordingly, in structural analysis it is becoming common practice to conduct FEM analysis for each component and make structural analysis of the entire system by the process of partial structure synthesis. We have prepared a tool for analyzing the structure of large satellites by this process. We will report it here in general, showing the results of our analysis with a sample model.

2. Subsystem Recovery in Partial Structure Synthesis

The entire satellite system, which is a large structure, is divided into a number of subsystems including the body, the antenna, and the solar paddle as partial structures and the dynamic characteristic of each subsystem is determined. The process of synthesizing the dynamic characteristics of these subsystems, thereby preparing a motion equation for the main system and computing the characteristic frequency and natural mode of the entire system as well as response acceleration and response stress is called the process of partial structure synthesis.

So that an evaluation of the interiors of the subsystems can be done in the main system, it is necessary to bring monitor points into the main system and, therefore, the degree of boundary freedom increases. In this tool, subsystem recovery is possible; thus, it can evaluate subsystem stress and strain energy and it is possible to make a detailed analysis, component by component, at the subsystem level.

3. Basic Equations

The basic equations for mode synthesis and subsystem recovery in this tool are as follows:

Explanation of symbols

mA:	model mass matrix of subsystem A	qA:	mode coordinate of subsystem A
mB:	model mass matrix of subsystem B	qB:	mode coordinate of subsystem B
M1C:	mass matrix of main system	ΦA:	mode vector of subsystem A
kA:	model rigidity matrix of system A	ΦB:	mode vector of subsystem B
kB:	model rigidity matrix of system B		
IKC:	rigidity matrix of main system C		
UA:	displacement vector of subsystem A	fA:	external force vector of subsystem A
UB:	displacement vector of subsystem B	fB:	external force vector of subsystem B
U1C:	displacement vector of main system C	IFC:	external force vector of main force C

The equation of motion for each subsystem is as follows:

Subsystem A $mA\ddot{q}A+kAqA=fA=0$ (1) $UA=\Phi A\cdot qA$

Subsystem B $mB\ddot{q}B+kBqB=fB=0$ (2) $UB=\Phi B\cdot qB$

Main system C $M1C\ddot{U}1C+K1CU1C=F1C$ (3)

$$U1C=\begin{pmatrix} UC \\ \hline UA \\ UB \end{pmatrix},\ F1C=\begin{pmatrix} FC \\ \hline FA \\ FB \end{pmatrix}$$

If these are consolidated into one equation

$$\left(\begin{array}{cc|c} mA & \cdot & \cdot \\ \cdot & mB & \cdot \\ \hline \cdot & \cdot & M1C \end{array}\right)\begin{pmatrix} \ddot{q}A \\ \ddot{q}B \\ \hline \ddot{U}1C \end{pmatrix}+\left(\begin{array}{cc|c} kA & \cdot & \cdot \\ \cdot & kB & \cdot \\ \hline \cdot & \cdot & K1C \end{array}\right)\begin{pmatrix} qA \\ qB \\ \hline U1C \end{pmatrix}=\begin{pmatrix} \cdot \\ \cdot \\ \hline F1C \end{pmatrix} \quad (4)$$

or

$$M1\cdot\ddot{U}1+K1\cdot U1=F1 \quad (5)$$

Here,

$$U1=\begin{pmatrix} qA \\ qB \\ \hline U1C \end{pmatrix}=\begin{pmatrix} qA \\ qB \\ \underline{UC} \\ UA \\ UB \end{pmatrix}=\left(\begin{array}{ccc} I & \cdot & \cdot \\ \cdot & I & \cdot \\ \cdot & \cdot & I \\ \hline \Phi A & \cdot & \cdot \\ \cdot & \Phi B & \cdot \end{array}\right)\begin{pmatrix} qA \\ qB \\ UC \end{pmatrix}=T\cdot V \quad (6)$$

$$T=\begin{pmatrix} I \\ \hline G \end{pmatrix}=\left(\begin{array}{ccc} I & \cdot & \cdot \\ \cdot & I & \cdot \\ \cdot & \cdot & I \\ \hline \Phi A & \cdot & \cdot \\ \cdot & \Phi B & \cdot \end{array}\right) \quad (7),\qquad V=\begin{pmatrix} qA \\ qB \\ UC \end{pmatrix} \quad (8)$$

The equation expressed by the Ul system is converted into the V/ system.

Multiplying $\mathbf{M}\ddot{\mathbf{U}}\mathbf{l} + \mathbb{K}\mathbf{U}\mathbf{l} = \mathbb{F}$ (5) equation by

$\mathbf{U}\mathbf{l} = \mathbf{T} \cdot \mathbf{V}\mathbf{l}$ (6) equation, the product is

$$\tilde{\mathbf{M}}\ddot{\mathbf{V}}\mathbf{l} + \tilde{\mathbb{K}}\mathbf{V}\mathbf{l} = \tilde{\mathbb{F}} \quad (9)$$

Here,

$$\tilde{\mathbf{M}} = \mathbf{T}^t \cdot \mathbf{M} \cdot \mathbf{T} \quad (10)$$

$$\tilde{\mathbb{K}} = \mathbf{T}^t \cdot \mathbb{K} \cdot \mathbf{T} \quad (11)$$

$$\tilde{\mathbb{F}} = \mathbf{T}^t \mathbb{F} \quad (12)$$

Namely, the system equation for the entire system can be expressed by equation (9) from equations (10), (11), and (12). This tool is the application of this conversion to FEM analysis.

4. Example of Application to Simple Model

Subsystem recovery for Panel 2 of the two-panel simple model shown in Figure 1 was conducted by characteristic frequency analysis and frequency response analysis by the process of partial structure synthesis. Figure 2 shows the flow of degeneracy and recovery.

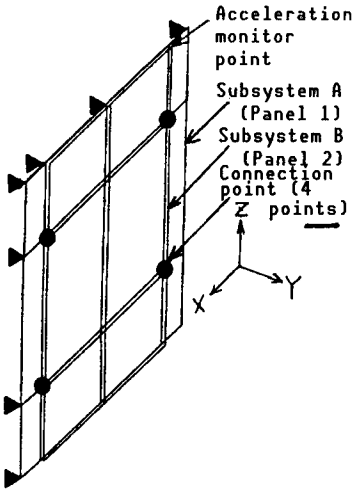

Figure 1. Simple Model

4.1 Results of Characteristic Frequency Analysis

Ten modes each were obtained from the low order for Subsystems A and B by the constraint mode process and the characteristic frequency of the entire system was obtained by the mode synthesis process. Table 1 shows the characteristic frequency while Figure 3 shows the natural mode.

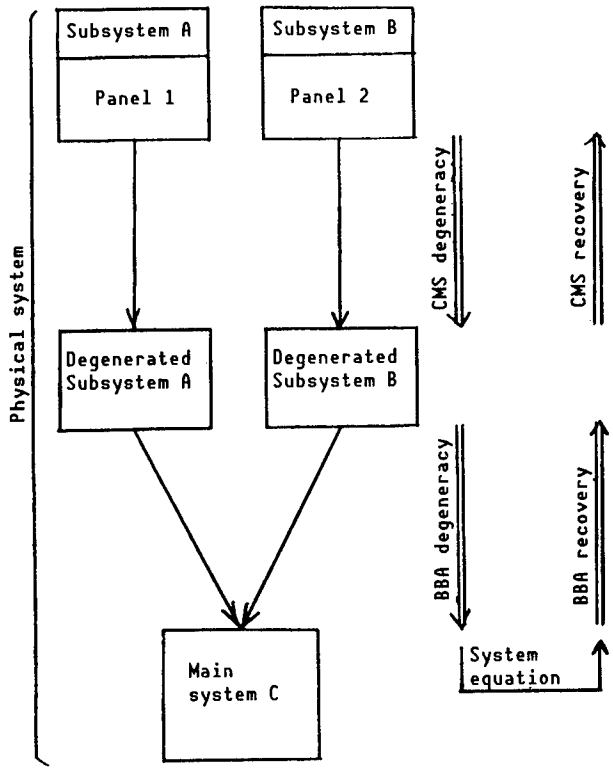

Figure 2. Flow of Degeneracy/Recovery

Table 1. Results of Analysis of Characteristic Frequency

Order	Result of synthesis of characteristic frequency (Hz) mode	Result of characteristic frequency (Hz) physical mode
1	36.560	36.551
2	41.870	41.868
3	50.476	50.447

4.2 Results of Analysis of Frequency Response

Figures 4 and 5 respectively show the response acceleration at the monitor point and the response component strength when panel 1 was excited by a 1G sine wave in the Y direction (outside the panel surface). $\zeta = 0.025$ was always assumed as the value of the model attenuation matrix.

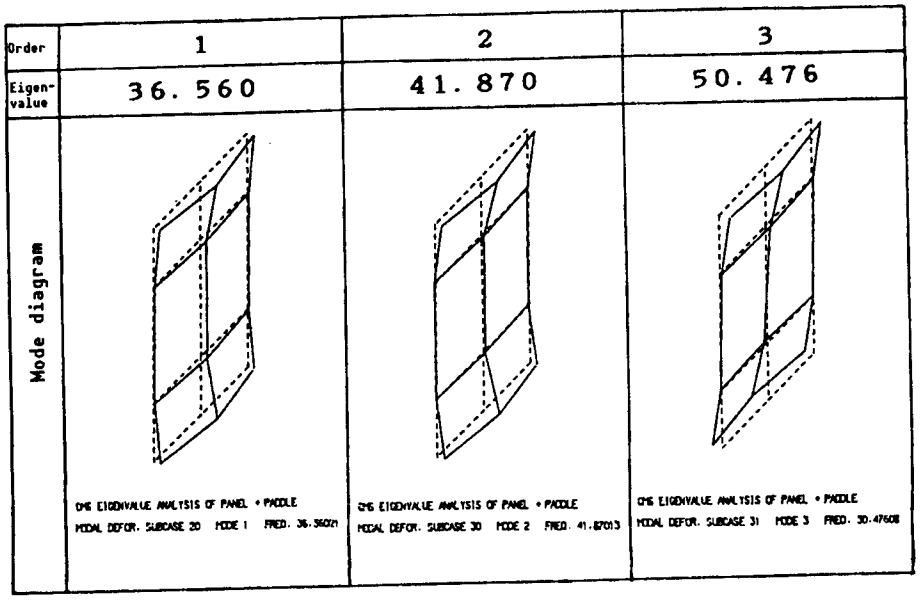

Figure 3. Diagrams of Subsystem Recovery Characteristic Modes

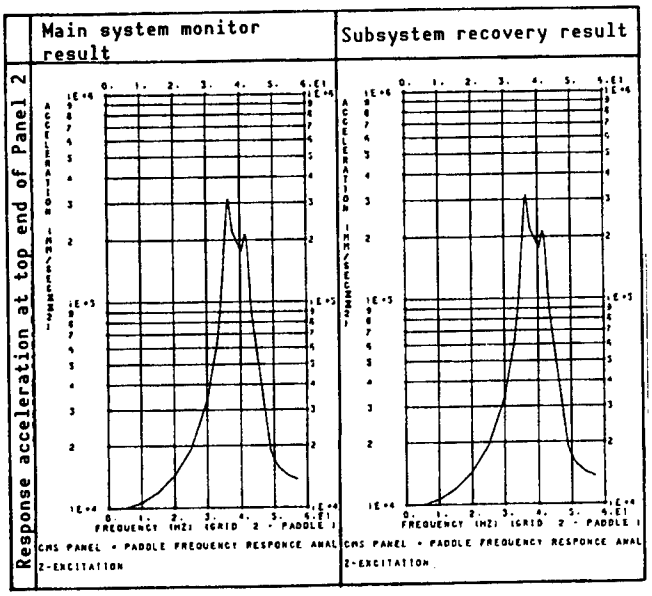

Figure 4. Response Acceleration

5. Summary

The results of analysis of the characteristic frequency agreed well with the results of physical model FEM analysis. As for the results of analysis of frequency response, the subsystem recovery results agreed well with the monitor results in the main system.

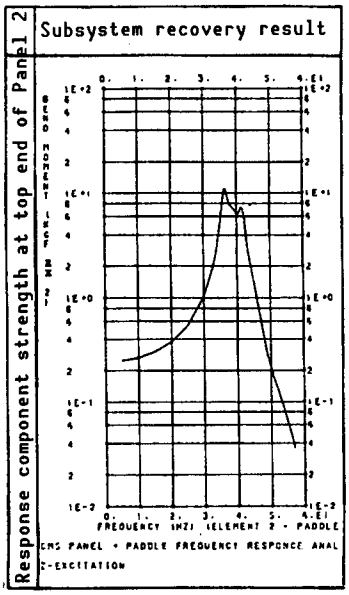

Figure 5. Response Component Strength

References

1. Manahu Kasai, "Subsystem Recovery by DMAP of Broad-Sense CMS of Constraint Mode Type," Collection of Papers for 5th MSC/NASTRAN Users Conference, October 1987, pp 3-9.

2. Akio Nagamatsu, "Mode Analysis," Baifu-kan, July 1985, p 190.

Vibration Test on H-II Rocket Model

43067502b Tokyo PROCEEDINGS OF THE JSASS/JASME STRUCTURES CONFERENCE in Japanese 14-16 Jul 88 pp 42-45

[Article by Masakatsu Minegishi, Masaaki Sano, Keiji Komatsu, and Motoyuki Morita, National Aerospace Laboratory; Yoshiki Morino, Kenji Tomioka, and Isao Ujino, National Space Development Agency of Japan; and Shigatoshi Aikawa, Kawasaki Heavy Industries: "Vibration Test on 1/5 Structure Model of H-II Rocket (continued)"]

[Text] 1. Introduction

This is continued from the previous report[1] on the vibration test we conducted, using a 1/5 structural model of the H-II rocket. This fiscal year, an ML (moving launcher) was designed. We manufactured a 1/5 ML model according to the design and tested it on a configuration relative to the vibration of ML.

2. Outline of ML

Figure 1 is a drawing of the ML. A solid propellant rocket booster (SRB) is fastened onto it at eight points. The core part is connected to the SRB and does not share a connecting part with the ML. The model was 1/5 the size of the real launcher and measured 4.4 m in width, 3.4 m in length, and 1.8 m in height. The 1/5 was used as the cross section of the truss member, and for the fixed launcher and other parts where flexural rigidity is predominant, priority was given to the simulation of flexural rigidity. Board rubber was used for the wheels of the real launcher.

3. Problem of Vibration of Rocket in ML Self-Supporting Form

Table 1 lists study subjects to which the dynamic characteristics of ML are related.

The previous test confirmed that the rocket-side model had been manufactured with fair precision as an analogous model and it can be expected to serve as basic data on the problem of vibration in the form of ML self-support if the ML is designed and manufactured with high precision as a model.

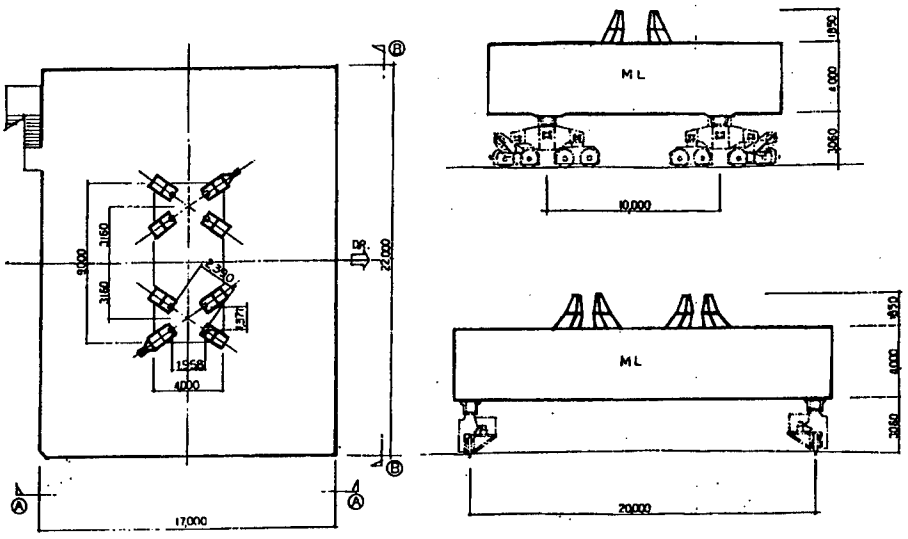

Figure 1. Three Views of ML (Real)

Table 1. Items of Analysis of Basic Design to Which Entire Machine Vibration Characteristics in ML Self-Support Are Related

Item of analysis	Study subject	Hardware affected	Vibration form related
Vibration load due to surface wind	• Collection of statistical data on launch point surface wind • Confirmation of dynamic response characteristics by model wind tunnel test • Reduction of acceleration in time of ML movement	• SRB chamber • SRB rear skirt/ fastening bolt • ML	• Entire machine pad self-support bending vibration pitch/yaw LOX: with/without Mainly primary mode
Earthquake load	• Collection of launch complex earthquake data • Earthquake response analysis	• Confirm that there are none	•Same as above
Vibration load at liftoff	• Setting of external force conditions (thrust buildup, ignition imbalance, transverse stress) • Response analysis (fastened → free)	• SRB/core separating bolt • Upper-stage structure (including satellite) transload	• Entire machine pad self-support liftoff Vertical, yaw and pitch LOX: full Primary-high order mode

4. Results of Test With 1/5 Model and Unit Test

Table 2 compares the test and computation results of the characteristic frequency of unit ML in Figure 2 [not reproduced] form. The ML unit weighed about 6 tons. In the test, free attenuation was measured by giving impact with a hammer or a log and then spectrum analysis was done. The computation was done using a real machine and conversion for a model was made by multiplying the computation results five-fold. The natural mode by computation is shown in Figure 3.

Table 2. Comparison of Characteristic Frequency of Single Unit ML Between Test Results and Computation Results

Mode form	Real machine computation	Conversion for model	Model test result
Yaw horizontal	3.13 Hz	15.7 Hz	13.5 Hz
Pitch horizontal	7.33	36.7	36.0
Vertical	10.32	51.6	46.8

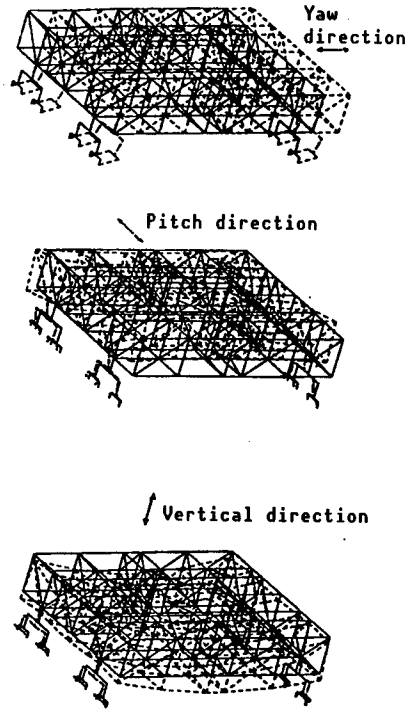

Figure 3. Natural Modes of Unit ML (From above, yaw horizontal, pitch horizontal, and vertical)

5. SRB-ML Compound Vibration Test Results

We then tested in the form of two SRB's mounted on an ML. Figure 4 shows the form of the test while Table 3 lists the results.

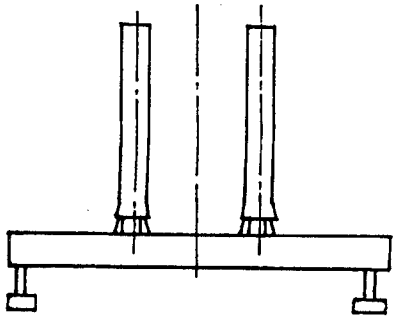

Figure 4. SRB-ML Test Form

Table 3. SRB-ML System Test Results
(SRB unit free-free binding primary and secondary characteristics frequencies were 42 Hz and 99 Hz and vertical primary and secondary were 135 Hz and 331 Hz.)

Excitation	Mode form	Characteristic frequency	Damping ratio
Yaw direction		29.3Hz	2.1%
		30.9	1.3
		72.3	0.8
		78.5	1.2
		81.6	1.3
Pitch direction		28.1	0.4
		32.0	1.1
		73.0	0.3
		76.6	1.0
		82.0	1.0
Vertical	In-phase	40.0	5.8
	Antiphase	63.0	2.2

6. Test on Form of Self-Support on ML With Full Fuel

Figure 5 [not reproduced] is a photograph of the entire model mounted on an ML. Entire-machine vibration characteristics were obtained by making excitation in vertical, pitch, and yaw directions. Figure 6 shows points of measurement of acceleration. Table 4 lists test results concerning characteristic frequency.

7. Conclusion

We manufactured a 1/5 structural model of ML and tested its vibration in the forms of ML, ML-SRB and on-ML self-support. As far as the test results and computation results on ML and ML-SRB are concerned, the precise FEM

modelling of ML seems possible. In the previous test, we used a truss structure as the pad corresponding to ML. There were no great differences, qualitative or quantitative, in test results between pad self-support in that test and ML self-support in this.

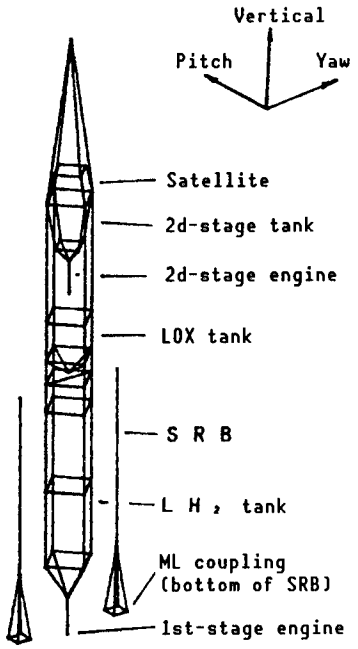

Figure 6. Acceleration Measurement Points

Table 4. Test Results on Self-Support on ML With Full Fuel

Direction of excitation	Natural frequency	Characteristics of natural mode
Vertical	17.3 Hz	Vertical primary, SRB reverse bending
	25.8	LH_2 tank hoop
	38.5	1st-stage engine bend
	40.2	Fairing
	42.7	2d-stage bend
	47.5	Front and back of core
Pitch	2.3	Primary bend
	11.3	
	19.7	
Yaw	4.0	
	12.0	Core bend primary
	13.8	Core-SRB
	21.3	
	40.1	

References

1. Masakatsu Minegishi, Motoyuki Morita, Masaaki Sano, Keiji Komatsu, Yoshiki Morino, Kenji Tomioka, and Isao Ujino, "Vibration Test on 1/5 Structural Model of H-II Rocket," 29th Lecture Meeting on Structural Strength, 1987, pp 50-53.

Heat-Resistant Structural Members of HOPE

43067502c Tokyo PROCEEDINGS OF THE JSASS/JASME STRUCTURES CONFERENCE in Japanese 14-16 Jul 88 pp 250-253

[Article by Tadashi Matsushita, Masataka Yamamoto, Tokio Onishi, Tomoyuki Kohayashi, and Motohiro Atsumio, National Space Development Agency of Japan: "Study of Heat-Resistant Structural Members of HOPE"]

[Text] 1. **Introduction**

The main structural members and the thermal protection system (TPS) of the H-II rocket-launched spaceplane (HOPE: H-II orbiting plane) must be light, strong, and heat resistant because they are exposed to severe thermal and mechanical environments in time of operation (launching, orbiting, atmosphere reentry, and landing).

Materials meeting these requirements will be selected for main structural members and the manufacturing technology will be established by conducting basic tests, component tests, and partial structure tests. In this report, we will discuss materials and the basic test to acquire the technology of molding polyimide CFRP, one of the most hopeful materials, and related design data. As for heat protecting materials, by 1986 we conducted the experimental manufacture and testing of ceramic tiles, carbon/carbon, and flexible heat insulators (conventional heat protecting materials). At present, we are conducting research on a thermal protection system including the experimental manufacture of Ti and Ni alloys and a high-performance carbon/carbon heat insulator (high-performance heat protecting material) and the attachment of these to the fuselage for the purpose of improved durability, reliability, and maintenance. Here, we shall mainly describe our conceptual design and partial experimental manufacture of heat protecting materials of Ti and Ni alloys. Figure 1 shows the conceptual diagram of the HOPE plane and an example of study of materials composing different parts of the plane.

2. Study of Main Structural Materials

2.1 Suggested Materials of Main Structural Materials

The chief basic performance required of the main structural members of HOPE are as follows:

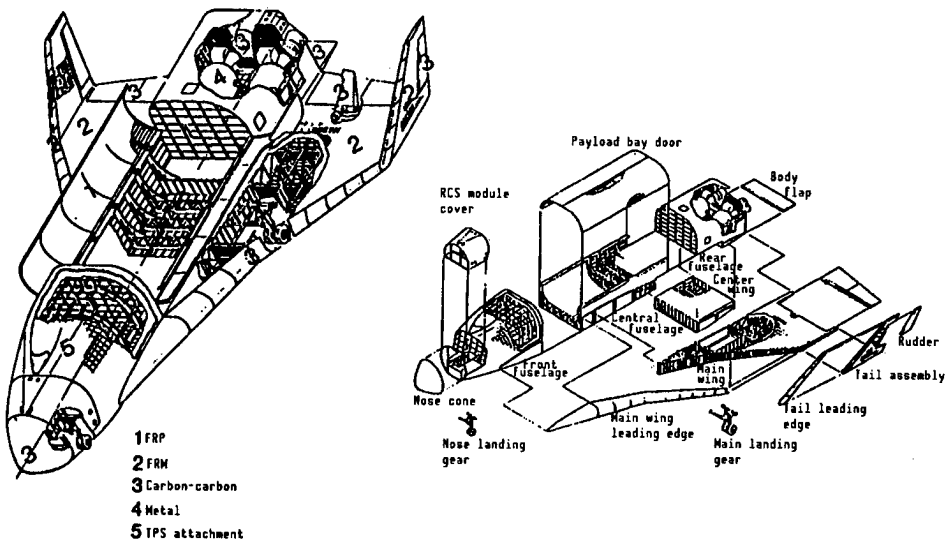

Figure 1. Conceptual Diagram of HOPE Plane and Example of Study of Materials Composing Different Parts of Plane

(1) Light weight: Weight reduction is possible by showing high specific strength and high specific rigidity under the given environmental conditions (temperature, load, etc.).

(2) Heat resistance: Weight reduction is possible by improving operating temperature and thereby alleviating the heat insulation requirement of TPS.

Besides these, moldability, development elements, cost, material availability, etc., must be considered as important matters in selecting materials.

To select materials meeting these requirements as main structural members, we studied the following candidate materials:

(1) Metallic materials: Al alloy and Ti alloy
(2) CFRP: Epoxy, bismaleimide and polyimide types
(3) FRM: SiC/Al and SiC/Ti
(4) Carbon/carbon: RCC (reinforced carbon/carbon)

Figure 2 shows an example of study for weight reduction by various main structural materials. Of these candidates, CFRP and Ti alloy excel in light weight and heat resistance as materials generally used for main structures. Of CFRP, the polyimide type is one of the strongest candidates for its high operating temperature (about 300°C) and is highly worth developing in the future. So, we are studying by a basic test its applicability to main structural members.

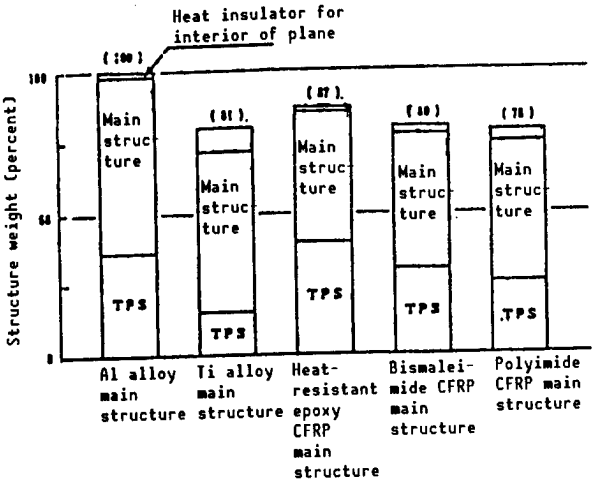

Figure 2. Example of Study of Weight Reduction by Different Main-Structure Materials

2.2 Basic Test

Table 1 shows the test items and test conditions selected to acquire design data for polyimide CFRP selected as a candidate material and the study items of molding technology. Table 2 shows an example of test data already acquired on matrix resin PMR-15.

3. Study of Heat Protecting Material

3.1 Outline of Reusable Heat Protecting Materials

HOPE will come under severe aerodynamic heating when it reenters the atmosphere. Figure 3 shows a computed example of radiation equilibrium temperature distribution. A heat protecting material to protect the airframe from this super-hot thermal environment must have the following capacities:

(1) Heat resistance and heat insulation
(2) Strength, rigidity, and shock resistance
(3) Reusability, reliability, maintainability, and serviceability
(4) Weight reduction

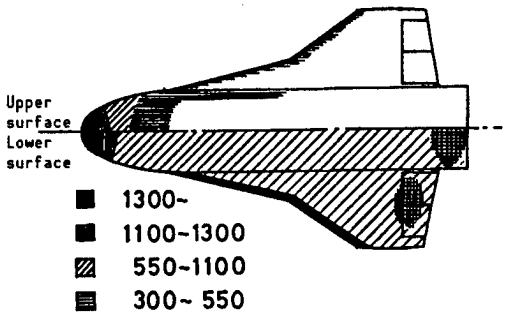

Figure 3. Example of Computation of Radiation Equilibrium Temperature Distribution on Surface of Plane (°C)

Table 1. Main Details of Test in Basic Test and Study Items

Details of test			
Test item			Test condition
Thermal and mechanical characteristic test			
Single layer board material characteristics	0°	Tension Compression	• Temperature condition: -100~300°C • Humidity condition: Dry, wet
	90°	Tension Compression	
	±45°	Tension	
	Interlayer shear		
	Bending test		
Laminated material characteristics	Nonporous board	Tension Compression	
	Porous board	Tension Compression	
	Damage allowability test (CAI)		
	Heat cycle test		
	Heat characteristic test		
	Heat radiation test		
	Edge delamination test		
	Fastener joint test		
	Fatigue test		
	Outgas		

Study items of molding technology	
• Prepreg characteristic	• Special machining
• Moldability	• Secondary materials and equipment
• Hardening conditions	• Small component experimental manufacture test
• Secondary hardening conditions	Etc.

Table 3 shows the outline of reusable heat protecting materials that we have been studying up to the present time. Of these, heat protecting materials on which study was started only recently have higher (2), (3), and (4) capacity requirements than the older types and these will be used for the main structures of the plane according to the different heat-resistant temperature zones.

3.2 Ti Alloy Heat Protecting Material

The Ti alloy heat protecting material is used in the temperature zone of 300~500°C. As indicated in Figure 4, it is composed of Ti alloy sheets and dimple cores and, for weight reduction, its different components use as

Table 2. Example of Basic Test Data on Polyimide CFRP

Fiber/ resin	Temperature and humidity conditions	Mechanical characteristics* 0°direction tensile strength (kg/mm^2)	0° direction compressive strength (kg/mm^2)	0° direction tensile elastic modulus (kg/mm^2)	Inter-layer
Material A /RMR-15	23°C Dry	195	157	13,000	11.5
Material B /RMR-15	23°C Dry	230	142	17,500	10.5
	300°C Dry	202	87	--	--

Note: *: The mechanical characteristics were computed, using the nominal board thickness when 60 percent was assumed as Vf, fiber content rate.

Table 3. Outline of Heat Protecting Materials for HOPE

Item / Name of IPS	Structural drawing	Temperature used °C	Specific weight kg/m³	Heat conductivity W/m°C	Coefficient of thermal expansion 1/°C	Tensile strength kgf/mm²	Present status of study	Development element
Ceramic tile		-100~1250	1.0 (550 °C) 2.0 (1250 °C)	0.11 (550 °C) 0.23 (1250 °C)	3.2×10⁻⁶	0.047	1st stage was completed in FY 1982-1985 (large coefficient of thermal expansion)	Method of attachment (adhesive) Maintainability Reliability
Carbon/carbon (RCC:Reinforced Carbon Carbon)	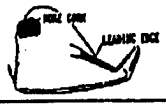	-100~1500 ~1700	15.0	10.8	-0.3×10⁻⁶	16.6	1st stage was completed in FY 1982-1985	Manufacturing equipment for large components is necessary Improved heat resistance
Flexible heat insulator		For medium temperature -100~650	3.5 (result)	0.14 (650 °C)	----	0.009	1st stage was completed in FY 1982-1985	Method of attachment (adhesive) Maintainability Reliability
Ti alloy heat protecting material	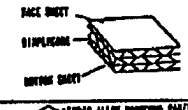	-100~550	3.7 (result) 2.5 (560 °C) (target	0.13 (550 °C)	TBD	12.5 (400 °C)	FY 86: preliminary experimental manufacture performance test	Superplastic molding, curved panel molding, coating, manufacturing, testing
Ni alloy heat protecting material		-100~1100	5.5 (550 °C) (result 9.4 (1100 °C) (target	TBD	TBD	Bend 5.6 (1000 °C)	FY 86: preliminary experimental manufacture performance test	Molding, curved panel molding, coating, manufacturing, testing
Carbon/carbon (ACC:Advanced Carbon Carbon) heat protecting material	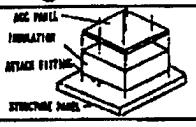	-100~1300 ~1700	10.0 (1100 °C) (result 12.8 (1300 °C) (target	TBD	TBD	TBD	FY 86: investigation	Baking, weight reduction, high strength, improved heat resistance, coating, manufacturing, testing

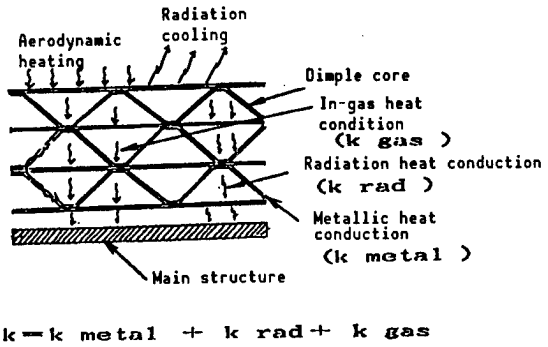

Figure 4. Heat Insulation Structural Drawing of Titanium Alloy Heat Protecting Material

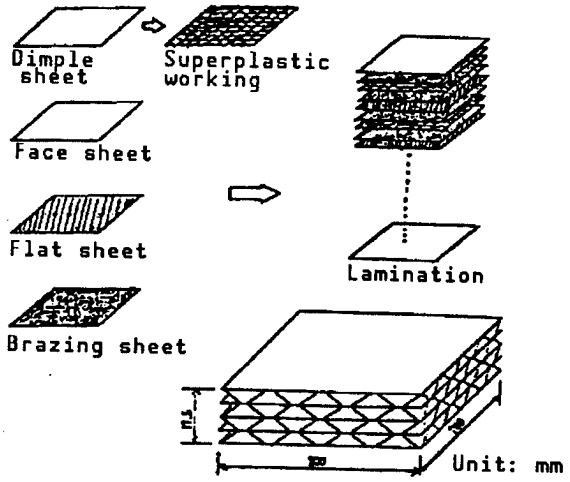

Outside dimension (mm)		200 x 200 x 17.3
Dimple dimension	Height (mm)	4.3
	Pitch (mm)	Approximately 19
Board thickness (μm)	Face sheet	90
	Flat sheet	50
	Dimple sheet	80
Material		Ti•6Al•4V, etc.
Specific weight (kg/m^2)		3.9

Figure 5. Manufacturing Process of Titanium Alloy Heat Protecting Material and Prototype

thin sheets as possible. Heat transfer in this material is by metallic heat conduction, in-gas heat conduction, and interlayer radiation.

The important technical tasks in the experimental manufacture of this heat protecting material concerned sheet rolling capacity, the molding of dimple sheets by superplastic molding, and the technique of laminate joining. Figure 5 shows the method of molding a dimple sheet by superplastic working and joining it with a flat sheet by brazing. Using the prototype, we confirmed strength and also confirmed strength and heat resistance by a heat resistance/heat insulation test.

3.3 Ni Alloy Heat Protecting Material

The Ni alloy heat protecting material is composed of an outer layer (550°C~1,100°C) using INCONEL 617 or some other Ni-based alloy honeycomb panel, an inner layer (~550°C) using Ti alloy honeycomb or dimple sheet and an intermediate layer filled with heat insulating material (Figure 6). It functions as a heat protecting material by radiation cooling from the surface panel and the heat insulating action of the heat insulating material used for the interior. The outer layer panel made of a heat-resistant superalloy must have high strength and high rigidity in order to withstand aerodynamic load, etc.

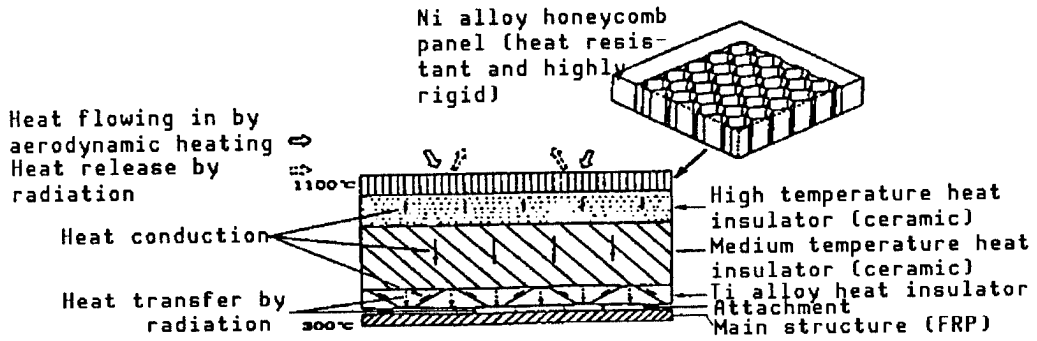

Figure 6. Conceptual Diagram of Ni Alloy Heat Protecting Material

Heat-resistant inorganic fibers which are light weight and excellent for heat insulation and heat resistance are promising as intermediate layer heat insulators and, of these, we are now studying ceramic heat insulators, such as silica fibers heat resistant up to about 1,000°C and aluminosilicate fibers heat resistant up to 1,260°C. Figure 7 shows an example of our recent Ni alloy honeycomb panel prototypes for the outer layer surface. Structurally, it is made by arranging a honeycomb core between the upper and lower face sheets and joining the whole. The element technology necessary to manufacture this honeycomb panel comprises the manufacture of the honeycomb core, the working of the face sheets and the brazing assembly of the whole.

We conducted preliminary tests, such as heat insulation, heat resistance, and load tests, using our recently made honeycomb panel prototypes, and thereby acquired basic temperature distribution data and confirmed their heat insulating capacities.

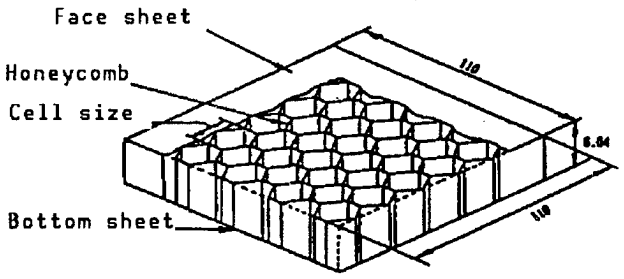

Outside dimension (mm)		110 x 110 x 6.04
Board thickness (μm)	Face sheet	100
	Bottom sheet	100
	Honeycomb	100
HOneycomb size (mm)	Core height	5.84
	Cell size	4.16
Material		INCO 600

Figure 7. Example of Ni Alloy Honeycomb Panel Prototype

4. Conclusion

We will continue our tests on heat-resistant FRP to be used for main structural members and acquire material data on polyimide CFRP.

Regarding heat protecting materials, we will conduct research and development to make Ti alloy and Ni alloy heat protecting materials practical and to develop a carbon/carbon heat protecting material.

References

1. Matsushita, Yamamoto, Onishi, and Kobayashi, 19th Technical Results Intracompany Announcement Meeting, 1987, p 54.

2. Yamamoto, Onishi, and Kobayashi, 31st Space Science Joint Lecture Meeting, 1987, pp 376, 378.

3. Iida and Nakamura, 30th Space Science Joint Lecture Meeting, 1986, pp 30, 31.

4. Matsushita, Yamamoto, Onishi, Kobayashi, and Atsumi, 4th Space Station Lecture Meeting, 1988, pp 143, 145, 147.

Structural Design, Static Load Test on ERS-1

43067502d Tokyo PROCEEDINGS OF THE JSASS/JASME STRUCTURES CONFERENCE in Japanese 14-16 Jul 88 pp 258-261

[Article by Yoshio Masuda and Susumu Toda, National Space Development Agency of Japan, and Toshio Inoue and Akira Iwamura, Mitsubishi Electric Corp.: "Structural Design and Static Load Test on ERS-1, Earth Resources Satellite No 1"]

[Text] **1. Introduction**

Earth Resources Satellite No 1 (ERS-1) is a large observation satellite with two large expandable structures and a gross load of 1.4 tons (Figure 1). Its satellite structure differs from the conventional satellite in such respects as shape, structural format and the formula of connection to the rocket. This article reports the outline of the structural design mainly with regard to the circumstances that led to its development and the results of the static load test.

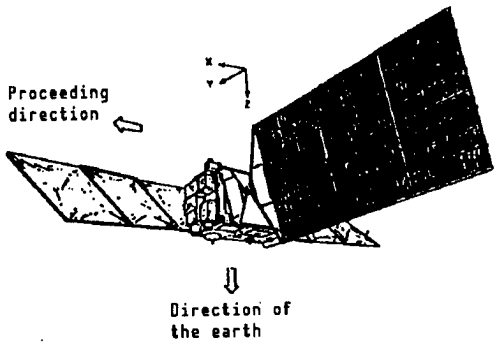

Figure 1. Shape of Satellite (on orbit)

2. Outline of Structural Design

2.1 Design Conditions

The main design conditions for the satellite structure are shown in Table 1. The point in designing it consists in achieving a shape to be able to hold its two large expandable structures in the allowable envelope besides securing area for mounting various equipment and necessary heat release area

Table 1. Main Design Conditions

Design load	Limit load: 2σ ceiling value of H-1 rocket flight load Ultimate load: limit load x 1.5		
Dimension limit	Can be held in allowable envelope of H-1 rocket fairing		
Characteristic frequency	35 Hz or more in axial direction and 15 Hz or more in axis-of-abscissas direction under boundary conditions of complete fixation of satellite's separating face.		
Gross weight	Less than 1,400 kg:	Mission apparatus:	533 kg
		Bus apparatus :	751 kg
		Fuel :	115 kg
Field of view requirements	Field of view requirements of different sensors and antennas must be satisfied		

and assuring necessary rigidity and strength in accordance with the result increase of body height.

2.2 Preceding Research Models

In developing this satellite structure, an actual size model prototype was manufactured during the development research that preceded the basic design. The precedent research model was developed, using 1) the modularizing of satellite structure; 2) divisional body structuring (dividing the body into two parts); and 3) the use of CFRP for the entire main structure frame as basic design policies. The modularizing consists of mounting different equipment in the form of thermally and structurally independent modules. It has the advantage of increasing development efficiency by not only enabling the different parts of the structure to be developed separately but also enabling the different tests to be conducted separately and in parallel, module by module. The policy of divisional structuring is due to the fact that testing the structure separately as two divided parts was initially planned because structural testing was ERS-1 as a whole was impossible with the testing equipment that was then available. The policy to use CFRP for the entire structural frame was decided to prevent thermal stress in the connections between materials having different thermal deformation and different coefficients of thermal expansion. This is especially necessary because module structures involve the possibility of undergoing great temperature changes. Figure 2 shows the outline of the precedent research model developed under the above basic policies. The body structure is composed of aluminum honeycomb boxes, panel-shaped modules, and a trussed main structure frame made entirely of CFRP to support these and capable of being divided into two parts: top and bottom.

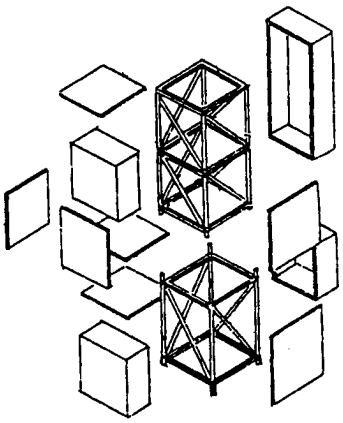

Figure 2. Precedent Research Model

2.3 Basic Design Model

1) Changes from precedent research model

Though the mission weight increased after the development of the precedent research model, it was necessary to further reduce the weight of the body because the gross load of the satellite had to be smaller than the launching capacity of the rocket. Therefore, there was no choice but to give up the module structure, which excelled in development efficiency but was inadequate in structural efficiency and weight reduction was difficult. Also, the division requirement was abandoned because testing ERS-1 as a whole had become possible through the improvement of satellite system test equipment. Thus, we decided on an integral body structure after all. This enabled the CFRP main structure frame to be controlled at the temperature level of on-board equipment and the aforementioned heat problem was thus solved. Therefore, we decided to improve strength and reliability by using metals for joints where the flow of load was complicated.

2) Outline of body structure

Figure 3 shows the outline of the satellite body structure in the basic design. The satellite body is a semimonocoque structure where boxes composed of honeycomb panels with aluminum and CFRP facings are reinforced with CFRP frames. The honeycomb panels not only carry equipment but also serve as structural members. The CFRP frames and structural members to lead the weight on the panels to the four points of connection with the rocket. They form an important load route and, at the same time, improve the rigidity of the satellite as a whole. Moreover, the main frames connected to the panels function as girders to reinforce strength and rigidity in the panel out-of-plane direction (Figure 3). All CFRP frames and metallic joints were connected by adhesion to reduce weight. Double-scuff joints with high strength and reliability are used for the structure of adhered parts. The body weight is 175 kg and the body weight/total weight ratio is 12.5 percent; thus the body of this satellite is much lighter than those of similar satellites.

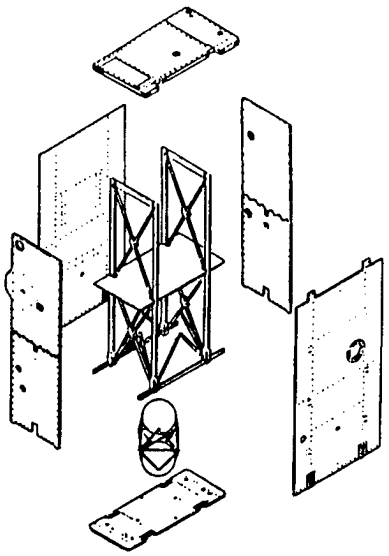

Figure 3. Basic Design Model (SLM)

3) Structure analysis

Static analysis: Static analysis by the finite element method was conducted to predict strength against the static load received by the satellite from the rocket during launch flight. Figure 4 shows the outline of the static analysis model while Figures 5 and 6 each show an example of analysis results.

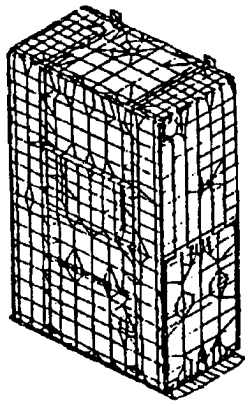

Figure 4. Static Analysis Model

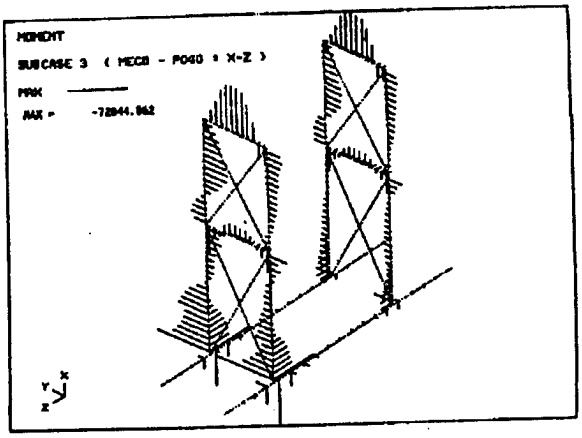

Figure 5. Static Analysis Results (bending moment)

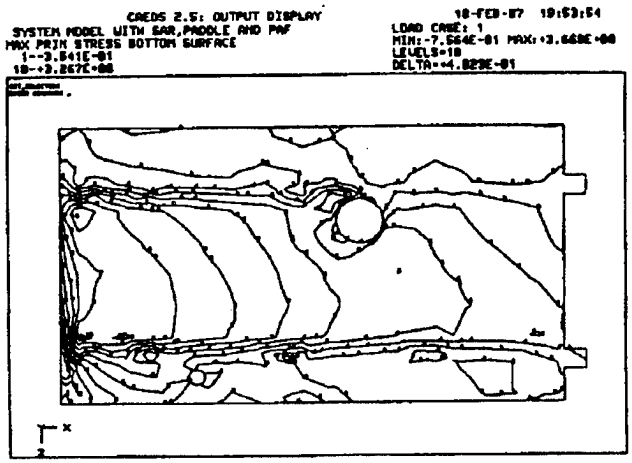

Figure 6. Static Analysis Results (panel stress distribution)

Dynamic analysis: Rigidity and strength against vibrational load were predicted by conducting specific dynamic analysis and frequency response analysis, using a dynamic analysis model. Furthermore, the vibrational environments of on-board equipment were presumed.

4) Member test

Strength at the level of structural elements was confirmed by prototype tests using partial structural models for the different parts of the body. A strength test using about 120 specimens was conducted in 9 areas.

3. Static Load Test

3.1 Outline

A static load test using a prototype model (SLM) was conducted to confirm that the body structure could withstand the aforementioned static load. Table 2 shows the load conditions of the static load test.

Table 2. Quasistatic Load Conditions (Ultimate level)

	Body axis (X-axis direction	Axis of abscissas Y-axis Z-axis directions
LIFT-OFF	3.6 G	3.0 G
MECO-POGO	12.0 G	1.5 G

3.2 Test Configuration

Figure 7 shows the test configuration. Load corresponding to the inertial force caused by the prescribed acceleration was charged to the different parts of the satellite by means of a hydraulic jack. In the static load test, efforts were made to reproduce a state close to an acceleration load by charging load at 70 points on the body, using 20 hydraulic jacks.

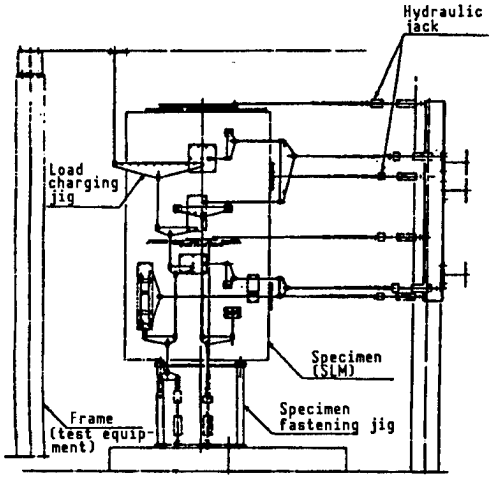

Figure 7. Static Load Test Configuration

Furthermore, our analysis confirmed that the load condition in the different parts of the body attained by test loading almost accurately matched the condition attained by acceleration loading.

3.3 Test Results

We measured strain at 487 points in the different parts of the body and displacement at 99 points by applying a prescribed load.

The normal external appearance, the good linearity in the load-stress/displacement chart for each point of measurement, the absence of permanent deformation and the failure of stress to exceed the yield point of the material. From these, we confirmed that the body satisfied its strength requirement.

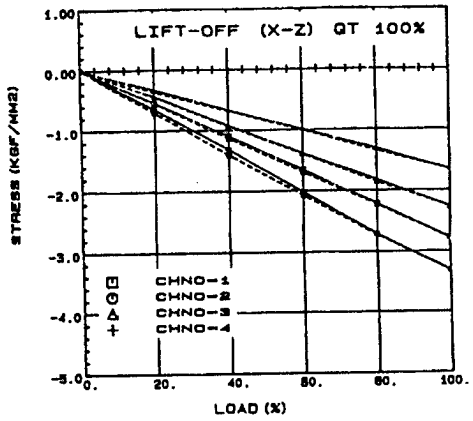

Figure 8. Test Results (Frame section, load-stress chart)

Figure 8 shows an example of load-stress charts.

The test results and the analyzed values agreed well, indicating that our structural design was appropriate.

4. Summary

(1) The body of ERS-1 was first planned to use a module structure but, due to the requirement of weight reduction resulting from the subsequent increase of mission weight and due also to the realization of large test equipment, the basic policy of design was changed and the semimonocoque integral structure composed of CFRP frames and honeycomb panels became a reality.

(2) In development, we predicted performance by the numerical analysis of the body structure and a member test and confirmed by a static load test using a body model (SLM) that the body satisfied its strength requirement.

References

1. Masuda, et al., "Structural Design of ERS-1 and Member Test," 3d Lecture Meeting of Space Structure Research Association.

Self-Excited Vibration Suppression for Liquid Fuel Rockets

43067502e Tokyo PROCEEDINGS OF THE JSASS/JASME STRUCTURES CONFERENCE in Japanese 14-16 Jul 88 pp 282-285

[Article by Shigeo Kobayashi, Tokyo Metropolitan Institute of Technology; Hiroshi Kojima, Mitsubishi Electric Corp.; and Masayuki Niitsu, Graduate School, Tokyo University: "Basic Study Concerning Self-Excited Vibration Suppression for Liquid Fuel Rockets"]

[Text] **1. Introduction**

POGO is the self-excited vibration of a liquid fuel rocket caused by the combination of a vibration mode in the vertical direction of a structure and the variation of thrust. When POGO occurs, vibration acceleration in several G's is exerted on the payload and this becomes the maximum load. In designing a liquid fuel rocket, therefore, it is important to suppress this.

The pump inlet accumulator is used to suppress POGO and, in fact, it is provided in the first stages of H-I and N-II but it does not fully function yet.

In this study, we conducted basic model experimentation and theoretical analysis to check for the possibility of POGO suppression by the pump inlet accumulator.

2. Experimentation

For the experiment, we used a simplified model composed of a fuel tank, a feed pipe, an accumulator and a discharge pipe. We put water in this model and fastened it on an electromagnetic platform. As force corresponding to thrust variation, we measured the flow in the discharge pipe and applied force proportional to this to the exciter. Figure 1 shows the outline of the experimental equipment used.

The displacement of the fluid in the discharge pipe was measured, using a mechanism illustrated in Figure 2. the displacement, Ud, of the target, painted black and white, which moved with the fluid was measured with an electronic optical displacement gauge and the flow (flow velocity), dU_d/dt,

was obtained by passing this through the differentiator. The exciter voltage is given by

$$E = \alpha \, (dU_d/dt)$$

α is a feedback gain.

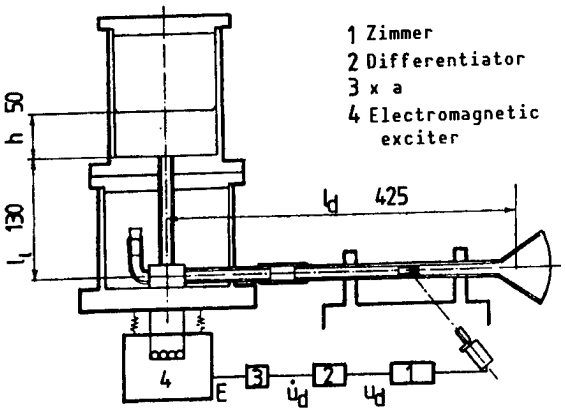

Figure 1. Experimental Equipment

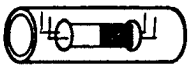

Figure 2. Flow Velocity Measuring Mechanism

If the feedback gain is gradually increased, self-excited vibration starts soon. α_{cr} is used for α of the time when α is gradually decreased and vibration stops after once causing self-excited vibration.

α_{cr} is measured by variously changing the volume of air in the accumulator. Similar tests were made by changing l_a, length of the pipe connecting the corresponding position of the pump and the accumulator.

3. Theoretical Analysis

3.1 Formulation of Accumulator Section

Pressure increases occur for the following four reasons (Figure 3):

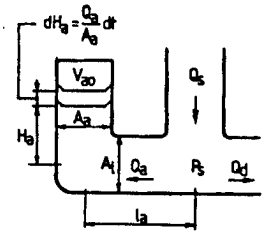

Figure 3. Accumulator Section

(1) Pressure increase of upper gas

$$dP_a = K_a Q_a dt \qquad K_a = \gamma \frac{P_{a0}}{V_{a0}} \qquad \gamma : \text{ratio of specific heat} \tag{1}$$

(2) Pressure increase on accumulator bottom reference plane when airframe steady acceleration of downward ng (in this test, n = 1) acts on liquid

$$dP_a = dH_a \times \rho n g = \frac{Q_a}{A_a} \rho n g \, dt \tag{2}$$

(3) Pressure increase on accumulator bottom reference plane due to inertial force of liquid caused by increase of acceleration of liquid

$$dP_a = \rho H_a d\left[\frac{d}{dt}\left(\frac{Q_a}{A_a}\right)\right] = L_{Ha} d\left(\frac{dQ_a}{dt}\right) \qquad L_{Ha} = \frac{\rho H_a}{A_a} \tag{3}$$

(4) Pressure increase due to acceleration of liquid (d^2U_1/dt^2) attending vertical motion of accumulator container

$$dP_a = \rho H_a d\left(\frac{d^2 U_1}{dt^2}\right) \tag{4}$$

From (1), (2), (3), and (4),

$$P_a = \rho H_a \frac{d^2 U_1}{dt^2} + L_{Ha} \frac{dQ_a}{dt} + \frac{1}{C_a} \int Q_a dt \quad , \quad \frac{1}{C_a} = \frac{\rho ng}{A_a} + K_a$$

Furthermore, if the length of the pipe connecting the accumulator and the inlet of the pump is taken into consideration and the resistance and inertial force in this section is added,

$$P_s = R_a Q_a + L_a \frac{dQ_a}{dt} + \rho H_a \frac{d^2 U_1}{dt^2} + \frac{1}{C_a} \int Q_a dt \quad , \quad L_a = \frac{\rho l_a}{A_a} + L_{Ha} \tag{5}$$

P_s is the pressure at the equivalent position of the pump inlet.

3.2 Transfer Function of Feed System

If the transfer function of the feed system is obtained with consideration for the accumulator section formulated above, it is as follows, provided that $A_d = A_1 = A_a = A$ and $\rho h/A = L_h$.

$$\frac{dU_d}{dt} = \frac{G_1}{G_2} \frac{dU_1}{dt} \equiv \beta e^{i\theta} \frac{dU_1}{dt} \tag{6}$$

$$\begin{aligned} G_1 &= [R_1/C_a - \omega^2 (L_{Ha} R_1 + L_h R_a + L_1 R_a + L_a R_1)] + i[\omega \{(L_h + L_1)/C_a + R_a R_1\} - \omega^3 (L_1 L_{Ha} + L_a L_h + L_a L_1)] \\ G_2 &= [(R_1 + R_d)/C_a - \omega^2 \{(L_1 (R_a + R_d) + L_a (R_1 + R_d) + L_d (R_1 + R_a)\}] \\ &\quad + i[\omega \{(L_1 + L_d)/C_a + R_1 R_a + R_a R_d + R_d R_1\}] - \omega^3 (L_1 L_a + L_a L_d + L_d L_1)] \end{aligned} \tag{7}$$

3.3 Equation for Body

If M is the weight of the body, K is the spring constant of the exciter and U_1 is displacement in the vertical direction, the equation of motion is

$$M\frac{d^2U_1}{dt^2}+\frac{\Gamma^2}{Z}e^{-i\psi}\frac{dU_1}{dt}+KU_1=\frac{\Gamma}{Z}e^{-i\psi}\alpha\frac{dU_d}{dt} \qquad Z=\sqrt{R^2+(\omega L)^2},\quad \psi=\tan^{-1}(\omega L/R) \tag{8}$$

Here, Γ is the magnetic field intensity and R and L are, respectively, resistance of the coil in the exciter and its self-inductance. The second term on the left side represents the damping force due to the fact that counter electromotive force is caused by the motion of the coil. When assuming a real machine, the following is used as the equation of motion.

$$M_1\left(\frac{d^2U_1}{dt^2}+\eta\frac{\omega_1^2}{\omega}\frac{dU_1}{dt}+\omega_1^2U_1\right)=\alpha\frac{dU_d}{dt} \tag{9}$$

3.4 Frequency Equation and Critical Gain

Assuming the harmonic vibration of angular frequency ω,

$$U_1=\frac{1}{i\omega}\frac{dU_1}{dt} \qquad \frac{d^2U_1}{dt^2}=i\omega\frac{dU_1}{dt} \tag{10}$$

If Equations (6) and (10) are substituted for Equation (7) and the imaginary parts of real numbers on the right and left sides are made equivalent,

$$\omega M\left(1-\frac{\omega_1^2}{\omega^2}\right)-\sin\psi=-\frac{\Gamma}{Z}\alpha\beta\sin(\psi-\phi) \tag{10}$$

$$\frac{\Gamma^2}{Z}\cos\psi=\frac{\Gamma}{Z}\alpha\beta\cos(\psi-\phi) \tag{11}$$

From Equations (10) and (11),

$$\omega M\left(1-\frac{\omega_1^2}{\omega^2}\right)=\frac{\Gamma^2}{Z}\left[\sin\psi-\cos\psi\tan(\psi-\phi)\right] \tag{12}$$

as a frequency equation.

Once the frequency is decided, α_{cr} can be obtained by the following:

$$\alpha_{cr}=\frac{\Gamma\cos\psi}{\beta\cos(\psi-\phi)} \tag{13}$$

If Equation (9) is used as an equation of motion, the frequency equation and α_{cr} are as follows:

$$\frac{\omega^2}{\omega_1^2}-1=\eta\tan\phi \qquad \alpha_{cr}=\frac{M_1\eta\omega_1}{\omega\beta\cos\phi} \tag{15}$$

4. Results and Discussion

Figures 4 and 5 show the experimental and computed values of frequencies of self-excited vibrations and Figures 6 and 7 show the experimental values and computation results of α_{cr}. In the experiment, self-excited vibration occurring at the characteristic frequency of the structural system and self-excited vibration occurring at the characteristic frequency of the feed system were observed. In Figures 6 and 7, self-excited vibration occurring at the characteristic frequency of the feed system corresponds to the line of stability limit on the lower side. In other words, the self-excited vibration greatly decreases the stability area. This has something to do with the fact that the force corresponding to structural damping abnormally increased due to the characteristics of the exciter. To see how η, coefficient of structural damping, affected α_{cr}, we computed using η as a parameter. The results were as indicated in Figures 8 and 9. The stability limit lowered as η increased. At η = 2 (approximately) hardly any effect as a suppressor can be expected of it. In the real rocket η = 0.01 (approximately) and, at this time, self-excited vibration occurring at the characteristic frequency of the feed system is all but negligible.

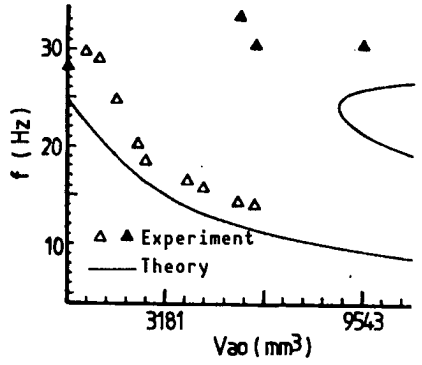

Figure 4. Frequency (1_a = 30)

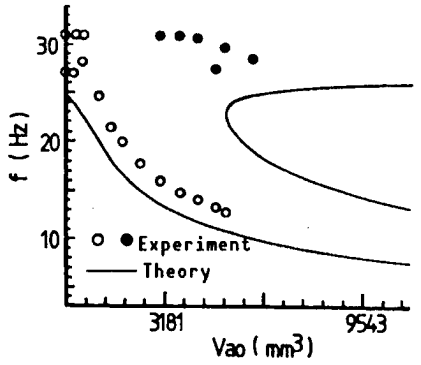

Figure 5. Frequency (1_a = 94)

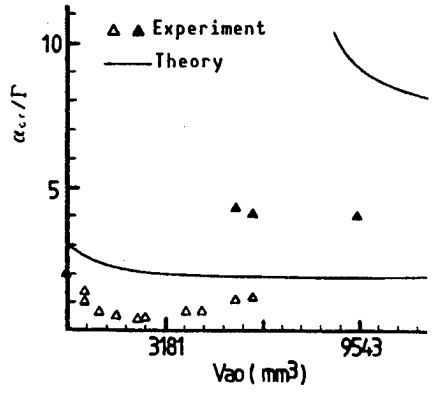

Figure 6. Critical Gain (1_a = 30)

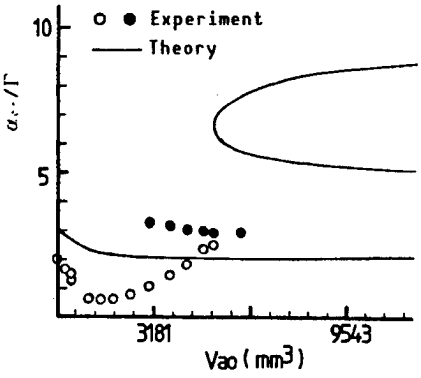

Figure 7. Critical Gain (1_a = 94)

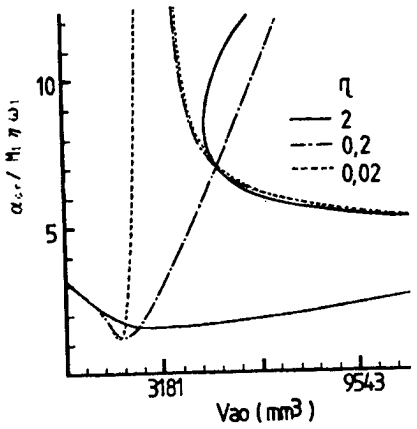

Figure 8. Critical Gain (parameter η)

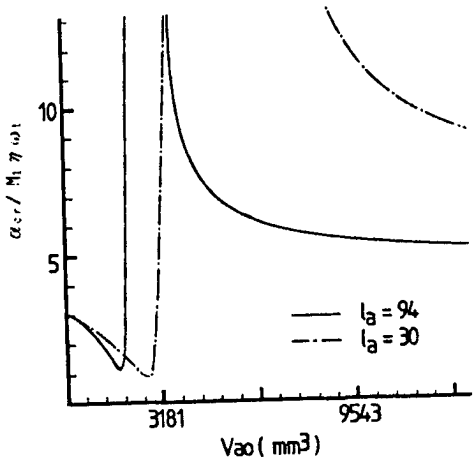

Figure 9. Critical Gain (η = 0.01)

We have learned that, as in Figures 6, 7, and 9, l_a, length of the pipe connecting the equivalent position of the pump inlet and the accumulator, greatly affects the stability area. The shorter l_a is, the larger is the stability area of the time when the amount of air in the accumulator is large.

References

1. S. Kobayashi and H. Kojima, "Self-Excited Vertical Vibration (POGO) of Liquid Fuel Rocket," JOURNAL OF AEROSPACE SOCIETY OF JAPAN, Vol 39, 1982, pp 354-363.

2. Ibid., "A Study Concerning Mechanism of Development of MECO POGO," Vol 33, 1985, pp 238-245.

Load Conditions of Large H-II Satellites

43067502f Tokyo PROCEEDINGS OF THE JSASS/JASME STRUCTURES CONFERENCE in Japanese 14-16 Jul 88 pp 286-289

[Article by Yoshiki Morino, National Space Development Agency of Japan, and Tokio Nara, Mitsubishi Heavy Industries: "On Load Conditions of Large Satellites To Be Carried by H-II Rockets"]

[Text] **1. Introduction**

The H-II rocket, a rocket capable of launching a large geostationary satellite of the 2-ton class, is being developed with the target to launch the first experimental machine in the winter of 1991. It is much larger than the H-I rocket, the largest rocket that has ever been developed in Japan. Moreover, the development of its large first-stage liquid propellant rocket supplemented with large solid propellant rockets, in view of its composition, involves many technical elements that cannot be regarded simply as an extension of the development of past rockets. As for the load conditions for satellites to be carried by H-II rockets, the design load must be set largely by analysis when no flight results whatsoever are available and it is necessary to allow some margin for unknown elements. It is also necessary to consider weight impact on the satellite and an excessive load requirement must be avoided as much as possible. Under these circumstances, we will, in this report, state our basic concept of the load conditions set at this point.

2. Composition and Flight Conditions of H-II Rocket

The general view of the H-II rocket is shown in Figure 1. It is a two-stage rocket and two solid propellant rockets (SRB) are provided on both sides of its first stage. The total weight of about 260 tons at the time of launch is supported by the lower parts of the SRBs contacting the launcher before launching. The SRBs and the first-stage rocket are connected at two places, one above and one below, but it is only the front connection that transmits force in the body-axis direction and the rear connection only transmits load in the lateral direction. The flight sequence after launching is indicated in Figure 2. At launch, the first-stage engine and the SRBs ignite and transient vibration develops with pad breakoff subsequent to the ignition. The acceleration to the satellite at this time is considered to be an important load criterion for the satellite. The rocket then climbs through

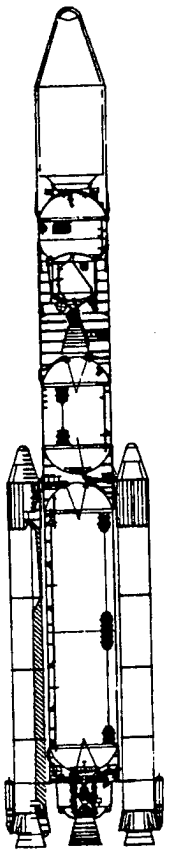

Figure 1. H-II Rocket

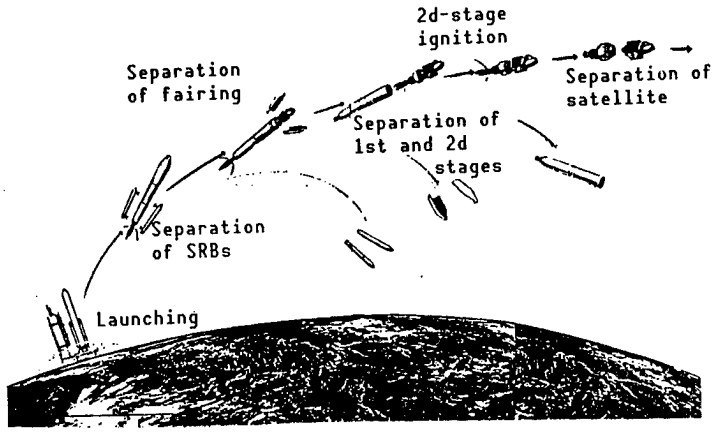

Figure 2. Flight Sequence of H-II Rocket

the atmosphere and the product of its dynamic pressure and its angle of elevation becomes maximal at an altitude of approximately 10 km. The conditions under which a gust works at this point is an important load criterion for the rocket body. The load of the satellite, which is protected in the fairing, does not constitute a criterion but the clearance between the fairing and the satellite is an important criterion point. The SRBs complete their combustion about 95 seconds after launching and are separated from the core body in about 100 seconds. Transient vibration in the core body and the satellite develops at the time of SRB separation but we do not regard it as a design load criterion to either the core body or the satellite. POGO vibration, which is the combination of propulsive system fluid vibration and body axial vibration, may possibly develop during the period from launching until the first-stage engine completes its combustion in about 315 seconds. The load setting for this will be described later. The greatest static acceleration in flight (about 4 G) develops at the end of combustion of the first stage. Transient vibration develops each at the end of the first-stage combustion, at the separation of the first and second stages and at the second-stage ignition but we regard none of these as constituting design criteria. POGO vibration may develop during the combustion of the second-stage engine, as in the case of the first stage, but from the flight results of the H-I rockets, we deem

that it is not necessary to make load setting for the second-stage POGO. Shock due to the action of ammunition develops at the time of satellite separation after the completion of second-stage combustion. This makes a shock environment condition of the satellite, rather than a load condition criterion.

3. Load Launch Time

Before the ignition of its engine, the H-II rocket has the rear ends of its SRBs constrained with separation nuts and bolts each at four points on the mobile launcher (ML). First, the liquid engine (LE-7) is ignited and, after confirming the rise of its combustion pressure, the constraint by the separation nuts and bolts is released and the SRBs are ignited at the same time. The thrust of LE-7 at launch is about 93 tons. This is smaller, compared with the SRBs, and the rise of this thrust takes several seconds; therefore, its contribution to the total vibration as an exciting external force is small. The thrust of the SRBs to be ignited later is about 150 tons each and their rise time is only 0.1~0.2 second and their effect in the vibration of the entire rocket including the satellite is, indeed, great. Also, if there is a difference in the igniting time of the right and left SRBs, the bending vibration of the entire rocket may result. In the response analysis of the launch time, a solution satisfying the boundary condition change at the lower end of the rocket is obtained by the mode method using natural vibration modes in the state of the rocket being fastened to the mobile launcher and the state of the rocket being in the free-free condition. The main analytic input conditions of response analysis are shown in Table 1. We are planning to acquire SRB characteristics to provide main external force conditions of the launch time from the four ground combustion tests scheduled before launching the real rocket. The values in this table show estimates plus characteristic value dispersions assumed for each serial rocket and margins for coping with future replanning. Figure 3 shows the launch time response acceleration at the center of gravity of the satellite. At the time of thrust rise of SRBs, the rear end of the SRB is pressed against the fixed launcher by the dilation of the solid propellant rocket motor. Therefore, the vibration characteristic of the mobile launcher seriously affects the satellite's load at launch. As for the characteristics of the mobile launcher, we are planning to confirm them with respect to the 1/5 vibration model and the actual mobile launcher. Regarding load in the vertical direction, 3.2 G is set for ETS-VI, allowing about 10 percent for the analytic error. In the lateral direction, load based only on the ignition imbalance of the right and left SRBs is about 1.0 G but 2.0 G is used for the safe side, considering unpredictable cases, such as the rocket leaving the pad in a state of bend by surface wind and in view of the results with large foreign rockets. It must be remembered that this condition is for the center of gravity of the satellite and can serve as a design condition for the main body structure of the satellite but acceleration several times as large develops for accessory satellite structures with low natural vibration.

Table 1. Launch-time Response Analysis Input Data

Item	Set value
SRB thrust	180 tons
SRB thrust rise time	100 msec
SRB ignition time difference	70 msec

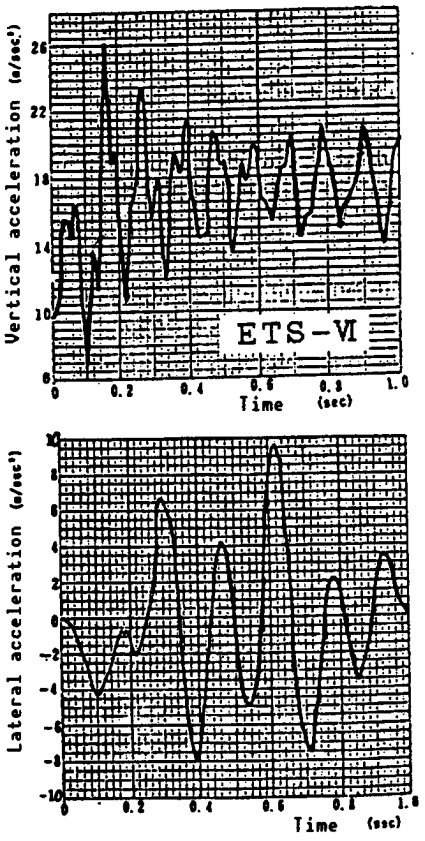

Figure 3. Vibration Response at Center of Gravity of Satellite at Time of Launching

4. POGO-time Load

Measures based on stability analysis have been initiated since the design period to prevent the occurrence of POGO vibration in the H-II rocket and we are planning to confirm the suitability and effectiveness of these measures in each phase of the development test.[7] However, the occurrence of POGO vibration in foreign rockets indicates that POGO prevention according to design has seldom succeeded and that the forms of POGO that occur are diverse and include many cases of POGO occurring in forms that had first been unpredictable. The development of the large first-stage liquid propellant rocket is a new experience for Japan and it is considered too risky to proceed with the design on the premise that we can certainly prevent POGO. So, in the initial test phase of or development of the H-II

rocket, we are now designing under a plan to set a load anticipating some POGO while also considering the impact of the satellite on the load. According to the POGO stability analysis conducted to date, in the worst case that can be predicted at this point the low-order vertical vibration mode may be unstable for 1 to 30 Hz if no POGO preventing equipment is available. We are designing to stabilize these unstable modes by using POGO preventing equipment but use 15-30 Hz as the zone of caution against the occurrence of POGO is consideration of unknown factors. As for the magnitude of POGO vibration generated, we set it after the examples of other rockets under the condition by which, in vertical vibration, 0.5~1.0 percent of the main engine thrust is the vertical resonance frequency and makes sine wave fluctuation. Regarding lateral POGO vibration, there are few examples of other rockets that can serve as reference and the mechanism behind this occurrence has not yet been clarified; but the case may be that vertical vibration excites bending vibration via the nonaxissymmetric characteristics (eccentricity, etc.) of the rocket body. Here, normally response in the lateral direction is not large but in a special situation where the combination of vertical and lateral vibration modes is important, lateral vibration of a considerable magnitude may possibly occur. In the H-II rocket, which has the design target to suppress POGO, the value set is "1.0 G (3σ ceiling value)" equivalent to the somewhat lower level of the normal value for the H-I rocket.

5. Sine Wave Vibration Environmental Conditions for Satellite

Properly, it is desirable for the sine wave vibration environmental conditions for a satellite to be determined by consolidating much rocket flight data but, as far as the satellite to be carried by the H-II experimental rocket is concerned, environmental conditions must be set in the total absence of flight data. Figure 4 shows the interface condition now set for ETS-VI. For 15 Hz to 30 Hz, it was set for POGO by estimating acceleration in the satellite separating part in accordance with the concept stated in the preceding section. The other frequency domain was set as a level for enveloping vibration environments occurring at launch time, the time being affected by a gust, at the separation time, etc. The vibration levels at these times are estimated by analysis. Figure 4 shows values in the satellite separating part. If they are applied as they are to a satellite sine wave vibration test, it follows that large acceleration in the interior of the satellite occurs at the resonance points of the satellite in the configuration of the test period. Some of these resonances are due to the test/flight difference in boundary and other conditions and the exciting levels at consonance points can be lowered through consultation between the rocket side and the satellite side. This step called notching was applied to past rockets but, in the case of the H-II rocket with the total absence of flight data, care must be exercised in applying it. Also, the condition in Figure 4 concerns the experimental rocket. We consider that, in the operational rocket, the exciting level can be lowered because POGO suppression must have already been realized in it.

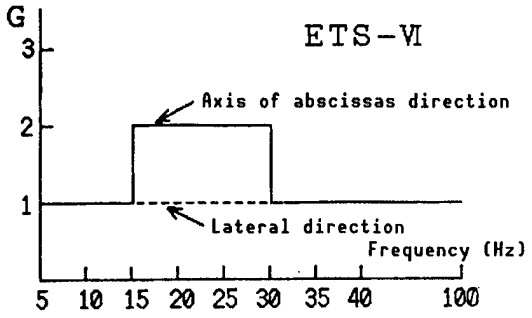

Figure 4. Sine Wave Vibration Environmental Condition

6. Summary

In this article, we stated our basic concept on the load conditions of the large satellite to be carried by H-II rockets. These concepts are not necessarily fixed. Instead, they may be modified, depending on the future progress of the development of the rocket, and we believe that the concept of the rocket and its details will finally be established by the results from launching several H-II rockets.

Trial Manufacture of Titanium Alloy for Heat-Protective Panel

43063810a Tokyo PROCEEDINGS OF THE 32ND SPACE SCIENCES AND TECHNOLOGY CONFERENCE in Japanese 26-28 Oct 88 pp 46-47

[Article by Tomoyuki Obayashi, Tadashi Matsushita, Masataka Yamamoto, Tokio Ohnishi, and Motohiro Atsumi, National Space Development Agency of Japan, and Shigeo Mikimoto and Toshiyuki Shimokawa, National Aerospace Laboratory: "Trial Manufacture of Titanium Alloy for Use in Heat-Protective Panel of Space Plane 'HOPE'"]

[Text] **1. Preface**

The National Space Development Agency of Japan [NASDA] is conducting research on the H-II rocket-launched winged recovery plane, HOPE. When HOPE reenters the atmosphere or when it makes a landing, it will be exposed to hostile thermal and mechanical environments. It is absolutely necessary to develop a highly strong, lightweight, and heat-protective system which has excellent heat resistance and heat insulation qualities and which can withstand such environments. This development work is an indispensable research subject.

Research on a heat-protective panel as a recovery technology was started in 1982, and trial-manufacturing and tests of ceramic tile, carbon, carbon materials, and flexible heat-insulating materials (conventional heat-protective materials) were conducted by 1986. At present, trial-manufacture of titanium alloy, nickel alloy, and advanced carbon carbon [ACC] heat-protective materials and research in these heat-protective materials mounted on an airframe, are being conducted with the aim of promoting further rises in heat-resistant temperatures and weight reductions.

We will hereunder describe the trial-manufacture of a titanium alloy heat-protective panel out of the above heat-protective materials.

2. Titanium Alloy Heat-Protective Panel

2.1 Concept of Heat Insulation

When the surface temperature of titanium alloy heat-protective materials is within a range from -100~550°C, it is regarded to be within an acceptable temperature range. The purpose of these materials is to protect the

radiation cooling of heat generated from the surface. They are laminated in structure, and are coated with multilayer films of highly rigid metal having load-carrying capacity and heat-insulating properties. Four kinds of forms shown in Figure 1 can be cited as structural forms of titanium alloy heat-protective materials having such a laminated structure.

Kind	Shape	Feature
Dimple-core multiwall	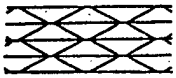	Structural system studied with Ti-alloy heat-protecting material by NASA
Insulated multiwall		Combination of dimple-core and heat-insulating material
Multi-honeycomb	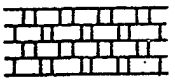	System frequently used for aircraft structure
Waved-core multiwall	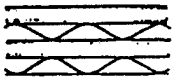	Easy-to-form core

Figure 1. Kind of Heat Insulating Structural Systems

As a result of studying these forms for heat insulating characteristics, moldability, and weight, it has been clearly observed that a dimple-core multiwall laminated structure is the best of all the structural types.

2.2 Study of Installing Method

The following functions are required in the method of installing titanium alloy heat-protective materials.

(a) It must be easy to install and remove these heat-protective materials on and from an airframe.

(b) It must be possible to absorb a difference between the coefficient of thermal expansion of the airframe and that of the heat-protective materials.

(c) These heat-protective materials must have high mounting reliability without detachment, deformation, etc., against sound, vibration, aerodynamic load, etc.

At present, the bolt-fastening method and the bayonet-clip method are being studied for the above-mentioned functions. Figure 2 shows an example of the bayonet-clip method.

3. Trial-Manufacturing and Test

Titanium alloy heat-protective materials are formed and assembled by joining and laminating flat sheets with dimple-core sheets. In this trial manufacturing work, Ti-6-4 and Ti-6242, very thin foil materials, were laminated and assembled by using was materials only at the junctions. As

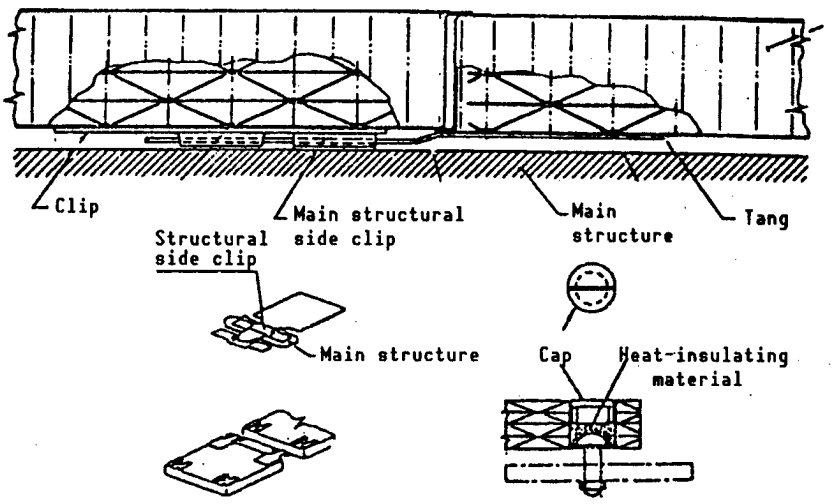

Figure 2. Example of Installation Structural System

a result, compared with the previous trial-manufactured product, this trial-manufactured one was lightened by at least 20 percent.

Figure 3 shows an example of the trial manufacturing method and that of the trial-manufactured product.

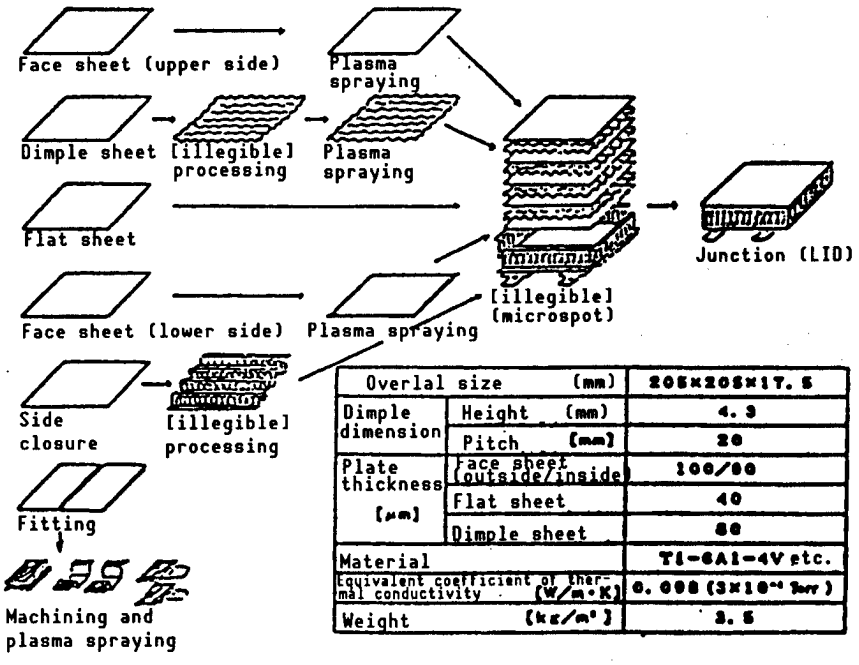

Overlal size (mm)		205×205×17.5
Dimple dimension	Height (mm)	4.3
	Pitch (mm)	20
Plate thickness (μm)	Face sheet (outside/inside)	100/80
	Flat sheet	40
	Dimple sheet	80
Material		Ti-6Al-4V etc.
Equivalent coefficient of thermal conductivity (W/m·K)		0.008 (3×10⁻⁴ Jw)
Weight (kg/m²)		3.5

Figure 3. Example of Trial-Manufacturing Method and Outline of Trial-Manufactured Product

Also, as a result of conducting the strength test and heat resistance test of this product, the value desired in this trial-manufacturing work was satisfactory.

4. Conclusion

Following on from the previous trial-manufacturing and test, advanced titanium alloy heat-protective materials were trial-manufactured and tested so that they become light weight. As a result, applicable data were obtained. From now on, we are scheduled to carry out the research and development of titanium alloy heat-protective material units on the basis of definite conditions required for functions so that these units can be applied as heat-protective materials to HOPE.

Trial Manufacture of Nickel Alloy for Heat-Protective Panel

43063810b Tokyo PROCEEDINGS OF THE 32ND SPACE SCIENCES AND TECHNOLOGY CONFERENCE in Japanese 26-28 Oct 88 pp 48-49

[Article by Tokio Ohnishi, Tadashi Matsushita, Masataka Yamamoto, Tomoyuki Kobayashi, and Motohiro Atsumi, National Space Development Agency of Japan: "Trial Manufacture of Nickel Alloy for Use in Heat-Protective Panel of Space Plane 'HOPE'"]

[Text] **1. Preface**

The thermal protection system [TPS] is one of the basic technologies important for research on the H-II rocket-launched winged recovery plane (HOPE: H-II Orbiting Plane). Of the re-use type TPSs, metal TPS is regarded to be promising from the standpoint of durability, reliability, ease of maintenance, etc. The authors, et al., have made a report on the result of studying nickel alloy heat-protective panels for a range of intermediate and high temperatures of about 550~1,100°C.[1,4] We will now describe the result of studying structural forms to judge whether or not they can be put to practical use; studying forming workability and fittings, and carrying out trial-manufacturing work and tests.

2. Nickel Alloy Heat-Protective Panel

The following matters are important to study structural forms of the TPS: 1) it must be easy to install and remove on and from the airframe; and 2) the TPS must be able to cope with thermal expansion. Various structural forms of the TPS for intermediate and high temperatures are shown in Table 2.1. The following items have been established as design conditions for the TPS, and it is necessary to study the design conditions so that they satisfy the TPS.

a) Load conditions shown in Table 2.2

b) Heat-resistant conditions

Even if the temperature history shown in Figure 2.1 is applied repeatedly to the TPS for 10 cycles, the TPS must not be seriously deformed.

Table 2.1 Structural System of TPS

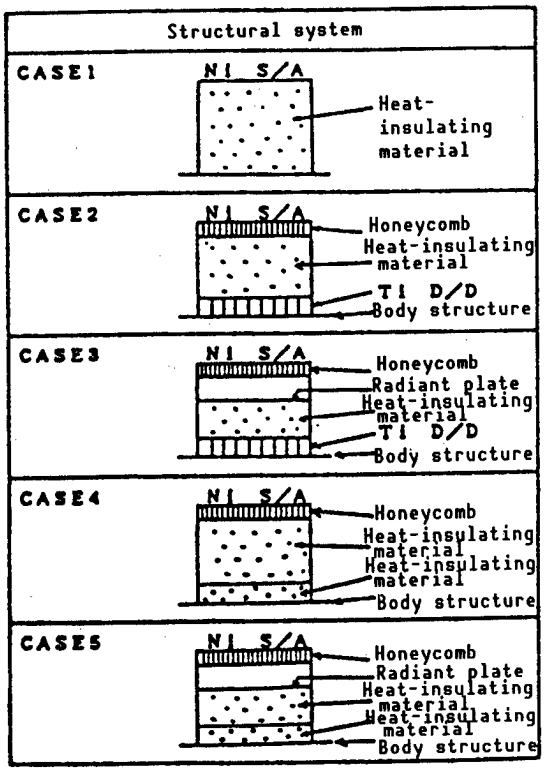

Table 2.2 Load Condition

Phase	Pressure (kg/cm^2)	Surface temperature °C
Launching	±0.48	Room temperature
Reentry	±0.13	1,000

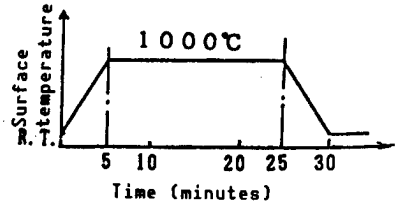

Figure 2.1 Temperature History

c) Heat-insulating conditions

The temperature of the main structure must not exceed the specified temperature (300°C in the case of CF/Pi) at the above-mentioned temperature load.

We are inexperienced in technologies for manufacturing and joining superalloy foils--such as INCONEL 617--having high strength at high temperatures. In order to carry out R&D on the TPS, it is necessary to solve the following subjects, including the manufacturing of honeycomb panels using such materials.

(1) Possibility of domestic production of materials equivalent to INCONEL 617
(2) Domestic production of very thin materials (foil materials) based on nickel alloy
(3) Honeycomb core forming and working technologies
(4) Foil material welding technology
(5) Foil material brazing technology
(6) Unit panel constituting and assembling technologies
(7) Technology for installing the TPS on the main structure
(8) Surface coating
(9) Evaluation of thermal characteristics
(10) Evaluation of mechanical characteristics

Figure 2.2 shows the results of a study of brazing conditions under the above-mentioned conditions.

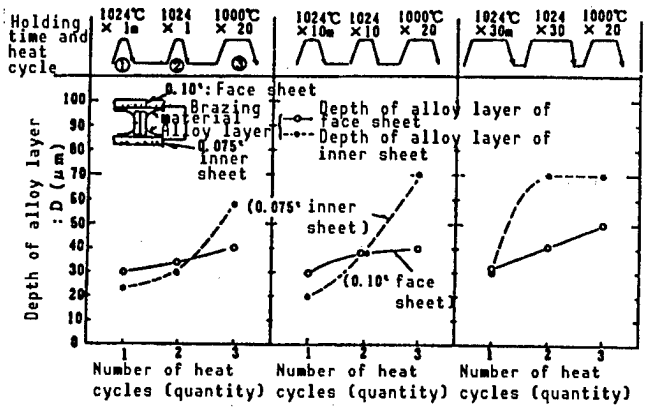

Figure 2.2 Example of Study of Brazing Conditions

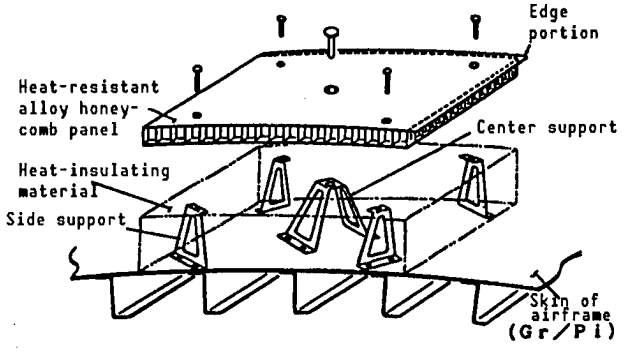

Figure 2.3 Example of Trial-Manufactured Nickel TPS

Figure 2.3 shows a product manufactured on trial under the above-mentioned design conditions and technical subjects. With regard to methods of installing the TPS on the main structure, we are studying a method of installing the lower portion of the edge of the TPS as a unit on the main structure as well as that of directly supporting the honeycomb panel shown in Figure 2.3.

3. Postface

As noted, we have studied the forming workability and structural forms of the heat-protective panel based on nickel alloy for HOPE, have manufactured products on trial, and have seen our way clear to developing the TPS for HOPE. In the future, we must carry out the R&D work to make the TPS practical to use for HOPE.

References

1. Ohnishi, Kobayashi, and Yamamoto, The 31st Space Scientific and Technical Union Lecture Meeting, 1987, p 376.

2. Matsushita, Yamamoto, and Ohnishi, The Fourth Space Station Lecture Meeting, 1988, p 147.

3. Matsushita, Yamamoto, Ohnishi, and Kobayashi, The 19th NASDA Technical Result In-House Announcement Meeting, 1987, p 54.

4. Matsushita, Ohnishi, Kobayashi, and Atsumi, The 30th Lecture Meeting Concerning Structural Strength, 1988, p 250.

Trial Manufacture of CC Heat-Protective Panel

43063810c Tokyo PROCEEDINGS OF THE 32ND SPACE SCIENCES AND TECHNOLOGY CONFERENCE in Japanese 26-28 Oct 88 pp 50-51

[Article by Tomoyuki Kobayashi, Tadashi Matsushita, Masataka Yamamoto, Tokio Ohnishi, and Motohiro Atsumi, NASDA: "Trial Manufacture of Carbon Carbon Heat-Protective Panel for HOPE"]

[Text] **1. Preface**

When the H-II rocket-launched winged recovery plane, HOPE, reenters the atmosphere, it will be exposed to very hostile thermal and mechanical environments. It is absolutely necessary to apply carbon carbon composite materials to these portions of HOPE exposed to the most hostile thermal environments. In other words, these materials must be used for portions in which the applicable upper-limit temperature of refractory metals exceeds 1,100°C.

Since FY 1984, NASDA has carried out research on reinforced carbon carbon [RCC] for the purpose of using RCC in nose cones and leading edges of wings. And NASDA has obtained a material which exceeds physical property values required for RCC used in the U.S. Space Shuttle. We will hereunder describe the results of studying heat-protective materials using advanced carbon carbon [ACC] having higher elasticity and strength and thinner walls than those of RCC, and the results of trial-manufacturing and testing the ACC panel.

2. Study of ACC Heat-Protective Panel

2.1 Insulation Concept of ACC Heat-Protective Material

The insulation structure of ACC heat-protective materials is that an ACC panel is provided on the surface of a heat-protective material and an insulating material is put between the main structure and the ACC panel. Also, combining the ACC panel and the main structure by use of posts is being studied. Figure 1 shows an installation structure with such posts. Also, heat-insulating properties mean cooling by radiation from the surface of the ACC panel and blocking off heat inside through use of heat-insulating materials with low thermal conductivity. At present, the combination of two layers of this heat-insulating material is being studied. One is an upper

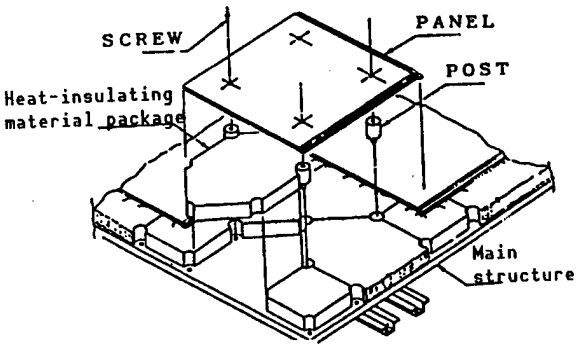

Figure 1. Outline of Installation Structure

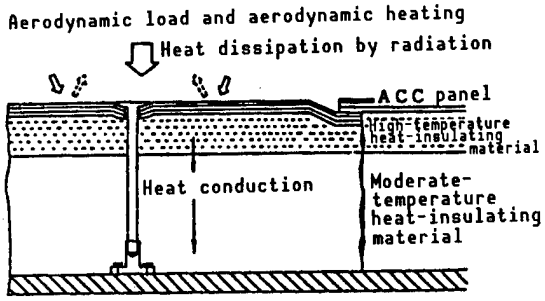

Figure 2. Concept of Heat Insulation

layer which is a heat-insulating material, has high heat resistance, and comes into contact with the ACC panel, and the other is a lower layer which is a high-performance heat-insulating material. Figure 2 shows a concept of the heat insulation.

2.2 Functions Required for ACC Heat-Protective Material

The following items can be regarded to be functions required for the ACC heat-protective material applied to HOPE.

(1) Heat-insulating properties

HOPE's structure and constituent elements, including equipment, etc., mounted on it shall be maintained within respective allowable temperatures or allowable inflow heating values.

(b) Aerodynamic shape

HOPE's facing shall be maintained at a design shape. The ACC heat-protective material shall be able to withstand loads, such as aerodynamic force, acoustic force, vibration, and impact in all operational environments anticipated, irrespective of strength. The ACC heat-protective material shall have strength and size enough to avoid buffeting and panel flutter.

(c) Installation and removal

It shall be possible both to install and remove the ACC heat-protective material to and from the outside to the main structure of HOPE. It shall

be possible to finely adjust the material during installation and to check the installation state after installation.

(d) Reusability

The surface of the ACC panel is coated with acid-resistant paint to prevent the ACC panel from deteriorating and wearing due to oxidization, because it is impossible to prevent CC materials from being oxidized. Also, it shall be possible to use the ACC panel repeatedly.

HOPE requires lightweight heat-protective materials which satisfy the above-mentioned functions.

3. Trial Manufacture and Test of ACC Panel

The ACC panel was reinforced two-dimensionally with UD material, woven fabric, etc., and was manufactured by using a resin-impregnated burning method. Figure 3 shows an example of mechanical and thermal characteristics of the ACC panel obtained by using this method. Target values are necessary to satisfy item (b) of the above-required functions. These target values were satisfactory in the trial-manufacture and test of the ACC panel.

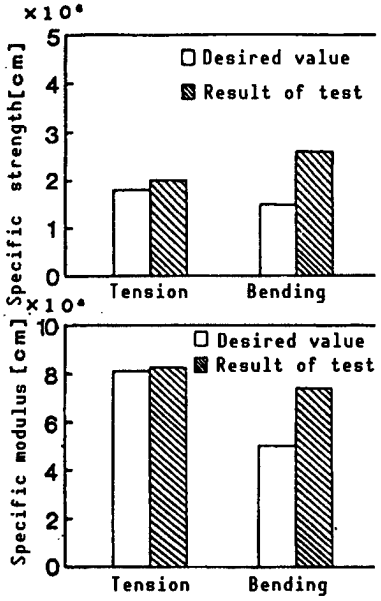

Figure 3. Result of Test of Trial-Manufactured Panel

Also, SiC films were formed for acid-resistant coating work by using a chemical vapor deposition [CVD]. Slight microcracks generated on the surface of these SiC films during the formation were sealed with silica or the like. With regard to the sealing work, satisfactory results were obtained by conducting tests in an arc-heating wind tunnel.

4. Postface

We have seen our way clear to applying the high-performance ACC heat-protective panel to HOPE by trial-manufacturing and testing this panel with the aim of lightening the panel. In the future, we are scheduled to carry out R&D of ACC heat-protective material units on the basis of prerequisites for applying such units as heat-protective materials to HOPE.

Trial Manufacture of CFRP

43063810d Tokyo PROCEEDINGS OF THE 32ND SPACE SCIENCES AND TECHNOLOGY CONFERENCE in Japanese 26-28 Oct 88 pp 52-53

[Article by Motohiro Atsumi, Tadashi Matsushita, Masataka Yamamoto, Tokio Ohnishi, and Tomoyuki Kobayashi, National Space Development Agency of Japan, and Shigeo Mikimoto and Toshiyuki Shimokawa, National Aerospace Laboratory: "Basic Test of Main Structural Members for HOPE"]

[Text] **1. Preface**

In the same way as heat-protective materials for TPS, the main structural member must be lightweight and excellent in respect of heat resistance, because the H-II rocket-launched winged recovery plane, HOPE, is exposed to severe thermal and mechanical environments during operations (launching, in orbit, reentry, and landing). This report covers basic tests for obtaining design data and technologies for forming and processing carbon fiber-glass reinforced plastics [CFRP] based on polyimide, which is one of the promising candidates for main structural material.

2. Candidate for Main Structural Member

Basic conditions required for the main structural member are shown below.

(1) Light weight: The weight is reduced with high specific strength and rigidity under given environmental conditions (temperature, load, etc.).

(2) Heat resistance: The weight is reduced by raising operational temperatures and by easing heat-insulating conditions required for TPS.

(3) It is easy to obtain, form, and work materials, and it is desirable to lower the developmental elements and cost of materials.

Candidates for main structural material were studied to select materials which satisfy the above required conditions. These candidates are shown below. Also, Figure 1 shows a conceptual drawing of the airframe of HOPE, and Table 1 shows an example of studies for applying these candidates to each section of HOPE.

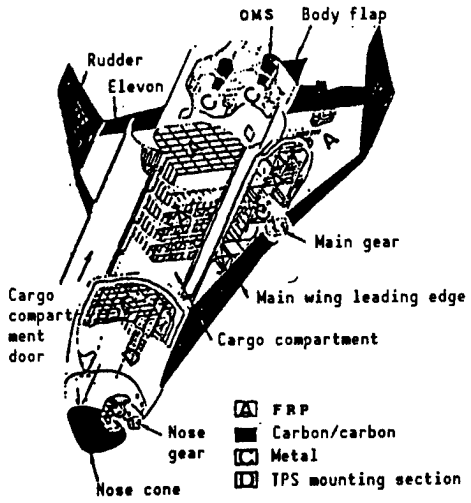

Figure 1. Conceptual Drawing of Airframe of HOPE

Table 1. Example of Application Study of Structural Materials

Portion	Material
Forward fuselage	
Main structure	CF/Pi
Nose cone	C/C
Nose gear door	CF/Pi or C/C
Intermediate fuselage	
Main structure	CF/Pi
Cargo compartment door	CF/Pi
After fuselage	
Main structure	CF/Pi
Thrust-supporting structure	Al alloy or FRM
Body flap	C/C
Main wing	
Main structure	CF/Pi
Leading-edge structure	C/C
Elevon	C/C
Main gear door	CF/Pi or C/C
Vertical tail plane	
Main structure	C/C
Leading-edge structure	C/C
Rudder	C/C
Various fittings	Ti alloy, Ni alloy, Al alloy, etc.

C/C: Carbon-Carbon
CF/Pi: Carbon Fiber/Polyimide

(1) Metal: Al alloy and Ti alloy
(2) CFRP: Based on epoxy resin
(3) Carbon/carbon: RCC [reinforced carbon-carbon]

Ti alloy is a promising candidate for metallic material used wholly for the main structure because of its light weight and heat resistance. CFRP based on polyimide having a high operational temperature of about 300°C is also a promising candidate for main structural material.

3. Basic Test

Table 2 shows study items and main contents of forming and working tests and mechanical characteristic tests of CFRP based on polyimide selected as a candidate material. Also, Table 3 and Figure 2 shows respective examples of results of the tests. Results almost equivalent to those of epoxy resin which have actually been used in aircraft, etc., were obtained from mechanical characteristics of laminated plates in which PMR-15, which is one of the polyimide resins, is regarded as a matrix.

Table 2. Main Contents and Study Items of Basic Test

Contents of test			
Test item			Test condition
Thermal and mechanical characteristic test			
Single layer plate material characteristics			
	0°	Tension	
		Compression	
	90°	Tension	•Temperature
		Compression	condition:
	245°	Tension	-100~300°C
	Interlaminar shear		•Temperature
	Bending test		condition: Dry
Laminated material characteristics			
	No hole plate	Tension	
		Compression	
	Holed plate	Tension	
		Compression	
	Damage allowable test (CAI)		
	Thermal cycle test		
	Edge delamination test		
	Fastener joint test		

Study item of fabrication technologies	
• Prepreg characteristics	• Hardening condition
• Molding process	• Special processing
• Lay-up properties	• Submaterial and facility
• Bug structure	• Compact parts trial-manufacturing test, etc.

Table 3. Example of Data on Mechanical Characteristics of CFRP Based on Polyimide

Fiber/resin	Temperature condition humidity condition	Tensile strength (kg/cm^2)	Compression strength (kg/cm^2)	Tensile modulus (kg/cm^2)	Compression modulus (kg/cm^2)
Colion 6K/PMR-15					
Single layer plate 0° direction	23°C DRY	195	143	13,700	12,800
	300°C DRY	167	78.5	15,000	13,700
Laminated sheet with no hole (+45/0/-45/90)45	23°C DRY	61.6	67.4	4,810	4,690
	300°C	50.0	21.1	4,710	4,500
T800/PMR-15					
Single layer plate 0° direction	23°C DRY	266	148	17,400	15,300
	300°C	175	100	16,700	14,700
Laminated sheet with no hole (?45/0/-45/90)45	23°C DRY	75.2	70.0	5,050	5,780
	300°C DRY	74.3	40.8	5,690	5,330

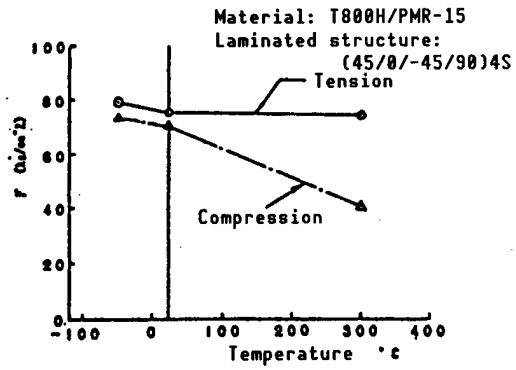

Figure 2. (1/3) Temperature Dependence of Strength of Laminated Sheet With No Hole

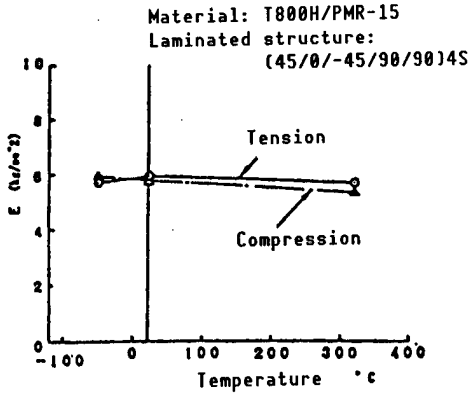

Figure 2. (2/3) Temperature Dependence of Modulus of Elasticity of Laminated Sheet With No Hole

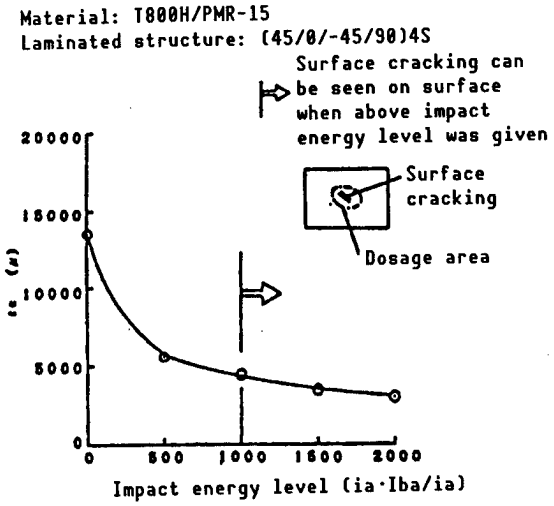

Figure 2. (3/3) Result of Test of CAI

Also, the forming process, bug configuration, hardening conditions, etc., have been obtained through trial-manufacture of plate levels and angle parts, and the purpose of forming and working technologies has appeared possible at the level of small parts.

4. Postface

From now on, we are scheduled to obtain data on thermal characteristics, fatigue characteristics, etc., of materials, to obtain the forming and working technologies and mechanical characteristics at the component level and partial structural level, and to study the applicability of main structural materials.

References

1. Yamamoto, Ohnishi, and Kobayashi, The 31st Space Scientific Allied Lecture Meeting, 1987, p 376.

2. Matsushita, Yamamoto, Ohnishi, Kobayashi, and Atsumi, The Fourth Space Station Lecture Meeting, 1988, p 143.

3. Matsushita, Yamamoto, Ohnishi, Kobayashi, and Atsumi, The 30th Structural Strength Lecture Meeting, 1988, p 250.

Trial Manufacture of TPS

43063810e Tokyo PROCEEDINGS OF THE 32ND SPACE SCIENCES AND TECHNOLOGY CONFERENCE in Japanese 26-28 Oct 88 pp 54-55

[Article by Tokio Ohnishi, Tadashi Matsushita, Masataka Yamamoto, Tomoyuki Obayashi, and Motohiro Atsumi, National Space Development Agency of Japan: "Thermal Analysis of TPS for HOPE"]

[Text] 1. **Preface**

When HOPE is operated, it will be exposed to mechanically and thermally hostile environments. The TPS mounted on the surface of the airframe and the heat-insulating material used in cabins are particularly indispensable for protecting the airframe and equipment mounted on HOPE for aerodynamic heat generated when HOPE reenters the atmosphere. We will hereunder describe results of thermal analyses conducted with a view to obtaining the weight of the TPS, weight of heat-insulating materials used in cabins, the amount of heat flowing into equipment mounted on HOPE, and thermal environments which affect main structural members.

2. Calculation Model of TPS

In this study, the radiant equilibrium temperature on the surface of the TPS was regarded as an input, and the equipment mounted on HOPE was regarded as a heat sink. The thickness of the TPS was obtained in the study. This thickness is necessary to lower the temperature of the main structure to less than the specified heat-resistant temperature, when the temperature of the surface of the TPS is raised by friction between the air and this surface. The temperature dependence was considered in respective physical properties. Figure 2.1 shows an outline drawing of a calculation model.

3. Calculation of Thickness of TPS

Table 3 shows a working temperature range and kind of TPS for the study. The temperature history of main structure, etc., was found by giving a temperature history generated with aerodynamic heat to the surface of the TPS, and the thickness of the TPS was found to lower the temperature of the main structure to less than the heat-resistant temperature. Figure 3.1 shows an example of a temperature history obtained from calculation results. Figure 3.2 shows results obtained in consideration of installation weight and weight per unit area of the TPS in each working temperature range.

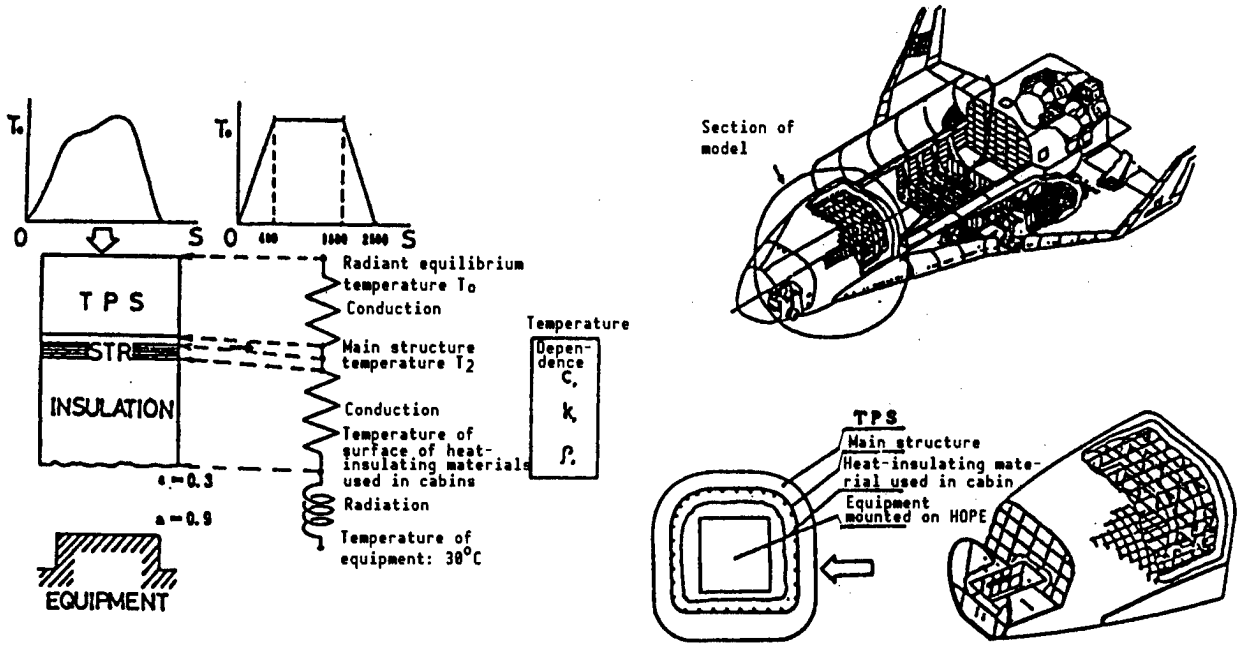

Figure 2.1 Calculation Model

Table 3.1 Kind of TPS

Items / Kind of Panels	OUTLINE SKETCH	ALLOWABLE TEMPERATURE (℃)
Ceramic tile	Coating; Alumina/silica Aluminoboro-silicate (illegible) felt; Structure panel	-100~1250 (RESULT)
Reinforced carbon carbon (RCC)	Nose cone; Leading edge	-100~1500 (RESULT); -100~1700 (TARGET)
Flexible reusable surface insulation (FRSI)	Silica films; Alumina/silica; Glass fiber	-100~ 650 (RESULT)
Titanium based alloy	Face sheet; Dimple-core; Bottom sheet	-100~ 550
Nickel based alloy	Super alloy honeycomb structure; Insulation; Ti dimple panel	-100~1100
Advanced carbon carbon (ACC)	Insulation; Attach fitting; Structure panel	-100~1300

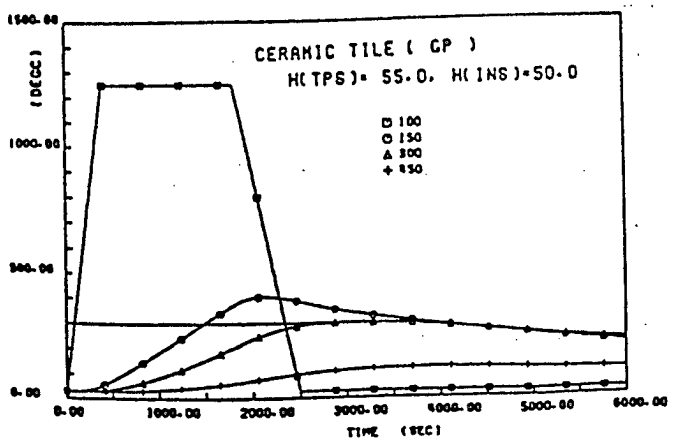

Figure 3.1 Example of Calculation of Temperature History

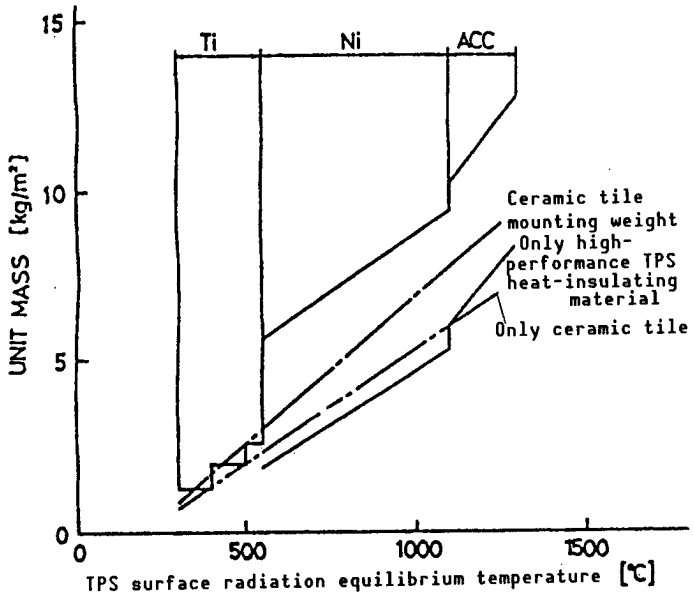

Figure 3.2 Example of Calculation of Unit Weight of TPS

Figure 3.3 shows results obtained from the amount of heat flowing into cabins and the thickness of the TPS necessary for the thickness of respective heat-insulating materials. The following items can be found from the results shown in this figure.

(1) Thicker TPS is required, because the thicker heat-insulating materials used in cabins, the smaller the amount of heat transferred from the main structure to cabins, and the main structure temperature rises.

(2) Thicker TPS is required in proportion to the thickness in the case when heat in cabins is insulated completely.

(3) When heat-insulating materials used in cabins are thick, the amount of heat flowing into equipment will decrease.

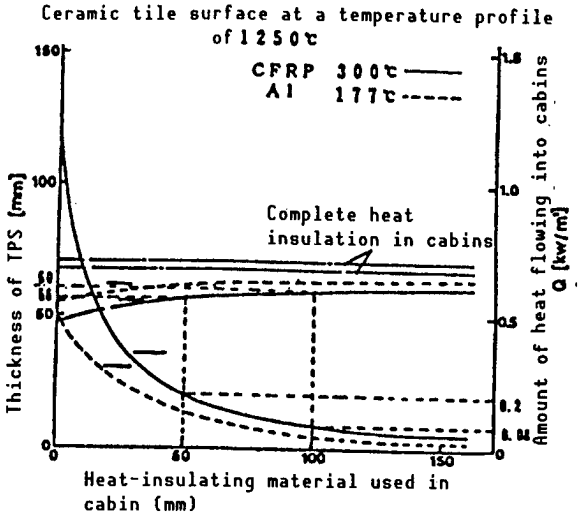

Figure 3.3 Necessary Thickness of TPS and Amount of Inflow Heat

(4) When the heat-resistant temperature of the main structure is decided, it is necessary to decide the minimum thickness necessary for the TPS and that for heat-insulating materials used in cabins in consideration of conditions required for the amount of heat flowing into equipment.

4. Postface

Typical sections were analyzed in this study, but it is necessary to analyze each section of the airframe in the future. It is also necessary to select the lightest heat-insulating material with high heat-insulating properties in accordance with the working temperature range.

References

1. Ohnishi, Kobayashi, and Yamamoto, The 31st Space Scientific Allied Lecture Meeting, 1987, p 376.

2. Matsushita, Yamamoto, and Ohnishi, The Fourth Space Station Lecture Meeting, 1988, p 147.

3. Matsushita, Yamamoto, Ohnishi, and Kobayashi, The 19th NASDA Technical Result In-House Announcement Meeting, 1987, p 54.

4. Matsushita, Yamamoto, Ohnishi, Kobayashi, and Atsumi, The 30th Lecture Meeting Concerning Structural Strength, 1988, p 250.

Present State, Future Outlook of Optic Industry

43066594 Tokyo OPTRONICS in Japanese Jan 89 pp 137-144

[Article by Masaaki Tsurumi and Satoshi Ishihara, Optoelectronic Industry and Technology Development Association]

[Excerpt] 1. Introduction

The optic industry is making an important contribution not only to the growth of the optic industry itself, but also to the advancement of other sectors, including electronics, information and energy. Further, it is also contributing to the realization of a high informationized society together with a high amenity society. [passage omitted]

4. Future Outlook for Scale of Optic Industry

With regard to the future of the optic industry, a report prepared in March 1988 by the Optoelectronic Industry Trend Survey Committee states that, based on production estimates for the 5-year period ending in FY 1992, production in FY 1992 will total Y3,470 billion, compared to Y1,230 billion in FY 1987. Breaking this total down, it is estimated that optical parts will be worth from Y370 billion to Y720 billion, optical equipment and devices from Y710 billion to Y2,370 billion, and optical application systems from Y150 billion to Y390 billion. There are many indefinite factors over the medium-term outlook 5 years from now. In particular, it is believed that the problem of when to introduce an optical communications system for subscribers will have a great influence on the future of the optic industry.

The results of estimates for the next 5 years based on the optic industry described in the previous chapter can be stated as follows:

In preparing the estimated, production quantity was computed from production value, and domestic demand was computed from domestic production while taking account of the export ratio. The optical products included in the estimate were basically those products included in production statistics for FY 1987. However, such products as

"optical application systems" and "semiconductor lasers," etc., were excluded because the average scale and use per sytem were indefinite and including them in the estimate was difficult. In short, greater importance was attached to production aspects than to demand, and the estimate was based only on existing products with definite images. The results of the estimate are shown in Table 3, and the trend of production value is shown in Figure 5.

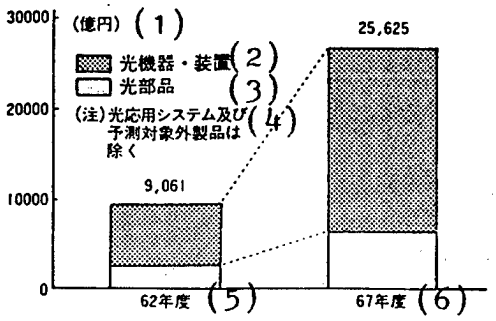

Figure 5. Production Value Trends for Optical Parts, Optical Equipment/Devices (FY 1987-1992)

Key:

1. Y100 million
2. Optical equipment/device
3. Optical parts
4. (Note) Excluding optical application systems and products excluded from estimate
5. FY 1987
6. FY 1992

The production value of Japan's optic industry for FY 1992 was estimated at Y2,560 billion compared with Y906 billion for FY 1987 for the total of optical parts and optical equipment/devices. The average growth rate of domestic production during this period is estimated at 23 percent, which is almost the same as that for the period from 1984 to 1987. The main reason why it was estimated that virtually the same growth rate can be maintained for the next 5 years is that it is believed high growth can be maintained through the functional development of an "optical disk" having the highest component ratio (from ROM to WORM, ERASABLE) with good prospects for commercialization in complex products (CD-V, CD-I, CD radio cassettes).

As mentioned above, the total domestic production value in FY 1987 for optical products included in the estimate was less than the FY 1987 estimate for those optical products excluded from the estimate. Therefore, in order to obtain a production scale for FY 1992

Table 3. Estimated Results of Optical Industry (Recapitulation)

Item \ Fiscal Year	Production Value (million yen)		Domestic Demand Value (million yen)		Growth Rate	
					Production Value	Demand Value
	FY87	FY92	FY87	FY92	92/87	92/87
1. Semiconductor laser	34,500	69,500	21,640	40,600	15.04	13.42
2. Gas laser	6,700	17,100	6,700	16,000	20.61	19.01
3. Solid state laser	2,500	9,600	3,220	13,320	30.88	32.83
4. Light-emitting diode	61,900	99,440	44,070	71,100	9.94	10.04
5. Discrete light-receiving element	21,750	46,200	16,400	33,090	16.26	14.94
6. Array type light-receiving element	26,000	52,000	22,750	46,800	14.87	15.52
7. Complex optical element	41,000	69,000	41,000	59,920	10.97	7.88
8. Solar cell	9,900	16,300	6,990	10,490	10.49	8.45
9. Optical fiber	68,710	85,420	47,510	67,890	4.45	7.40
10. Handle fiber	2,400	10,000	2,400	9,000	33.03	30.26
11. Passive optical parts	15,850	50,200	14,200	36,450	25.93	20.75
Optical parts subtotal	291,210	524,760	226,880	404,640	12.50	12.26
12. Optical transmission equipment and devices	62,950	156,200	59,110	139,380	19.93	18.72
13. Measuring equipment for optical transmission	13,510	42,670	11,360	27,810	25.86	19.62
14. Laying equipment	5,000	10,000	2,500	5,000	14.87	14.87
15. Optical sensors (laser or sensors using fibers)	5,950	20,850	5,950	17,910	28.50	24.66
16. Optical disk player	351,000	1,189,100	119,660	444,100	27.64	29.99
17. Optical printers	110,670	419,000	54,660	133,200	30.51	19.50
18. Laser, LED scanner (bar code reader)	10,900	28,000	10,900	28,000	20.77	20.77
19. Medical laser equipment	4,830	19,900	3,310	11,620	32.73	28.58
20. Laser application production equipment	36,080	131,000	36,080	82,700	29.42	18.05
21. Printing/processing equipment	14,000	21,000	11,200	16,800	8.45	8.45
Optical equipment/devices subtotal	614,890	2,037,720	314,730	906,520	27.08	23.56
Optical parts, optical equipment/devices total	906,100	2,562,480	541,610	1,311,180	23.11	19.34

corresponding to the production scale for FY 1987, it is necessary to make a correction taking the above-mentioned difference into account.

If a correction is made based on the products excluded from the estimate, a production scale of about Y910 billion (Y200 billion for optical parts, Y320 billion for optical equipment/devices, and Y390 billion for optical applications) will be added. As a result, the domestic production scale for FY 1992 will be about Y3,470 billion.

The corrected value, Y200 billion, for optical parts for FY 1992 was derived from an estimated Y100 billion for micro-optical parts, etc., included in other optical parts, and also from about Y100 billion for a production scale estimated for other elements used in semiconductor lasers.

Also, the corrected value of Y320 billion for optical equipment/devices was derived from an estimate for production expansion for optical fiber utilization, laser utilization sensors and other elements in addition to Y300 billion for optical disk media such as CD-ROMs. However, an optical communications system for a subscribers system, a solid state camera, displays, etc., were not considered. Therefore, considering the above-mentioned trial computation results, there is a possibility that Y400 billion for a subscribers system, Y1 trillion for a solid state camera, Y400 billion for displays, etc., will be added.

The production value for only those optical parts included in the estimate was Y290 billion in FY 1987, but the production scale for the same optical parts in FY 1992 was estimated at Y520 billion. The annual average growth rate for this period will be 12 percent. The production value breakdown for optical parts in FY 1992 is shown in Figure 6.

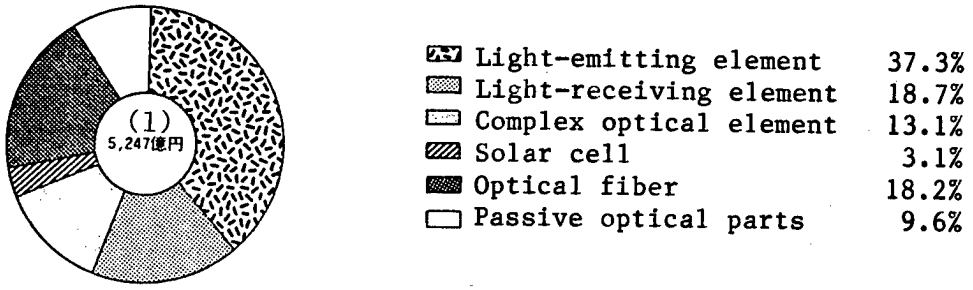

Figure 6. Breakdown of Production Value Estimates for Optical Parts (FY 1992)

Key:

1. Y5,247 billion

Next, the production value for only the optical equipment/devices included in the estimate was Y610 billion, while in FY 1992 the same optical equipment was estimated at about Y2 trillion. The annual average growth rate for this period is 27 percent. This is more than double the above-mentioned growth rate for optical parts. The production value breakdown for optical equipment/devices in FY 1992 is shown in Figure 7.

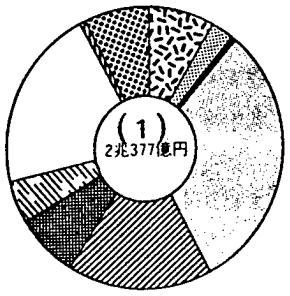

Optical transmission equipment and devices	7.7%
Optical measuring equipment	2.6%
Sensors using optical fibers	1.0%
Compact disk devices	29.5%
Replayable video disk devices	15.1%
Writable optical disk devices	7.4%
Rewritable optical disk devices	6.4%
Optical input-output devices	21.9%
Laser devices for medical use	1.0%
Laser processing equipment, etc.	7.4%

Figure 7. Breakdown of Production Value Estimates for Optical Equipment/Devices (FY 1992)

Key:
1. Y2,037.7 billion

Also, in the estimate work for this fiscal year, practicalization of a subscribers system was not presupposed. In other words, it is believed that practicalization of an optical communications system for subscribers will be realized in the near future, but the exact time remains indefinite.

5. Future Problems for the Optical Industry

The FY 1987 report prepared by the Optoelectronic Industry and Technology Development Association shows that the production scale for FY 1992 was estiamted at Y3,470 billion, and assuming that a high growth rate can be continuously maintained, there is a possibility that the optic industry will be a Y10-trillion industry by the year 2000.

In the future, if the possibility embodied in the estimated is realized, this will mean that the optic industry will play a great role in contributing to the development not only of Japan, but also to the world economy. The optic industry is Japan's second leading industry following the electronics industry. At the same time, it is also true that the optic industry has many problems to solve.

The optic industry is a typical high-technology industry; it is supported and developed by the progress of optical technology. Just as the field of optical technology is related to the broader fields of industry and society, so the fields connected with the optical industry are also broad.

Although technological development competition among the advanced countries in this high-technology field is severe, Japan's optical technology is fortunately leading the world together with the United States. In order to continue to lead the world and to ensure technological strength in the future, it is most important to solve the various problems facing optical technology by promoting research and development among industry, government and academia. In particular, five fields that require active technological development are as follows:

a. Technological development necessary to meet the demands of a subscribers system and high vision.

b. Technological development for the realization of optical technology that can be handled easily, such as light-electricity/electron interface.

c. Technological development for the realization of functional complex products as exemplified by the CD-V, etc.

d. Technological development concerning highly functional semiconductor optical elements, especially integrated optical elements (OEIC, OIC) that constitute key parts.

e. Development of optical elements to make it possible to enlarge usable optical wavelengths and of optical technology to make it possible to utilize the coherence of laser light.

To ensure the future development of the optic industry, it will also be necessary to maintain international cooperation. Based on the extensive experience gained from confronting the various problems generated during the development of semiconductors, it will be necessary to set up a more active structure than ever before to avoid creating problems or to solve problems rapidly instead of merely adopting the passive attitude of looking for measures only after a problem has arisen.

As in the case of the subscribers system, it is fundamentally important to form excellent international relations in order to actively promote the development of new optical products and systems leading to the creation of new markets. The development of new optical products also falls within the international responsibility imposed on Japan, which takes pride in its position as an optically advanced country.

Optical technology is growing rapidly. Consequently, new products are being marketed one after another. However, in some cases the disorderly development of new products will only serve to confuse users. Although technological progress must not be hindered, the promotion of standardization is also important, while keeping a close eye on future technological trends. From Japan's perspective, it is especially important not only to promote standardization domestically, but also internationally.

6. Optoelectronization Index

The optoelectronization index is an index to measure the progress of the diffusion of optical technology and optical products. This index uses the Gompertz curve. The Gompertz curve is a curve defined by the equation: $Y=KxA^{BX}$, where A and B are invariable numbers based on actual result data, X is a variable representing time, and K is the least upper bound of penetration.

Optoelectronization indexes for major items are as follows:

a. Optical Transmission Equipment

Fiscal trends in the ratio of optical communications equipment against wire carrier communications equipment is designated as the optoelectronization index. Based on the assumption that application fields favorable for telecommunications will continue to exist in the future, the final diffusion rate for the least upper bound was designated as 50 percent. It is believed that the upward fiscal trend, which is slow compared to the optoelectronization rate for optical fibers, is governed by the fact that electronic equipment, such as multiplex devises, is being used in the optical communications system. Computation results are shown in Figure 8.

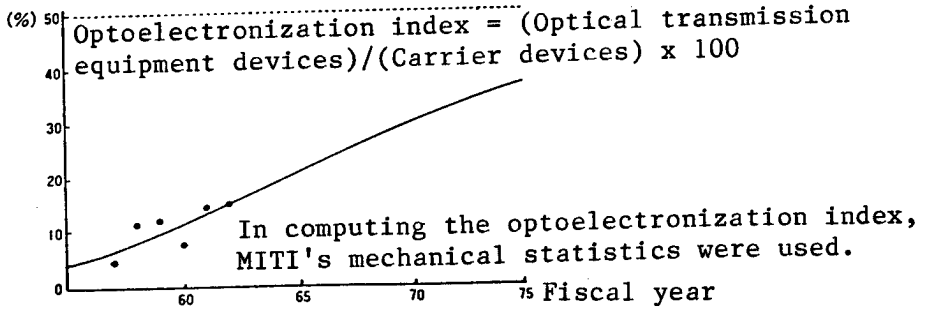

Figure 8. Optical Transmission Device Optoelectronization Index

b. CD Players

The diffusion of CDs is progressing rapidly. It is likely that analog players will completely disappear. Here, the least upper bound is 100 percent. Computation results are shown in Figure 9.

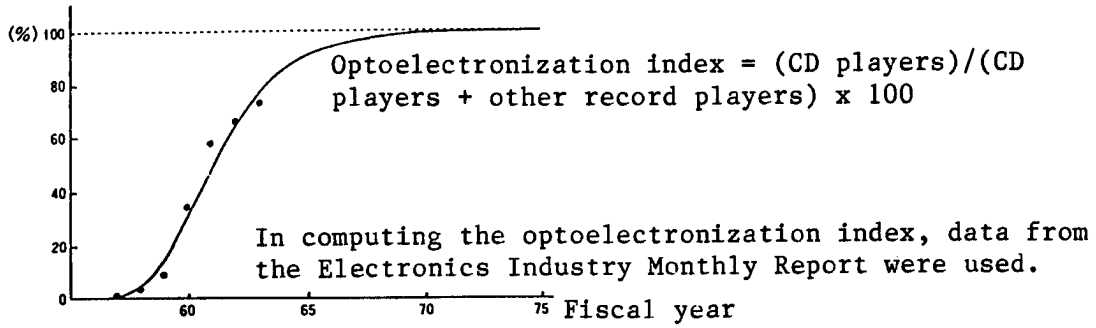

Figure 9. Optoelectronization Index for Number of CD Player Units

c. Lasers for Industrial Use

Lasers for industrial use were compared with mechanical optical devices. Such devices include cameras, telescopes, microscopes, etc. In these comparisons, the least upper bound was set at 10 percent. Computation results are shown in Figure 10.

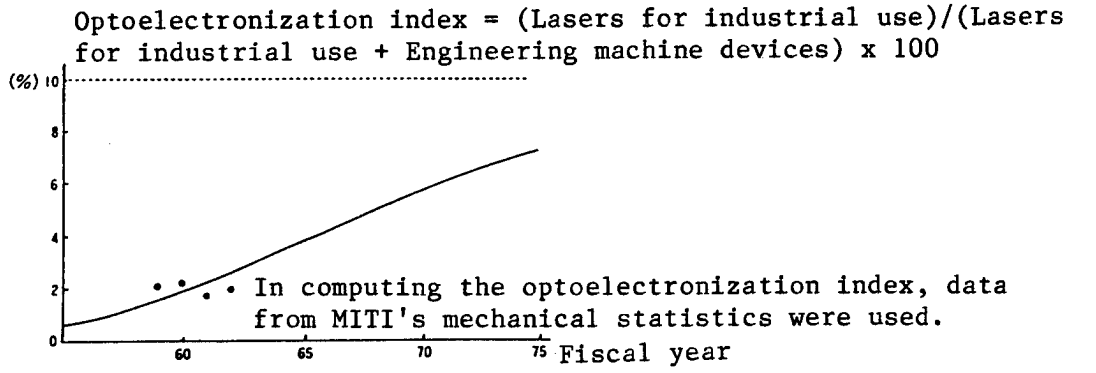

Figure 10. Optoelectronization Index for Lasers for Industrial Use

d. Optical Fibers

Since existing electrical wires include electrical wire not only for communications use, but also for power transmission, only data on existing electrical wire for communications use was used. The computation results are shown in Figure 11.

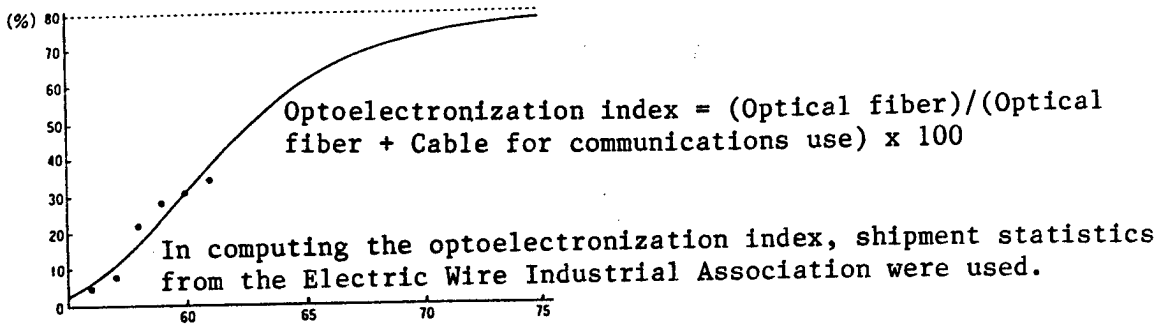

Figure 11. Optical Fiber Optoelectronization Index

e. GNP

Finally, the optic industry's percentage of GNP is targeted at 5 percent. The production value of the optic industry was computed by avoiding duplication among parts, equipment and systems in order to keep its balance with GNP. Construction results are shown in Figure 12.

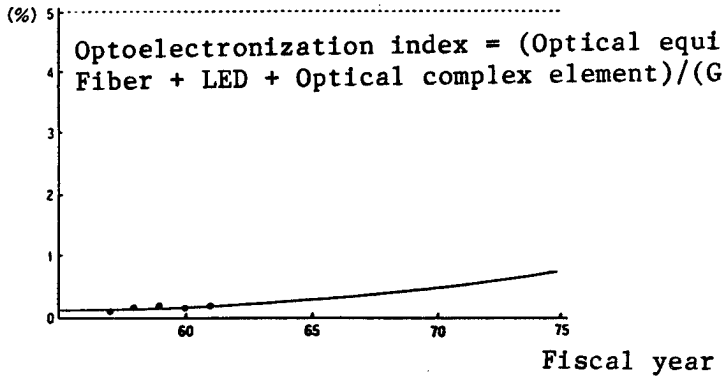

Figure 12. Optoelectronization Index Compared to GNP

7. Conclusion

The rapidly growing optic industry is a typical high-technology industry. Its production value has reached Y1,230 billion. Some optical products are shifting to the stable growth stage. With regard to these products, it is necessary to deal with trade problems with the advanced countries, as in the case of electronic products, and also with catch-up problems in the newly industrialized countries. On the other hand, it seems necessary to make further efforts directed toward market exploitation, highly advanced technological development and new product development in order to sustain the growth of the optic industry.

Now that the responsibility to perform both domestically and internationally has become great because of the expansion of industrial scale, it can be said that the necessity of reestablishing definite guidelines for the future of Japan's optic industry, together with appropriate international relations, is growing. Expectations for optical technology are also growing. If very high-performance optical communications, optical computers, laser nuclear fusion, optical control chemistry, optical biology, etc. are achieved, it will not be a dream that the optic industry will become a key industry in the 21st Century.

REFERENCES

1. "Trends in the Optic Industry for FY 1987," Optoelectronic Industry and Technology Development Association.

2. "Survey and Research on the Present State of Japan's Optical Application System," Optoelectronic Industry and Technology Development Association.

Nuclear Energy Laser Developments Reported

Nuclear Excited Lasers Discussed

43063015a Tokyo HIGH TECHNOLOGY in Japanese 19 Jan 89 p 1

[Text] Nuclear Excited Laser

The Power Reactor and Nuclear Fuel Development Corporation [PNDC], as a new development in nuclear energy engineering, a new field of technology, has been working with Professor Seiji Nakazawa of the Nuclear Engineering Section of Tokyo University's Engineering Department to advance the development of a nuclear excited laser neutron detector which can be applied in the nuclear engineering of lasers. Recently, they succeeded in a new method of nuclear excited laser oscillation by means of the neutrons, gamma rays, and X-rays of a nuclear reactor core. This was achieved by experiments inside a reactor, using the research reactor, "Yayoi [Spring]" which belongs to the nuclear engineering research facility affiliated with the Tokyo University Engineering Department.

Nuclear Excited Lasers

In the field of nuclear energy use, the research and development of new technologies and the introduction of applied technologies from other fields are moving forward positively to make the next generation of reactors, including the fast breeder reactor, superior in safety.

A nuclear excited laser is a laser oscillation device which converts energy generated by the nuclear reaction of an atom's nucleus into emitted laser light. In the past, research had been carried out on this subject as a means to extract directly the energy of a nuclear reactor (see Figure 1). However, because laser radiation requires a high degree of neutron bundling (to the extent of 10^{15} ($n/cm^2.s$) and because the rate of conversion from neutrons to laser energy in the nuclear reactor core is extremely poor at 0.03 percent, no research is now being conducted on a method to extract energy from a nuclear fission reactor.

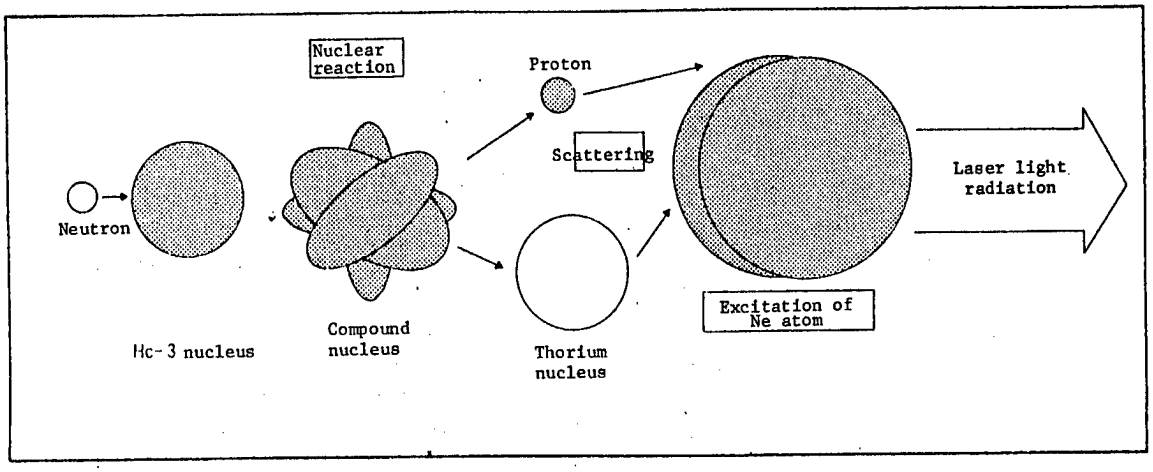

Figure 1. Concept Diagram of the Process From Neutron Injection to Laser Radiation

Using a Laser in a Neutron Detection Device

The laser light excited by a nuclear reaction inside the nuclear reactor can be used as a beneficial source of information that conveys to the outside the condition of neutrons inside the nuclear reactor. If this laser light is measured as an information source, this new concept will enable direct measurement of the quantum status within the nuclear reactor, something that could not be achieved by the traditional nuclear reactor instrumentation system.

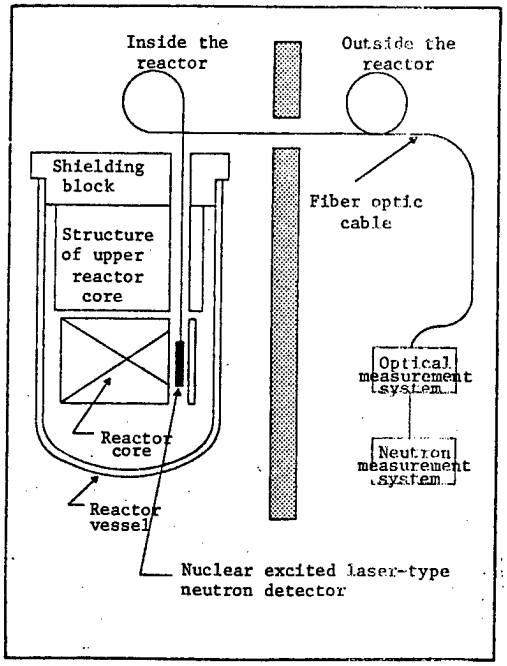

Figure 2. Nuclear Reactor Instrumentation System Using Nuclear Excited Lasers

Figure 2 is an outline of the nuclear reactor instrumentation system that uses nuclear excited lasers. The nuclear excited laser-type neutron detector is of simple composition and has an output signal to handle the laser light. It is a system with a simple structure. This is unlike the

many varieties of neutron detectors that were used in the past for the measurement of nuclear reactors and neutrons. Because laser light is essentially a superior means to convey information such that the use of telecommunications will expand, the information conveyed by a nuclear excited laser is quantitatively and qualitatively greater than that of past detection devices.

The new type of nuclear excited laser is a hybrid model. It uses helium-neon gas as the excitation medium; uses neutrons, gamma rays, and X-rays of the reactor core as triggers in a condition where electric voltage is added preparatory to excitation of the medium; and produces laser radiation by combining the voltage discharge and the radiation discharge.

In the recent experiments, a reactor experiment was carried out (see Figure 3) by means of neutrons from the fast breeder research reactor "Yayoi," as well as by X-ray experiments (see Figures 4 and 5) external to the reactor to verify the reaction to radiation of this hybrid-type nuclear excited laser.

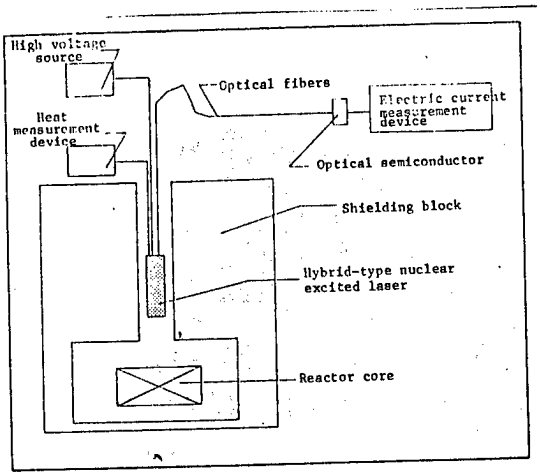

Figure 3. Outline Diagram of Nuclear Excited Laser Radiation Experiment in "Yayoi"

These experiments confirmed that laser oscillation occurs from nuclear excitation even under low nuclear bundling (from 10^{9} - 10^{1} $1(n/cm^{2}.s)$), which had never before oscillated at less than 10^{11} $(n/cm^{2}.s)$. Moreover, these experiments confirmed that reactor core gamma rays and X-rays can produce hybrid-type nuclear excited laser light.

The fact that light generation by experiments with neutrons in the reactor core, gamma rays, and X-rays external to the reactor core means that it is possible to use the hybrid-type nuclear excited laser to detect many types of radiation, not just neutrons. Moreover, this method is not only able to use the added voltage of an excited medium, but can also avoid the effects of electromagnetic waves within the nuclear reactor because it is a light measurement instrument.

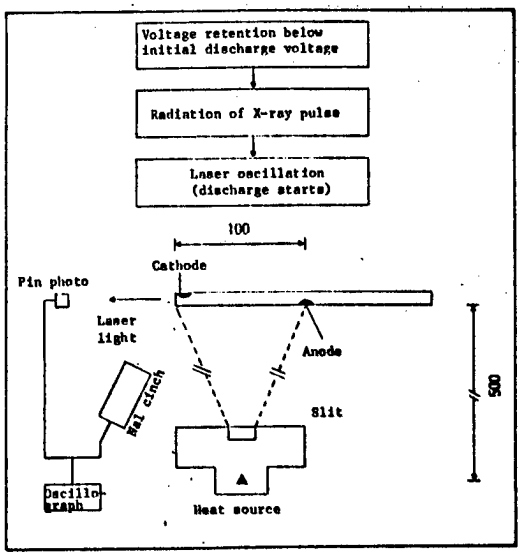

Figure 4. Outline Diagram of X-ray Experiment External to the Reactor

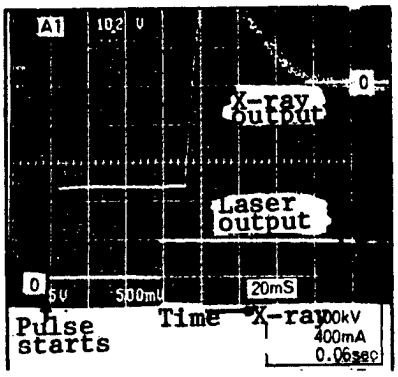

Figure 5. X-ray Pulse and Laser Oscillation

There are no examples in the world of the use of neutron detectors which use the nuclear excited lasers now moving forward by research and development, and it is hoped that this will provide new knowledge in such fields as measurement control, nuclear physics, and nuclear reactor physics. Moreover, PNDC says that it can apply the laser radiation principles derived from this new method to other media and semiconductor laser radiation devices.

Decommissioning Reactors Lasers Developed

43063015b Tokyo GENSHIRYOKU SANGYO SHIMBUN in Japanese 26 Jan 89 p 5

[Text] Success in Maximum Laser Oscillation

On 18 January 89 Mitsubishi Heavy Industries, Ltd. [MHI] and the Industrial Development Laboratory [IDL] announced that they had achieved a maximum output of seven kilowatts by means of a CO (carbon monoxide) laser oscillation device of the five-kilowatt class. Moreover, they succeeded in continuous oscillation at the five kilowatt level for over four hours.

Industry now uses a CO_2 (carbon dioxide) laser in such processes as the cutting and welding of metals. However, the CO laser, in contrast to the CO_2 laser, has only one-half its wavelength at five micrometers. As a result, its minimal spot diameter in the focusing of laser light is about one-half, and it has four times as much energy intensity. Moreover, since it can double the focus depth to obtain the same spot diameter, it is useful for the cutting of thick plates. Furthermore, since its absorption rate for metals is high, metals are easily melted. In addition, transmission by optical fibers is anticipated in the future, so this laser also has the advantages of a processing machine that can be miniaturized and made lightweight, while at the same time, it can be used in the fabrication process in narrow places.

Consequently, MHI and the Laser Research Center of IDL (Tomotada Fujioka, Center Director) worked together on the development and trial manufacture of a CO laser oscillation device of the five-kilowatt class.

In the cutting experiments that the two parties have carried out up to now, the CO_2 laser was able to cut, at an output of three kilowatts, carbon steel with a maximum thickness of 20 mm and stainless steel with a maximum thickness of 16 mm. In contrast, a CO laser, with an identical three-kilowatt output, was able to cut carbon steel 70 mm thick and stainless steel 40 mm thick.

They were able to achieve the maximum output and long-term oscillation by carrying out research to find the best discharge method, discharge electrodes, and laser gas combination, as well as carrying all sorts of tests for the parameters of the speed of the electric current, the temperature, and the pressure within the laser oscillator. Consequently, they found the ideal conditions.

Their future plan is to carry out oscillation experiments to achieve even higher performance, and to develop a CO laser device of the 20-kilowatt class.

High output and continuous oscillation was difficult to achieve in the CO laser device, and the seven-kilowatt output achieved is the world's highest output for a CO laser. Moreover, continuous oscillation for over four hours at an output of five kilowatts was achieved for the first time in

Japan. It is reported that the continuous oscillation record up to now had been one hour at an output of three kilowatts.

Because of this, they are working to develop a 20-kilowatt class CO laser device to be used fully in the decommissioning of nuclear reactors.

Moreover, this device is to be used in the implementation of the "reactor structure cutting technology verification tests," which are tests entrusted to MITI's Atomic Energy Engineering Test Center (Tadashi Fujii, Managing Director), which is among the verification tests being carried out by that ministry in regard to the disuse of nuclear reactors.

Atomic Lasers for Uranium Enrichment Tested

43063015c Tokyo GENSHIRYOKU SANGYO SHIMBUN in Japanese 2 Feb 89 p 1

[Text] Atomic Lasers and Uranium Enrichment

The Laser Uranium Enrichment Technology Research Association (Masatoshi Toyota, Director), which seeks to verify the possibility of commercial use of uranium enrichment technology by an atomic laser method, on 1 Feb 89 signed a nuclear power safety agreement with Tokai-mura in Ibaraki Prefecture, where it plans to install test equipment (with uranium enrichment capacity of one ton SWU per year). Having achieved this, it plans to present to the Science and Technology Agency on 2 Feb 89 an application for permission to use nuclear fuel materials. It will begin to construct its laboratory structure in the spring and to conduct experiments in FY90.

This association plans to install its experimental equipment on the grounds of the Japan Atomic Energy Research Institute [JAERI], which is north of Japan Atomic Energy Reactor's Tokai-mura reactor in Tokai-mura. The site will be on loan from JAERI.

The nuclear safety agreement that Ibaraki Prefecture, Tokai-mura, and this association signed on 1 Feb 89 is identical to past agreements signed by atomic energy entrepreneurs in the prefecture. It prescribes specific measures to ensure safety, such as control of radioactive waste materials, pollution prevention, environmental safety, an agreement on new and expansion design plans, and measures demanded from a safety standpoint. Lieutenant Governor Seiichi Takeuchi, Mayor Tomio Sudo, and Director Toyota signed the agreement.

This research association is a research corporation whose establishment has been licensed by the Science and Technology Agency and by MITI. It was founded in April 1987 and consists of 12 members, including the Tokyo Electric Power Co. Ltd., Kyushu Electric Power Co., Ltd., Japan Atomic Energy Reactor, Japan Nuclear Fuels Industrial, and the Central Research Institute for Electric Power.

For the four years up to FY91, the association will receive investments totalling Y20 billion, including a government subsidy. Its aim is to establish the technological feasibility of atomic laser uranium enrichment technology and to verify the possibility of its commercial use.

In the two years since 1987, the association has proceeded with research and development of the basic devices such as the laser device and the separation device along with design of the test equipment.

In the future, the association plans to improve the devices that it has developed up to now, to assemble them as test equipment at its "Tokai Uranium Enrichment Laboratory," and to conduct experiments in FY91.

The cost of building this laboratory, including the building and the equipment, will be about six billion yen. The association is building a labroatory of 3,600 m^2 in a two-story steel structure, with attached rooms, such as administrative offices.

This association signed a cooperation agreement with JAERI in Jun 87 to ensure close liaison when carrying out its research and development. This cooperation is proceeding smoothly and includes exchanges of technical information and the sending of technicians.

Omega Project for High Level Radioactive Waste

43062024a Tokyo ENERUGI FORAMU in Japanese Nov 88 pp 132-135

[Excerpt] [Passage omitted] At the annual meeting of the Japan Atomic Industrial Forum, Inc. (JAIF), held on 15 April this year, Junnosuke Kishida, chairman of the Japan General Research Institute, expressed his belief in and laid emphasis on changes in the way of thinking in regard to technical development involved in the commercialization of nuclear fuel cycles. He emphasized the necessity for the introduction of the "group partition" technology into the spent fuel reprocessing process. In other words, it is necessary to recover the platinum group, such as rhodium and palladium (rare metal) contained in waste liquids and residue. If rhodium is recovered from the fuel spent by the nuclear power plants currently in operation, the equivalent to one-fourth of 1.2 tons, the annual total demand of the industry, can be satisfied by so-called "alchemy." Chairman Kishida presented this trial calculation. It can be said that the recovery of the platinum group from spent fuel is a frontier technological development in which spent fuel is likened to an "artificial mine."

The above research and development conducted nationwide, aiming at the peaceful utilization of nuclear power, is being carried out at the Japan Atomic Energy Research Institute [JAERI], the Power Reactor and Nuclear Fuel Development Corp. [PNC], and the Central Electric Energy Research Institute. The Atomic Energy Commission of Japan, however, has decided to promote the above research and development as a national project beginning next year. The Radioactive Waste Disposal Expert Sectional Meeting (Yoshio Ikuta, chairman and chief director of the Energy Research Laboratory), which has conducted the final study of the "Long-Term Plan on Nuclear Power Development and Utilization" (established last summer) for the 21st century, finalized and reported its 12-year program on 11 October. Then, the Science and Technology Agency made a request to the Ministry of Finance for an appropriation of ¥500 million for the first year of the above program.

The above project is called the "Omega Plan," using the last letter of the 24-letter Greek alphabet to represent the task of nuclear power development. Engineering-scale tests involving group partition (nuclide separation) are planned to be conducted not later than the year 2000, aiming at the effective utilization of natural resources, such as the recovery of rare metals from high-level radioactive wastes and residue. Long-life nuclides, such as transuranic elements (TRU), strontium, and cesium, are intended to

undergo "annihilation disposal" and "nuclear transformation" to stable elements capable of reducing radioactivity and preventing its irradiation. This alchemy involves the study and development of the following three items:

(1) Utilization of existing fast breeders
(2) Development of fast reactors to be used exclusively for combustion
(3) Nuclear transformation using accelerators

Technical Development Conducted 17 Years Ago

Before discussing details of the project, it is necessary to first introduce the new technical developments concerning radioactive waste disposal in the"Long-Term Plan" established last year by the Atomic Energy Commission of Japan.

"Nuclides contained in high-level radioactive wastes undergo group partition according to their half-life, purpose of use, etc., and the necessary nuclides are utilized effectively. Along with this, long-life nuclides are transformed to short-life nuclides or nonradioactive nuclides (annihilation disposal). This is a very important research subject when converting high-level radioactive wastes to resources and improving the efficiency of disposal. To this end, JAERI, PNC, etc., must cooperate in systematically carrying out the necessary research and development work." (Excerpt from Chapter 2, "Nuclear Power Generation and Nuclear Fuel Cycle," Section 4, ("Radioactive Waste Treatment and Disposal.")

High-level radioactive waste liquids are solidified using borosilicate glass, confined in a steel canister, and stored for 30 to 50 years while being cooled to remove decay heat. They are finally buried in layers more than several hundred meters below the ground surface. This is the basic policy of the Long-Term Plan that encompasses the 21st century. The Omega Plan is an extension of the above basic policy of the Long-Term Plan, i.e, the pursuit of frontiers of the high-level radioactive waste disposal technology. The relationship between the basic policy of the Long-Term Plan and the Omega Plan is given in Table 1. Another purpose of the Omega Plan is to open the way to effectively utilizing nuclides (produced in spent fuel) other than plutonium. It will also be possible to enhance the required safety (several thousands of years ahead) for the high-level radioactive waste "layer" disposal technology. These issues cannot be disregarded.

Research on the recovery of rare metals and the annihilation of radioactivity is currently being highlighted, although such concepts germinated 17 years ago, i.e., in the autumn of 1971. In order for the concept of nuclear power, "innovative, industrial technology and systems accompanied by radioactivity," to deeply take root in human society, it is necessary to educate the general public concerning the effective utilization of nuclear power. Saying so, Seinosuke Hashimoto, managing director of JAIF, has advocated the necessity of spreading "nuclear culture." He has emphasized, "Unless high-level radioactive waste treatment and disposal technologies are established, the age of the full utilization of nuclear

Table 1. Relationship Between Basic Policy and Omega Plan

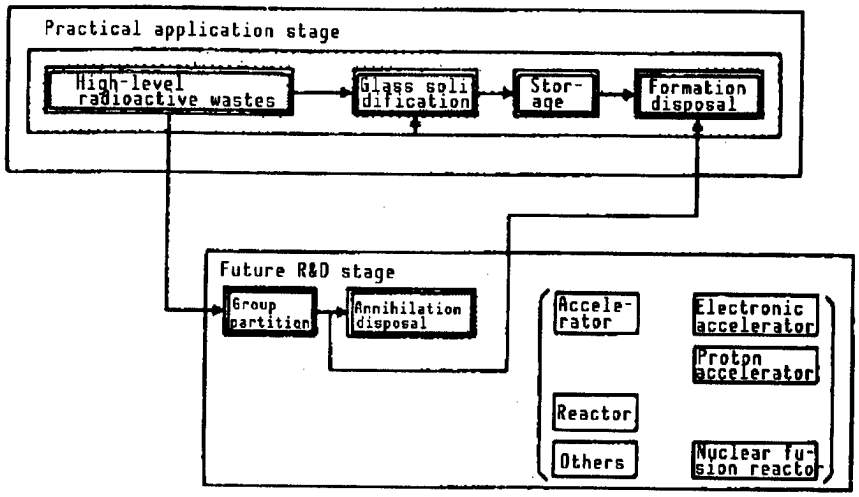

power will never come." Therefore, Hashimoto asked six scholars of the JAERI and the Institute of Physical and Chemical Research (with Kenjiro Kimura, honorary professor, Tokyo University, as the leader) to design research for the recovery of rare metals and the annihilation of radioactivity. This marked the start of research on the recovery of rare metal from radioactive wastes and the annihilation of radioactivity. In spring of 1973, 2 years later, a report entitled, "Radioactivity Closed System Concepts" was prepared. This concept was made public by Professor Kimura at the JAIF annual meeting and was proposed to electric power companies and manufacturers, including the government authorities concerned. With this as a turning point, basic research was initiated at research institutes and universities. Consequently, the "Environmental Safety Research Department" was established in 1978 as a subsidiary organization of JAERI.

In the Long-Term Plan prepared last summer, a policy to further accelerate the above research and development was established. It should be noted, however, that residents are concerned about high-level radioactive waste disposal, raising such cries as "Anti-nuclear power" and "Stop dependence on nuclear power generation" since the accident occurred at the Chernobyl nuclear power plant in the USSR, which is regarded as a turning point. The nuclear power generation promotion side, including the electric industry, must frankly recognize the fact that the commencement of research and development of high-level radioactive waste disposal technology has been delayed due to the fact that it was not studied in earnest 17 years ago.

Overview of Group Partition/Disposal 12-Year Plan

Figure 1 shows the overview of the Omega Plan. Before introducing the details of the plan, the principles of the "group partition" and "annihilation disposal" will be explained.

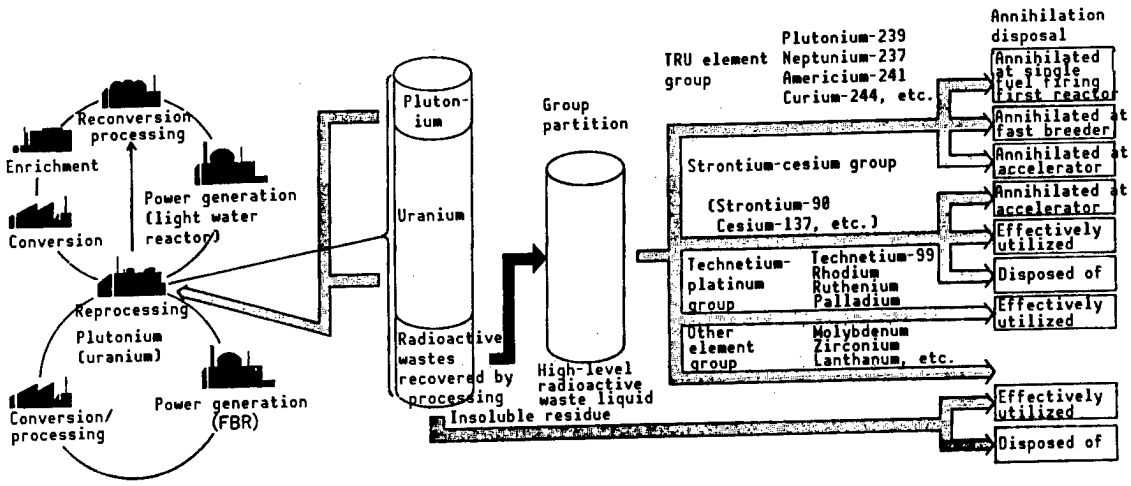

Figure 1. Conceptual Drawing of Group Partition and Annihilation

Spent fuel is reprocessed and is separated into half-burned uranium and plutonium. The remaining radioactive wastes are classified roughly into high-level waste liquids and undissolved residue. Reprocessing of spent fuels produces high-level radioactive wastes at a rate of less than 1 m^3 per ton of spent fuel. Such high-level radioactive wastes contain various types of nuclides, such as the following:

(1) Transuranium (TRU) group having a long half-life;
(2) Strontium-cesium group whose half-life is comparatively short, but whose decay heat is large;
(3) Platinum group elements which are rare metals;
(4) Other element group

These element groups and nuclides undergo chemical treatments, such as extractive separation, and are grouped according to their characteristics. Such a process is called "group partition."

Then, the so-called corpuscular beams, such as neutrons and gamma rays, are applied to grouped elements (1) and (2) to annihilate radioactivity. In this way, the grouped elements are transmutated to "safe elements," and their half-life is also shortened. Such a process is called "annihilation disposal."

Let us explain "annihilation disposal" using element group (2), the strontium-cesium group, which can be explained easily. As mentioned above, glass-solidified products confined in a canister must be left cooled and stored for 30-50 years because strontium and cesium emit decay heat. However, if corpuscular beams are applied to strontium and cesium, their nucleus takes in or emits neutrons according to the types of corpuscular beams, and these elements are transformed to other elements not completely emitting radiation. If proton rays are applied to strontium 90 with a half-life of 28 years, it is transmutated to yttrium with a half-life of 59 days. Further, if proton rays are applied to cesium 137 with a half-life of 30 years, it is transmutated to barium, a "safe element," which does not emit

radiation. Therefore, it is possible to artificially transmutate elements. The above process can definitely be termed the "alchemy" of the day. Practical application of such technology, if achieved, will serve to greatly shorten the cooling and storage period of 30-50 years, and also to noticeably improve economic efficiency in the treatment and disposal of high-level radioactive wastes.

Then, the major goals of the 12-Year Plan established (based on the original draft of the Omega Plan) by the Group Partition/Annihilation Disposal Technology Study Subcommittee (headed by Yurusu Amano, chairman and professor, Plasma Research Laboratory, Nagoya University) and the targets of the institutes executing the above plan are introduced as "group partition" and "annihilation disposal."

Laser Refining of Extracted Rare Metals

Elements and nuclides contained in high-level radioactive waste liquids can be separated into the following four groups:

(1) TRU (plutonium, neptunium, americium, curium, etc.)
(2) Strontium-cesium group
(3) Platinum group, rare metal
(4) Other element group

The above separation is a chemical field for research and development. Basic tests and actual waste liquid tests are scheduled to be completed not later than 1996, and process engineering tests are planned to be repeatedly conducted for 4 years so that pilot plant-scale research can be carried out around 2001.

In parallel with the above research and development, it is intended that technology be established for recovering and refining rare metals, i.e., the platinum group (ruthenium, rhodium, palladium, etc.) contained in undissolved residue, which, unlike high-level radioactive waste liquids, is discharged during reprocessing.

As shown in Table 2, rare metals are indispensable for Japanese hi-tech industries. Japanese industries, however, depend greatly on overseas markets for the supply of rare metals and, therefore, are placed in a very unstable position from the standpoint of securing future natural resources. The United States has already started storing such rare metals as international strategic materials. These are the reasons that the technology for recovering and refining the platinum group from undissolved residue is receiving so much attention. Such technology, therefore, can be referred to as "resource producing technology."

Ruthenium of 1.7 kg, rhodium of 0.4 kg, and palladium of 0.9 kg can theoretically be recovered per ton of spent fuel. Consequently, ruthenium (1.2 tons), rhodium (0.3 tons), and palladium (0.6 tons) are potentially contained in 600 tons of spent fuel (taken from electric power companies during 1985).

Table 2. Demand and Supply of Platinum Group Elements

	Ruthenium	Rhodium	Palladium
World production quantity (ton)	11	6.6	100
Japan's consumption (ton)	1.9	2	45
Major use worldwide [() shows percentage of use]	• Electrode materials (46%) • Electronics industry (45%)	• Catalyst for metals for vehicles (49%) • Chemical industry (21%)	• Electric/ electronics industry(41%) • Dental treat ment (31%)
Price Yen/g	250	5,500	500

At the Tokaimura Reprocessing Plant, the PNC is continuously conducting the research and development of technology for recovering rare metals from "raw materials," i.e., spent fuel, and refining them so that they can be used similarly to natural resources.

The PNC has already developed the method of refining recovered platinum group metals using laser beams, as shown in Figure 2, in order to remove radioactive substances from the recovered metals.

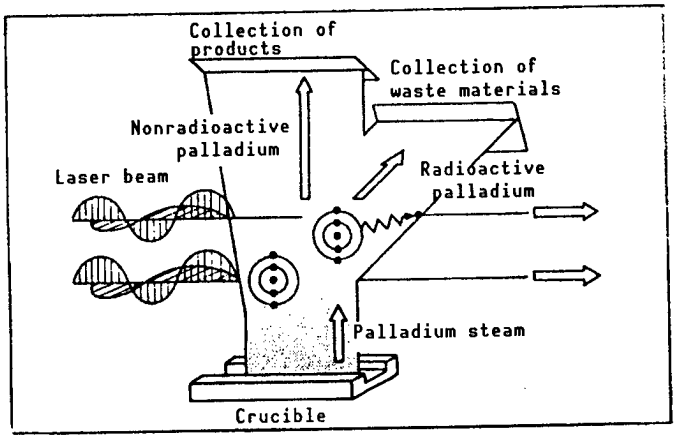

Figure 2. Conceptual Drawing of Palladium Laser Isotope Separation Process

Utilization of Accelerator To Expedite Annihilation Disposal

The Omega Plan describes three major "annihilation disposal" systems to change group partitioned radioactive wastes (after radioactivity has been annihilated) to "stable elements" or to shorten the half-life. In other words, the following three measures can be cited if arguments are narrowed

to include only TRU radioactive wastes whose half-life can be measured in 10,000 year units. Nuclides contained in TRU radioactive wastes are fissile materials and are burned (transmutation), together with fuel, in the prototype reactor "Monju" (scheduled to be operated n the near future) and other demonstration reactors, including the "Jo-yo" (fast experimental breeder), currently in operation. Fast reactors exclusively used for burning TRU nuclides have been developed. Further, spallation (transmutation) is carried out using electron accelerators or proton accelerators. The former two types of fast breeders are utilized as will be described later, with test irradiation scheduled to be initiated in 1990 using the Jo-yo. Reactor physical data are intended to be available not later than the year 2000 in order to prepare for the conceptual design of single fuel firing reactors.

As a final measure, TRU spallation using high energy protons is intended to be used by accelerators for annihilation disposal. Along with this, TRU nuclear fission caused by "strong" neutrons generated by TRU spallation will be used for annihilation disposal. To this end, the construction of a 10 mm ampere, 1,500 million electron voltage class accelerators, capable of applying protons to TRU nuclides, will commence around 1993 for the preliminary development of the elementary technology required for practical-scale accelerators, which is intended to be started around 2001.

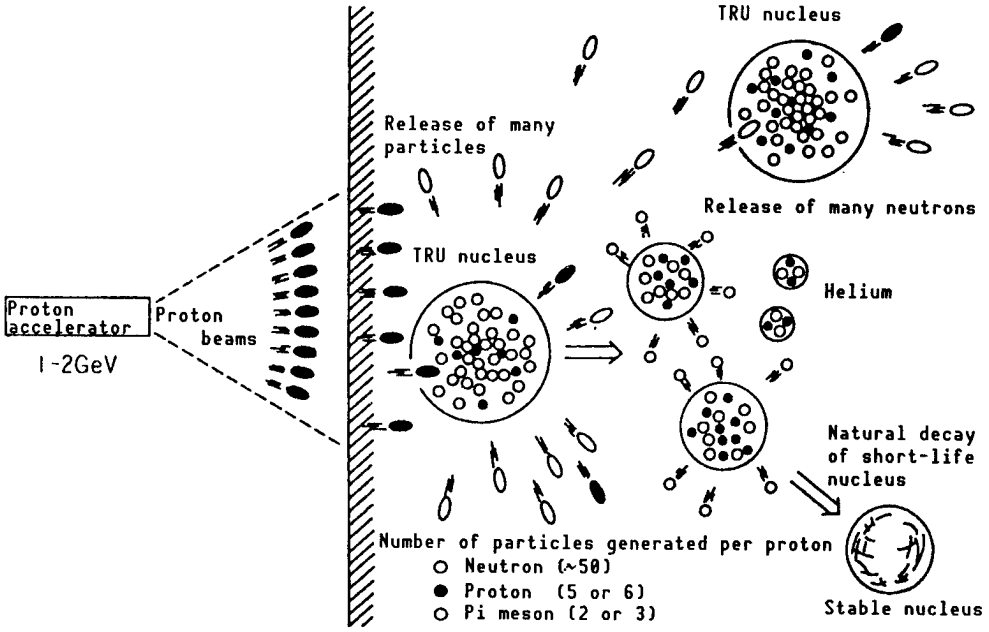

Figure 3. Annihilation Disposal of TRU Nucleus Using High-Energy Protons

JAERI has conducted continuing research on proton accelerators characterized by their fast annihilation disposal rate (Figure 3, a conceptual drawing). In order to utilize the "strong" neutrons generated by spallation, the amount of "burning" uranium contained in natural uranium must be increased

after the annihilation disposal of TRU nuclides has been completed. Therefore, JAERI is forming concepts for a double-purpose nuclear power plant with certain breeding functions.

However, JAERI is also attempting to achieve the annihilation disposal of a wide range of nuclides, such as strontium, cesium, and TRU, by developing large-current proton accelerators utilizing the electronic accelerator technology currently underway at the industrial level. JAERI plans to start constructing an electronic accelerator of the 100-milliampere, 100 million electron voltage class around 1993, so that annihilation disposal tests can be started around 2001 using a pilot plant.

PNC intends not only to carry out research on long-life TRU nuclides, but also to shorten the cooling period of vitrified products put in a canister. PNC, therefore, has already applied for a patent on a system in which the said accelerator, although small in scale, can be manufactured by Japanese technology. This electronic accelerator system is illustrated in Figure 4.

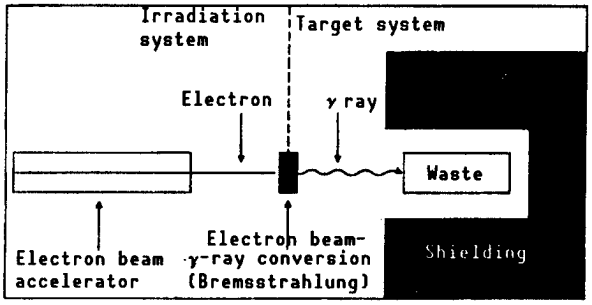

Figure 4. Conceptual Drawing of Nuclide Transformation Test System Using Gamma Rays

Configuration of Development System

It seems that the above problems must be settled under the direction of the Atomic Energy Commission of Japan. The practical application of "annihilation disposal" depends greatly on the progress of the "group partition" technology, as well as on the development of good accelerators, just as the nuclear fuel cycle technology is indispensable for nuclear power generation.

It is not easy to recover the platinum group, which is the leading technology of the group partition technology, because many unknown solution and powder chemical issues regarding the platinum group exist from a scientific point of view. Furthermore, it is necessary to resolve chemical/engineering problems such as the economical separation of elements within the platinum group, together with the same plant engineering problems as those confronting spent fuel reprocessing. It is not exaggerating to say that the solution of the above chemical/engineering problems holds the key to the success or failure of the technological development of group partition.

Overseas, it appears that the TRU Research Institute of EC (European Communities) is being confronted with budget shortage problems, although the Institute enjoys an established reputation for its collection of basic data. Japan has decided to tackle, though a little too late, research on group partition and annihilation disposal on a full scale, as seen in the Omega Plan. It may be necessary, therefore, for the Japanese research institutes to promote international cooperation with EC and American research institutes and to offer portions of engineering research to the EC and United States, if circumstances require.

It should be noted, however, that no research and development systems for the Omega Plan are indicated in Japan's 12-year plan. How is the relationship among JAERI, PNC, and the Central Electric Research Institute coordinated? Who is in charge of the Omega Plan? As an advisory council for the director of the Nuclear Bureau of Science and Technology Agency, the government authorities concerned have established the "Radioactive Waste Nuclide Partition/Annihilation Disposal Technology Development Promotion Committee" (chairman, Hiroshi Yamamoto, honorary professor, Tokyo University) consisting of representatives from academia, the electric industry, and manufacturers. Heavy responsibility, however, is vested with the above committee.

Specifically, radioactive waste problems cannot be handled at the same level as general wastes because the government authorities concerned must also assume the responsibility for disposal. It appears that electric power companies generating radioactive wastes should relinquish their conventional views as a "process industry," and cooperate in the disposal of radioactive wastes.

Collecting Uranium From Seawater

43062024b Tokyo ENERUGI FORAMU in Japanese Nov 88 p 136

[Article by Teruo Nakamura, Research Administration Section, General Affairs Department, Agency of Industrial Science and Technology, Ministry of International Trade and Industry]

[Text] Japan is not rich in natural resources, and cannot survive without securing resources. Therefore, Japan is forced to import most of its oil and uranium resources from overseas, although uranium may be collected from seawater in the future. The Japanese islands are surrounded by the sea and, therefore, if the above dream is realized, unexpectedly large profits will be gained from the sea.

Seawater contains 4-5 billion tons of uranium in solution. The amount of uranium that can be collected on land is estimated to be about 3.5 million tons. These figures show that extensive amounts of uranium dissolve in seawater. To our regret, however, uranium dissolves in seawater at very low concentrations, i.e., about 0.003 ppm, although the concentration differs from place to place. Seawater containing uranium at such a low concentration is worthless and must be concentrated in the range of 1 million to 10 million times.

How can we effectively collect uranium from seawater? Several processes have been devised so far to collect uranium effectively from seawater. However, many problems remain to be solved before the technology for collecting uranium can be developed. Such problems can be classified as follows:

(1) Seawater is a thick electrolytic solution and contains various types of electrolytes in large quantities. Of these electrolytes, the required elements of a very low concentration must be selectively collected.

(2) It is necessary to handle tremendous amounts of seawater. This poses engineering problems.

(3) The pH buffering property of seawater is large. It is impossible, therefore, to vary pH values by processing seawater when handling tremendous amounts of seawater as well.

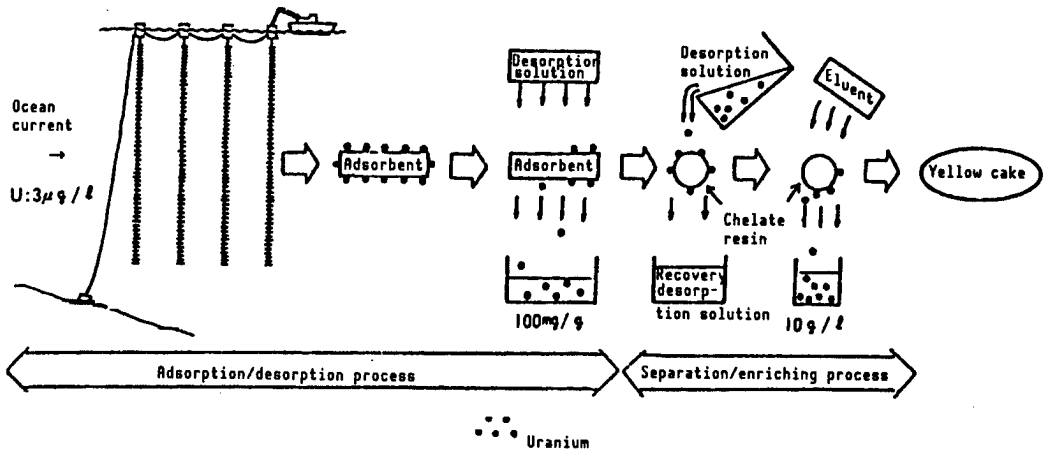

Uranium Extraction From Seawater

(4) It is necessary to assess the effects on the oceanic ecosystem.

When studying the above problems, it is deemed preferable that uranium be collected in such a way as to avoid drawing up seawater, changing pH values, installing large equipment, etc., as illustrated in the figure. The figure shows a method in which uranium comprises the adsorption collected while a large number of adsorbents are suspended in the seawater and exposed to the ocean current. It appears that as the adsorbent, an amido compound type fiber is superior in adsorption rate, adsorption performance, durability, handling, etc. This adsorbent is being studied by the Shikoku Industrial Science and Technology Laboratory, Agency of Industrial Science and Technology. Improvement of the fiber is serving to enhance the uranium collection rate every year, i.e., the adsorption of 2.6 mg/g of uranium in 10 days is possible. We are optimistic of the extent to which the adsorption performance can be improved. Therefore, Japan's energy supply structure may be able to be basically changed in the future.

JPDR Decommissioning Sets Standards for Future

43062021 Tokyo PUROMETEUSE in Japanese Dec 88 pp 46-50

[Article by Mitsuo Yokota, Chief of Decommission Section, Power Demonstration Reactor Division, Tokai Laboratory, Japan Atomic Energy Research Institute]

[Text] 1. Foreword

The Japan Power Demonstration Reactor (JPDR) of the Japan Atomic Energy Research Institute (JAERI) succeeded in atomic power generation for the first time in Japan in 1963. Twenty-odd years have passed since the first reactor in the Tokai Power Plant of Japan Atomic Power Co started its commercial operation in 1966. Thirty-five atomic power plants are in operation today, and nearly one-third of the electric power demand in Japan is supplied by atomic power generation.

On the other hand, the life of a reactor is generally considered 30 to 40 years, and the disposal of reactors completing their operation has become a matter of great concern in the world and it is an important factor in the progress of atomic power generation. In Japan, the basic policy on the methods of and measures for disposal of reactor facilities is indicated in the "Atomic Power Development Utilization Long-Term Plan" prepared by the Atomic Power Commission in 1982.

According to the policy, the principle is to dismantle and remove a reactor as soon as possible after completion of its operation. It also indicates that the technology required should be improved and the appropriate legal system be in place by the time atomic power plants are decommissioned. As a part of it, the development and tests of dismantling technology that can be utilized for atomic power plants in the future will be conducted using the decommissioned JPDR of the JAERI. Based on this policy, the JAERI began developing essential atomic reactor dismantling technology under authority given by the Science and Technology Agency as of 1981, and started the JPDR dismantling tests as of fiscal 1986.

2. Development of Dismantling Technology

Atomic reactor facilities to be decommissioned are strong structures containing a large amount of radioactivity. Most of the radioactivity is in the pressure container of the reactor, but some radioactivity is disseminated in the facility through the reactor cooling system, etc.; thus the dismantling of atomic reactor facilities is technically difficult and different from that of ordinary structures. For the dismantling and removal of such atomic reactor facilities, the development of a complicated engineering system that can freely use the dismantling technology in a radioactive situation and can manage the waste disposal and the accurate knowledge of reactor types, the amount of nuclear fuel contained, and the state of radioactivity in the atomic reactor facility is required.

The strong point of the JAERI technology development plan is that it aims at the establishment of a total system covering all technical fields required for dismantling atomic reactors, and it confirms its effectiveness by actually applying the technology in the dismantling of the JPDR, although it is small and used for testing and research, is an atomic reactor facility for power generation. The purpose of the dismantling of the JPDR is not merely offering a place for verification of the developed technology, but also offering useful information and data for the dismantling of atomic power plants in the future.

Figure 1 shows the items of essential technology that have been advanced, and a check and review was conducted on the results of technical development and the progress of the plan by the "Atomic Reactor Dismantling Technology Committee" consisting of men of learning and experience from within and outside the JAERI in 1985 when the development of essential technology was almost completed. As a result, it was found that the required technology was developed as expected, and it was evaluated that the plan should proceed to the next phase of the practical JPDR dismantling test--which was started in December 1986.

At present, the manufacturing of various cutting devices, etc., to be used for dismantling and removing the JPDR has already been completed based on the results of technical development, and their mock-up tests prior to practical use are being conducted in order and the plan is in the final phase.

3. Practical Dismantling Test of JPDR

The JPDR is an atomic power plant with a boiling water reactor of 90 MW (45 MW in the beginning) for testing and research. Since successful power generation in 1963, it has contributed to the experience of operation and maintenance, various tests and research, irradiation tests of fuel, training

of engineers for atomic power generation, etc., and finally ceased operation in 1976. The dismantling test of the JPDR is a plan for the establishment of a safety standard for the disposal of atomic reactors in addition to conducting the confirmation of appropriateness and the verification of technology developed so far.

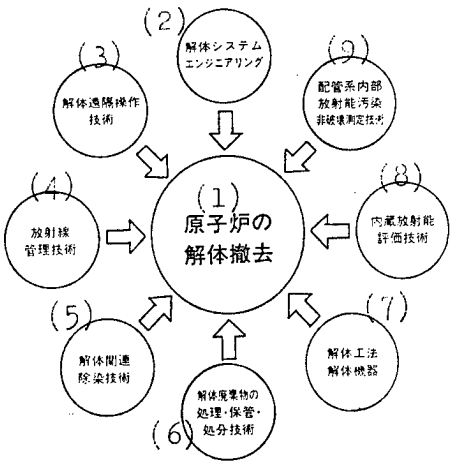

Figure 1. Developed Reactor Dismantling Technology

Key:

1. Dismantling and removal of an atomic reactor
2. Dismantling system engineering
3. Remote-control dismantling technology
4. Radiation control technology
5. Dismantling-related decontamination technology
6. Waste processing, storage, and disposal technology
7. Dismantling engineering and equipment
8. Contaminated radiation evaluation technology
9. Non-destructive technology for measuring radioactivity contained in the piping system

A. Dismantling Plan

When decommissioning the JPDR, the " Report of Decommission" which contained a decommissioning plan, based on the atomic reactor control law and was submitted to the STA in fiscal 1982 during the development of decommissioning technology. The results of technical development were reviewed and the "Report of Change in the Decommissioning Method" was submitted to the STA, and the decommissioning was started in December of the same year.

All the buildings and equipment, etc., at the site, excluding the office buildings in the non-radiation control area, are the target of dismantling and removal, and the ground will be leveled after the facility is removed. About 99.9 percent of radioactivity contained in the facility is concentrated in the atomic reactor pressure container, structures in the reactor, and the shield; the amount of contamination in other equipment, pipes, and buildings is about 0.1 percent. The remaining radioactivity immediately after stopping operation of the atomic reactor was 20,000 curies, but it is down to about 4,600 curies at present; it still contains many nuclear species, such as cobalt-60 and iron-55. The highly contaminated structures, such as the atomic reactor pressure container, the structures in the reactor, and the shield, will be dismantled by the remote-control cutting technology developed. The reactor containment and the building are to be removed in the final stage of dismantling because they will be used to shield the environment from contamination by the radioactive dust arising from the removal of the contaminated equipment and structures. The radiation monitoring equipment, the ventilation equipment, and the waste water disposal plant are to be maintained and controlled for safe supporting of the radiation control area, and they are to be utilized for the disposal of gas and liquid wastes discharged from the dismantling work.

The amount of the radioactive waste produced by the dismantling of the JPDR is estimated at about 4,000 tons. It is planned to eventually dispose of this waste after the establishment of the laws on rational disposal of radioactive waste. For now, the waste will be kept in the JPDR facility by properly classifying it by type of materials and level of radioactivity. The dismantling period is scheduled for 7 years from fiscal 1986 to fiscal 1992, with 63,000 man/days estimated to be required for the work and the amount of radiation exposure estimated at about 100 persons/rem. Table 1 shows the schedule of the practical test, etc.

B. Process of Dismantling and Removal

The atomic reactor pressure container, the structures in the reactor, the shield for living bodies, etc., are the most difficult targets of dismantling and removal, and these work processes will be critical in the entire work process. Table 2 shows the methods developed for use in this dismantling work, and the dismantling procedures are stated in the following.

Table 1. Schedule for Atomic Reactor Dismantling Technology Development and Practical Dismantling Test of JPDR

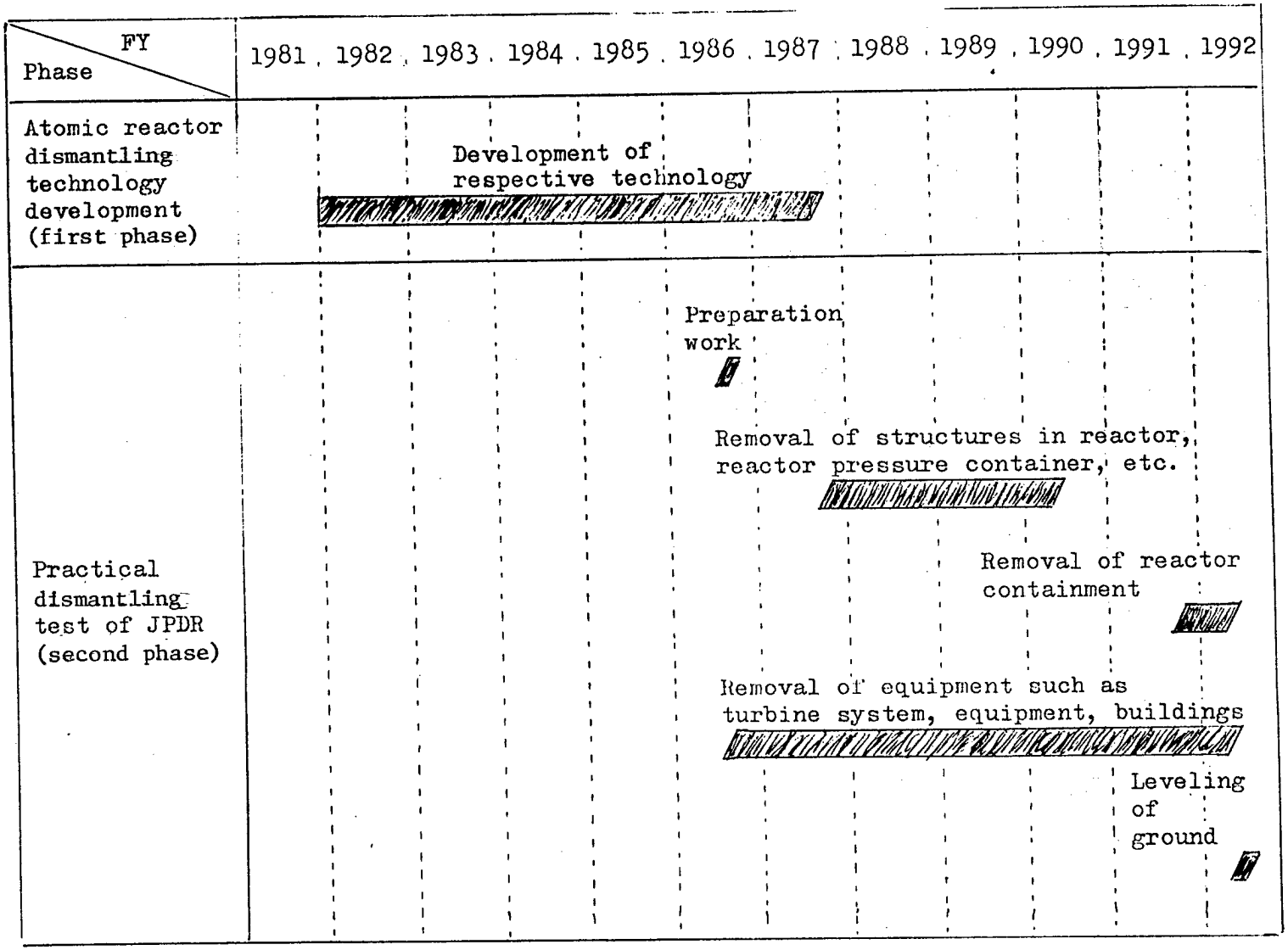

The removal work in the atomic reactor containment will be conducted as follows: 1) Remove the atomic reactor's peripheral equipment first and make the work in the narrow containment thereafter easy; 2) next, remove the structure in the reactor which is separated from the pressure container using the remote-control underwater plasma-arc cutting technology; 3) then, cut and remove the pipes connected to the pressure container. The shaped charge that can be remote controlled and the disc-cutter technology will be applied for this work. Some pipe cutting is conducted underwater, but the pipes in the forced circulating cooling system are cut after the water is drained; and 4) before cutting the pressure container, a cylindrical tank is placed in the gap between the pressure container and the shield, which is filled with water. The pressure container is cut horizontally and vertically in this water by the arc saw technology, 5) for dismantling the highly activated area of the shield, the technology of the diamond cutter that can be used by remote-control, mechanical cutting by core boring, and water-jet cutting using abrasives are applied. For an effective disjointing of the low activated area, the control explosion technology is applied.

The existing cutting equipment is mainly used for the dismantling of the facility excluding the reactor body, etc. Buildings are dismantled after removing contaminated floors, walls, etc., and canceling the designation of the controlled area. Figure 2 shows the procedure for the atomic reactor containment.

Table 2. Targets of Dismantling and Dismantling Engineering

Targets of dismantling	Dismantling engineering
Atomic reactor pressure container	Arc saw cutting
Structures in the reactor	Plasma arc cutting
Pipes connecting to atomic reactor pressure container	Disc cutter cutting Shaped explosion cutting
Living body shielding concrete	Mechanical cutting Water jet cutting Controlled explosion

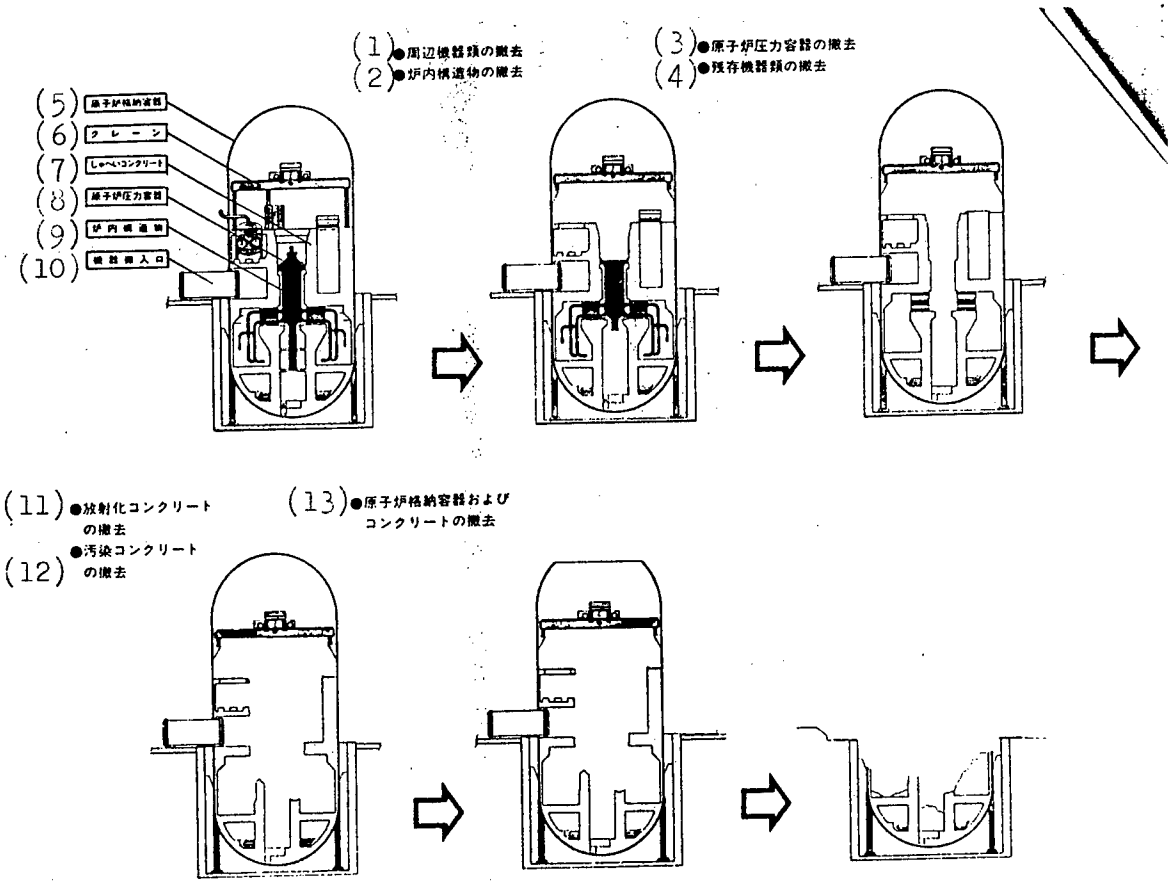

Figure 2. JPDR Atomic Reactor Containment Dismantling Procedure

Key:

1. Removal of peripheral equipment
2. Removal of structures in the reactor
3. Removal of atomic reactor pressure container
4. Removal of residual equipment
5. Atomic reactor containment
6. Crane
7. Shielding concrete
8. Atomic reactor pressure container
9. Structures in the reactor
10. Equipment carrying-in place
11. Removal of activated concrete
12. Removal of contaminated concrete
13. Removal of atomic reactor containment and concrete

C. Progress of Dismantling

The dismantling work is started from the removal of the upper lid of the reactor pressure container. The dismantling and removal of the reactor's peripheral equipment in the reactor containment have been almost finished by that time. The dismantling and removal of the dump condenser building equipment that were conducted at the same time were almost finished, and the site whence the equipment was removed is used for a temporary storage place for the dismantled waste. All of this dismantling work has been smoothly progressing, and the dismantling of the structures in the reactor was successfully conducted with the plasma arc cutting device by robots. Figure 3 shows the concept of this work. At present, the dismantling of the incore structures, the fuel frame, etc., kept in the containment is in progress.

As preparations for the dismantling and removal, such things as the identification of the scope of dismantling and the classification of radioactive level by marking the piping and equipment, the drainage of the system, and the cutoff of the power source are important for safety. These tasks were completed by personnel familiar with the JPDR facility, and the dismantling work is progressing smoothly. About 20,000 man/days were spent as of the end of August, with radiation exposure about 600 person/millirem.

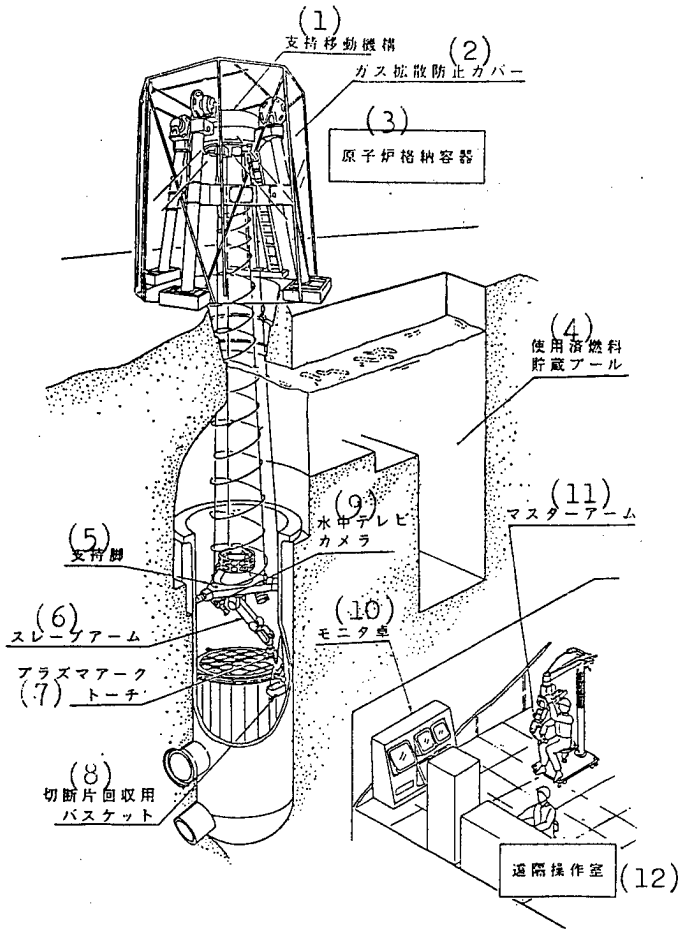

Figure 3. Conceptual Sketch of Underwater Plasma Arc Cutting Work Using a Robot

Key:

1. Support-moving mechanism
2. Gas diffusion prevention cover
3. Atomic reactor containment
4. Used fuel storage pool
5. Supporting leg
6. Slave arm
7. Plasma arc torch
8. Cut-piece-collecting basket
9. Underwater television camera
10. Monitor console
11. Master arm
12. Remote control room

4. Conclusion

The JAERI project has been called the main technological development on the decommissioning of an atomic reactor in Japan. Other countries are advancing their projects in this internationally important subject. Their contents vary depending on the conditions of facilities and the situation of the country. As one of the international exchanges, the Organization for Economic Cooperation and Development (OECD) started a "Cooperation Plan for the Exchange of Science and Technology Information on Atomic Reactor Facility Decommissioning Projects" in late 1985 to collect these various technologies and experiences systematically. At present 9 countries and 12 projects are participating in this cooperation plan. The JAERI, as an organization, and the JPDR as a project, are participating in this plan from Japan. Since international cooperation has been increasingly active every year, it is believed that a reactor decommissioning technology that can obtain worldwide concurrence will be established.

STA Projects, Budgets for 1989

43066143 Tokyo PUROMETEUSU in Japanese Dec 88 pp 72-80

[By General Affairs Division, Director General's Office, Science and Technology Agency]

[Text] Promotion of science and technology is one of the most important issues on the national agenda facing us today as we are about to enter into the twenty first century. It is a vital concept for ensuring the continuing prosperity of Japan and of the world, and for establishing an ensuing world peace. In consideration of the gravity of the issue, the Science and Technology Agency [STA] has been actively engaged in implementing strong policies in accordance with S&T Policy Guidelines (cabinet approval 28 March 1986).

Today, Japanese economic activity on the international scene is hitting an all time high, and the call of foreign countries for Japan to play an active international role in the advancement of science and technology is even louder.

Under these circumstances, STA has renewed its commitment to advancing Japan's contribution to world science and technology and at the same time promoting domestic advancement in basic areas of science and technology to ensure Japan's continuing leadership role.

I. International S&T Cooperation

Expectations are high that Japan will make even greater contributions to science and technology than ever before. In this regard, STA will push the implementation of the human frontier science program, and will establish a new organization for the comprehensive and systematic management of research projects designed to promote international cooperation. The agency is particularly committed to the formulation of policies which echo support for the concept of reciprocity in scientific exchange, an issue raised by many Western nations.

1. Human Frontier Science Program: Establishment of Overseas Management Offices for Management and Financial Support

Through the advancement of creative endeavors in basic research, contributions may be made to the welfare of the world community, as such efforts lead to fundamental innovations which become the common assets of mankind. In pursuit of this concept, STA will sponsor a multilateral basic research program, namely the human frontier science program, which seeks to reveal outstanding human biological capabilities. A non-profit organization with overseas offices will be established to coordinate the operation of the program. The aim is to set up an international framework which will be more conducive to tapping the full potential of the program. Funds for execution of the program will be channeled through this organization.

2. Organization for S&T International Cooperation: Accommodation of Foreign Guest Researchers

An administrative body, provisionally designated as the Organization for S&T International Cooperation, will be established to coordinate the overall operation of programs for the international exchange of research personnel and information. The aim is to create a dedicated office with a streamlined management environment. Also, the office will be responsible for providing accommodations and counseling for foreign researchers, who may find it difficult to make a successful transition to Japanese life.

3. International Cooperation Projects

STA will be instrumental in promoting multilateral scientific research projects, i.e., the international space station and nuclear fusion programs, and the collaborative programs by the Summit nations for photosynthesis research and the design of testing procedures for advanced materials. The agency will seek opportunities to support S&T projects being conducted by international organizations. It will uphold the spirit of the scientific cooperation agreements Japan has made with other nations. In this respect, Japan's S&T ties with the United States are especially important. Since a new agreement was reached and put into effect in June of 1988, there will be ample opportunities to push collaborative research programs, and to construct an even more mutually beneficial relationship.

International fellowship programs for basic scientific research will be implemented, and the International Frontier Research System which receives guest researchers from foreign research institutions of developed and developing countries will be supported. In the area of atomic energy, technical assistance programs, e.g., the atomic energy research exchange program, will be expanded in order to generate active involvement, on Japan's part, in world nuclear energy research. Also,

surveys will be taken to identify the requirements of neighboring Asian countries for assistance in atomic energy research.

With regard to the international proliferation of research information, efforts will be made to translate research literature published in Japan into English, and to maintain a working English database which may be accessed online from anywhere in the world via the International Scientific Information Network. Also, the development of a realistic machine translation system will be pushed.

II. Promotion of Creative Basic Research

It is becoming increasingly critical for the Japanese to break away from the conventional mold of borrowing ideas and improving upon them, and to become more independent in the basic areas of science, the creation of original ideas and products. A true scientific contribution to the world community can best be made in this way.

1. Basic Science Fellowship Program

Often it is the younger generation of researchers who make significant contributions to basic research. It takes original and innovative thinking to initiate a pioneering effort. The responsibility of policy makers is to ensure that these individuals can work in a low-interference environment.

In this regard, STA will establish a fellowship program with the Institute of Physical and Chemical Research [RIKEN]. Aimed at stimulating innovative work in basic areas of science, the program will be designed to provide aspiring researchers with more freedom in their research pursuits.

2. Program for Advancement of Creative Studies in S&T

The program for advancement of creative studies in S&T, operated by the Research Development Corporation of Japan will be carried over this year. The program seeks to mobilize outstanding researchers from industry, academia and government, in and outside of Japan, under common leadership for a predetermined length of time, and to help plant the seeds for creative research topics in S&T.

For fiscal 1989, the program will continue coverage of the 12 topics carried over from last year, such as that of the quantum wave. Added to these are 3 new topics: phase information, atomic-level control of the surface, and genome dynamism.

3. International Frontier Research System

The International Frontier Research System was set up with RIKEN as a lab committed to long term programs for advancement of basic research in

pioneering areas of science. These programs will provide the vital ground work needed for technological revolution in the coming century. Designed to be flexible in recruitment, the system will invite scientists from diverse fields to work on unexpolored topics.

For fiscal 1989, the topics of physiological homostasis, frontier materials, and cognitive processes will be continued. The construction of a new laboratory dedicated to cognition research will commence.

III. Modernization of R&D Facilities

Rapid advances in science and technology have led to a shift in research orientation toward highly specialized and complex topics that often encompass multiple disciplines. Under such extensive research conditions, heavy investment in research facilities has become increasinly critical. The agency is actively implementing a wide range of policies including tax incentives and loan programs to encourage installation of large scale research facilities and equipment for the shared use of basic pioneering research. These policies will be also designed to support S&T programs for regional research, programs of interdisciplinary research, and research exchange programs for both information and research personnel, in an effort to consolidate the diverse efforts of different institutions.

1. Construction of Large SOR

It is believed that the large-scale synchrotron orbit radiation (SOR) facility will play a significant role in basic research in a broad range of fields: materials science, life science, information science, electronics, and nuclear science. SOR is also considered critical in advancing optical engineering. Regardless of the applications, it is important to design such a facility with special provisions supportive of international team work. The design work will be carried out jointly by RIKEN and JAERI. Construction will begin in fiscal 1989.

2. Promotion of Regional Research

In order to maximize the research potential of selected regional areas of Japan, and at the same time to upgrade their research capacity, a research information network connecting these areas and Tsukuba Academic New Town will be constructed. Supplimentary programs will be drawn up which will take advantage of the network to promote researcher exhange, joint research, and the transfer of lab work to industrial applications. Fiscal 1989 will see a couple of new developments. The high-tech consortium system of the Research Development Corp. will be put into effect to accelerate regional research in pioneering fields. In accordance with the (multi-polarized national land utilization act), interest-free loans from Japan Development Bank will be provided to regional labs for installation of facilities for basic pioneering

research with the aim of promoting the improvement of regional economies and strengthening the overall national research capacity.

In a related matter, research in ocean engineering will be pushed under ongoing joint regional research and development projects participated in by the national government and concerned prefectural offices.

3. Research Exchange between Industry, Academia and Government

STA laboratories will be instructed to organize projects of joint research work with private industries. These projects will be carried out with funds from the special government-private company joint research program. Also, the guest researcher program will be taken advantage of in this regard. Researchers of public institutions will be encouraged to attend scientific conferences and seminars. Training programs will be given to them as well.

Another measure utilized to strengthen ties between government research labs and private institutions is the continuation of the high-tech consortium system this year. In this program, researchers at national research institutions, mainly the Research Development Corp., will cooperate with private corporations in developing applications based on the results of basic research produced under government programs, e.g., the program for advancement of creative studies in S&T. Basic patents that the government holds have enormous potential for yielding useful applications.

Finally, the Research Development Corp. will provide contracts to private companies for research jobs. This is yet another drive to transfer emerging technology from government labs to industrial applications.

4. Exchange of S&T Information

In order to update the S&T information exchange system, the Japan Information Center of Science and Technology will implement several measures. Data bases of scientific literature will be expanded. Fact data bases with experimental data will be updated. An online service will be available to provide research information. A new Online Information System (JOIS-III) will be developed. Once inaugurated, JOIS-III will provide researchers with access to an integrated environment full of research literature and experimental data. Also, programs for the promotion of the international exchange of scientific information will be devised.

5. Tax Incentives and Loans

Vital to the advancement of science and technology is the sustenance of research strength by the private sector. In this respect, the current taxation system will be reviewed, and a proposal will be written in

support of S&T research related activities. Also, a loan program will be devised to provide interest-free loans from the Japan Development Bank to qualifying private companies.

IV. Administrative Functions for Comprehensive Promotion of S&T Activities

The administrative functions of STA need to be strengthened in order to handle the load of additional tasks. In particular, an increase in the budget for the S&T advancement fund will be sought. The agency's S&T policy making process will be revamped. Administrative functions responsible for the planning and coordination of S&T projects will be strengthened. Also, public relation programs will be expanded to reach not only the Japanese people but also the people of foreign countries, since the support not only of the Japanese public but also of the international community is critical for a successful S&T advancement campaign. To handle the increase in educational tasks, the agency's public relations functions will be upgraded.

1. S&T Advancement Fund

The Council for Science and Technology has issued guidelines for stepping up across-the-board research efforts in vital areas of science. To handle the coordination of added programs effectively, a budgetary increase for the S&T advancement fund will be introduced. The programs which will be expanded are the fellowship program for foreign guest researchers--a support program for basic research projects requiring recruitment of short-term international personnel--the resource consolidation program for establishing closer ties between industry, academia and government, and the vital basic research program.

2. S&T Policy Research

Guidelines for designing major national S&T policies are formulated by the Council for Science and Technology which is the nation's supreme decision making organ for S&T matters. Assessment functions of the council's policy committee are critical for timely formulation of comprehensive policies, and thus are in need of constant upgrading. Thus, the committee's ability to perform such assessments will be reassessed, and the appropriate action will be taken for improvement.

The influence that today's science policy exerts is extensive. Not only does it affect domestic social and economic activities, it can also complicate international relations. Thus, obtaining accurate assessment data for policy formulation in a timely fashion is critical. In this regard, policy research functions of the Science and Technology Policy Research Institute will be strengthened. Also, programs for involvement in policy research with other governments will be sought.

3. Public Relations Functions

Successful implementation of S&T policy is not possible without wide support from the Japanese public. Also, support and collaboration from other countries are becoming increasingly indispensible. Strong public relations functions will be an integral part of the effort to win this support. Therefore, comprehensive efforts will be mounted to boost the government's PR functions, i.e., the preparation of promotional literature, the making of documentary films, the broadcasting of special interest programs via television and radio, and the holding of public hearings. Opportunities will be sought to inform and solicit support from scientists and science related institutions in foreign countries as well as from those in Japan's regional areas.

V. R&D in Leading-Edge, Vital S&T Areas

1. Development and Utilization of Atomic Energy and Plans for Safety Issues

Nuclear power is positioned as Japan's primary source of energy. The design of a R&D policy for the applied technology of nuclear energy is guided by the long term program for atomic energy development and utilization which was revised in June of 1987. Gaining support from the public is of the utmost importance, and patience is the key to making progress in research in this area. The primary concern of the national government continues to be the upgrading of reactor safety. The implemention of safety measures notwithstanding, several other issues will also have to be given priority consideration. These are the establishment of a complete [domestic] nuclear fuel cycle technology, the development of an advanced reactor design, and research in nuclear fusion. In promoting these programs, special attention will be paid to innovative research works as they hold the key to development of brand new technologies. Finally, supplimentary programs will be planned to gain public support for nuclear energy.

(1) Strengthening of Safety Measures and Compliance with Nuclear Non-Proliferation

In years past, [the government and industry] have put forth maximum effort in securing reactor safety by effecting strict regulations and security control. Stringent controls will continue with increased intensity. More administrative effort will be put into the design of tougher safety regulations. The ability to monitor radiation leakage into the environment will be strengthened. The subject of disaster prevention will be given extra consideration in producing stronger measures for accident prevention. Research in reactor safety will be stepped up. Stronger measures for the prevention of radiation induced hazards will be introduced.

Compliance with the nuclear non-proliferation treaty will be sought. Measures that warrant accident free use of nuclear energy will be put into action. Tighter security for radioactive waste materials will be organized.

(2) Nuclear Fuel Cycle Technology

Achieving independence in nuclear fuel cycle technology continues to be a primary national goal. In this respect, active efforts will be mounted to execute and coordinate nuclear energy related projects. These efforts concern the survey of uranium mines abroad, the construction of commercial cascade testing equipment, the development of a laser-based uranium enrichment technology, the development of a spent fuel reprocessing technology, research in nuclear fuel processing technology for fast breeder reactors, and research in radioactive waste treatment and disposal, i.e., radioactive nuclide separation and incineration technologies. Private programs to build nuclear fuel cycle-related facilities by industrial concerns will be reviewed, and will be given appropriate administrative support and financial incentives designed to expedite the venture.

(3) Development of Advanced Power Reactor

Construction will continue on the prototypical fast breeder reactor "Monju". At the same time, the irradiation test and other fact finding tests will be conducted with the experimental reactor "Joyo".

As part of the development of a new converter reactor, the project for the test running of the prototype reactor "Fugen" will be initiated. This will be followed by design work on a commercial model.

(4) Construction of High-Temperature Engineering Test Reactor and Promotion of Pioneering Nuclear Fusion Research

Ground breaking research will be launched in the design of a high-temperature gas reactor to establish a viable technological basis and to advance the level of Japan's high temperature engineering resources. In particular, a test reactor will be constructed, and with it, pioneering efforts will be mounted in basic aspects of the technology.

In the area of nuclear fusion, the series of experiments with the JT-60, the engineering testing facility for studing critical plasma-density states, will be continued. Related studies, i.e., plasma confinement, and reactor design, will be actively sought. Also, Japan's participation in the program for the International Thermonuclear Experimental Reactor (ITER) will be pushed.

In the area of radialogical sciences, development of applied technology continues to be of vital interest to Japan. In this respect, the construction of the heavy particle [accelerator] facility for cancer

treatment will be continued, and experiments using the research-purpose heavy ion accelerator will be continued.

With respect to the R&D program for nuclear-powered vessels, data collection using the nuclear vessel "Mutsu" is the primary task. The goal is to establish the research basis for design of a motor for commercial liners. A minimum number of experiments aboard Mutsu will be carried out to test the power output characteristics of the ship's engine, among other items. In the meantime, the evaluation of proposed design modifications for next-generation reactors will be continued.

(5) Support Technologies

In order to establish a firm foundation for building an advanced nuclear engineering facility, and to lay the ground work for emerging innovative technologies, active efforts will be mounted in nuclear and laser research by using the resources of JAERI, the Power Reactor and Nuclear Fuel Development Corp., RIKEN, and other national labs. In particular, programs for reactor materials, artificial intelligence for nuclear reactor [operation], lasers used in nuclear reactors, and risk evaluation and reduction of radiation exposure will be continued. Also, the program for particle physics experiments with a tandem accelerator will be continued, and basic research on the fast converter light-water reactor will be shifted into high gear. National research resources and facilities will continue to be made available to industrial and academic concerns to consolidate public and private efforts.

(6) Measures to Obtain Public Support

Public support is essential for successful implementation of nuclear energy programs. Relocation/compensation programs, e.g., compensation from the (compensation fund for reactor site selection) which was created under the (three power facility construction acts), will be designed to improve the welfare of residents near planned reactor sites. Also, public hearings will be held to provide the public with a comprehensive matter-of-fact explanation regarding nuclear energy. At the same time, improvements in nuclear power generation safety will be made by conducting more verification tests on safety-related reactor functions.

2. Space Technology

With respect to the exploration of space, mankind's new frontier, research emphasis will continue to be placed on gaining technological self sufficiency. Attaining reliability and safety in the technology is essential. By mobilizing the resources of the National Space Development Agency [NASDA], the development of artificial satellites for commercial use in communications, broadcasting, the monitoring of meteorological and oceanographic phenomenon, and surveys of geological resources, as well as the development of rocket systems to launch these

satellites will be actively pursued. Also, to expand the scope of Japan's space exploration, projects related to Japan's participation in the [multilateral] space station program will be implemented.

(1) Space Transport System: H-II Rocket

The high demand for the launching of large satellites is anticipated in the 1990's. To meet this demand, the H-II rocket project has been conceived. It seeks to develop a satellite launcher with a payload capacity of about 2 tons. The present stage of development concerns preparation for the planned launch of the first test model in 1991. For this purpose, active efforts are under way.

In a related move, a research program will be inaugurated to develop Japan's own reusable space orbiter, called HOPE, that will be launched aboard an H-II rocket. Such a vehicle will provide an effective means to bring back to earth the fruit of research conducted in a space station in the future.

(2) Artificial Satellites

The development of the broadcasting satellites BS-3a and BS-3b (scheduled for launch in 1990 and 1991, respectively) will be continued. These satellites will provide relay capabilities for communication and broadcasting concerns. Also, research will be begin in geostationary satellite-based data relay and tracking technologies. In particular, the experimental data relay and tracking satellite (EDRTS) will be developed.

To respond to the need for monitoring of geological resources and phenomenon, various satellite development programs have been initiated. Ongoing projects deal with the development of the geostationary meteorological satellite GMS-4, the marine observation satellite MOS-1b, the earth resource satellite ERS-1, and the geostationary meteorological satellite GMS-5. Also, the development of the advanced earth observation (platform) engineering satellite ADEOS will be pushed.

The development program for the engineering test satellite ETS-VI will be continued as well.

(3) Space Station Related Projects

A space station can provide a significantly improved working environment in space, and can make space activities that were unimaginable before come true. It can add a whole new dimension to the concept of space exploration, not to mention the wide range of spin-off benefits it may bring to our understanding of space science, to the promotion of space environment utilization, to the advancement of leading edge technology, and to the encouragement of international cooperation.

Japan is scheduled to participate in the [international] space station program by contributing its own space laboratory to the station facilities. This lab is called the Japanese experiment module JEM, and is scheduled for launch in 1996. Currently, active development efforts are under way.

Administrative preparation will be conducted to guarantee successful participation by Japan in the planned multilateral collaborative activities which will follow the completion of the JEM development.

The ongoing project for developing a reusable space freeflyer unit (SFU)--for conducting diverse space experiments and monitoring tasks--will be pursued. As part of the national effort to establish a firm research footing in space exploration, a new program will be launched to develop a small rocket for space experiments (TR-IA), and to design a crew training system.

With respect to the collaborative space project with the United States to which Japan will contribute by sending Japanese astronauts and engineers aboard the Space Shuttle for conducting materials science experiments--called the first materials production test (FMPT)--the development of the systems for the planned experiments will be continued. Also, in preparation for the planned participation in the first international micro-gravity laboratory program (IML-1), the ongoing development of onboard testing instruments will be pushed.

(4) Basic Research in Space Vehicle Design

The National Aerospace Laboratory [NAL] is developing a reusable reentry vehicle as part of the national effort to come up with innovative space transport technology. The current stage of development involves preliminary designs of orbiter components. This year, component development will be joined by the construction of the testing facility for the vehicle's ram jet engine. NAL will also resume research in liquid oxygen and liquid hydrogen fuels for large rocket engines.

3. Ocean Development

For the sake of the multi-purpose development and utilization of the waters off the Japanese coast, a comprehensive package of diverse research activities will be administered. The Japan Marine Science & Technology Center will act as the principle coordinator in consolidating research efforts by related institutions both inside and outside of Japan.

(1) Deep See Submarine Surveys

The program for the development of the 6,000-meter survey submarine "Shinkai 6500", and its mother ship "Yokosuka" will be continued. Also, the full scale design work for a 10,000-meter unmanned deep-sea probe

vehicle will be started. These underwater crafts will be used to survey sea bed minerals like manganese nodules and ocean techtonics--needed for better earthquake prediction--and to study deep sea marine microorganisms.

Underwater exploration will be conducted by using the 2,000-meter survey sub "Shinkai 2000" teamed with its mother ship "Natsushima", and by using the remote-controlled probe the "Dolphin-3K".

(2) Underwater Technology

Fundamental to the technology of marine utilization is the possession of expertise in underwater work. By using the underwater experiment vessel "Kaiyo", field tests at a depth of up to 300 meters will be conducted with the aim of improving skills for deep water operations.

(3) Comprehensive Utilization of Marine Resources

Japan and China will conduct a joint research project to study the Kuroshio Current. The research into underwater remote survey techniques will be pursued. These represent a part of the ongoing efforts to unravel the mechanisms responsible for the oceanographic changes [around Japanese coasts]. As a related move, research for better marine observational technology will be introduced to develop a laser based distancing technique, and an automatic marine observation system.

In addition, joint projects for marine resource utilization between the national government and local prefectural governments will be pursued. These projects will form a part of the Aquamarine Project which is designed to advance comprehensive utilization of marine resources.

4. Earth Science Research

Studies of abnormal weather patterns and global variations in ocean plate techtonics will be conducted. These studies will have to be backed by sophisticated remote sensing technology. The technology of earth observation satellites will be utilized to develop the needed technology basis. Also, research programs for prevention of natural disasters will be pushed.

(1) Studies of Global Geological Effects

A long term international collaboration project will begin in 1989 to study the mechanism responsible for the generation of the Asian monsoon, and to study deep crust faults in the earth's plates--to unravel the driving force behind plate techtonics. Part of the S&T advancement fund will be spent on studies of meteorological variations over the Pacific Ocean, and the geological structures of ocean plate boundaries.

(2) Technology for Earth Observation

The development of the marine observation satellite 1b, the geostationary meteorological satellites 4 and 5, and the earth resource satellite 1 will be resumed. Coupled with satellite development, the development of remote sensing technology and its application will be pursued. For the latter efforts, Japan's first earth observation satellite--marine observation satellite 1--and the American satellite LANDSAT will be utilized. Research will concern signal processing technology for the processing of data received from these satellites. These technologies will provide Japan with the necessary independence in global monitoring technology.

(3) Prevention of Natural Disasters

The Earthquake Predication Advancement Headquarters will coordinate earthquake prediction-related monitoring activities and research work that is conducted by related geological institutions. The National Research Center for Disaster Prevention will continue research in the areas of earthquake prediction, the study of measures for disaster assistance after earthquakes, typhoons, snow-related disasters, and volcanic eruptions for the Kanto and Tokai regions.

5. Materials Science

Materials science provides a basis for every branch of science and technology. Active research efforts will be provided in this area.

(1) Superconductors

A project category of the Multi-Core Project has been formed for superconductor research with the National Research Institute for Metals [NRIM], the National Institute for Research in Inorganic Materials [NIRIM], and the Japan Atomic Energy Research Institute as the principle "core" member labs. This program seeks to consolidate the research strength of industry, academia and government in order to pursue key and basic aspects of oxide superconductor research. Research in metal superconductor materials will also continue.

(2) Basic Research in Pioneering Fields of Materials Science

NRIM and NIRIM will pursue active involvement in basic research in pioneering fields. In the meantime, the International Frontier Research System will conduct investigations into physical phenomenon of advanced materials applicable to information technology. It is being hoped that such research will lead to discoveries of wonder materials--referred to as "frontier materials" here--which possess such outstanding properties that they can be used to launch a yet-to-be-thought-of field in information science.

6. Life Science

Advancements in life science contribute to improvement of the welfare of mankind through a broad range of applied fields. In this area, research of cancer-related and aging problems will be actively pursued. Also, intensive efforts will be expended on basic research activities for advancement in the pioneering fields of the life sciences.

RIKEN will pursue cancer research by employing recombinant DNA techniques. Funded by the S&T advancement fund, the lab will mount research efforts in developing general purpose support technologies for cancer research. The National Institute of Radiological Sciences will resume work on the program for developing cancer treatment techniques based on radiation treatment, and the program for construction of a cancer treatment instrument which uses the technique of irradiation by heavy particle beams.

RIKEN will also conduct human genetic research. It will analyze the genes in human chromosomes. Genetic findings may bring about tremendous advancements in cancer research, genetic disease research, immunological research, and gerontological research. The genetic research of RIKEN will also cover investigation into the genes of the nervous system and immune system. AIDS research will also be conducted by the institute. The International Frontier Research System will conduct research in cognition processes. It will begin the construction of the cognition research laboratory in the coming fiscal year.

Information-carrying materials found in plants will be studied under funding provided by the program for advancement of creative studies in S&T. The S&T advancement fund will be used to fund life science studies: the development of key technologies necessary for the research of brain functions, and for research concerning the immunological response mechanism.

In addition, the tasks of collecting and preserving the cells and genes of animals and plants in storage facilities (e.g., a gene bank) will be performed at RIKEN.

7. Other Vital Research Areas

o The National Aerospace Laboratory will conduct studies of support technologies needed in development of a hypersonic transport vehicle. This topic is an integral part of the national program to develop innovative aerospace transport support technologies. Results of the completed program for development of the experimental fan jet short take-off and landing plane (STOL) "Asuka" will be organized into a data base. Upgrading of large research facilities will be performed as well. Tasks will include modification of the spiral wind tunnel facility. These facilities constitute the foundation of research and development in aerospace technology.

o Basic research in laser physics will be pushed by RIKEN.

o Formulating a comprehensive policy for utilization of natural resources is critical for the long-term security of Japan. Surveys will be conducted to provide assessment data needed for such policy formulation.

Summary Tables of STA Budget for Fiscal Year 1989

Category	FY88 budget	Proposed FY89 budget	Difference	Comparison to FY88 budget (%)
1. General account	(debt) 140,925 340,410	(debt) 150,052 353,857	(debt) 9,127 13,447	104.0
2. Special account for industrial investment	4,700	5,200	500	110.6
3. Special account for promotion of electrical energy R&D	(debt) 79,410 95,083	(debt) 36,225 106,124	(debt)-43,185 11,041	111.6
(1) Site selection related	15,032	19,135	4,103	127.3
(2) Multi-purpose applications	(debt) 79,410 80,051	(debt) 36,225 86,989	(debt)-43,185 -6,938	108.7
STA Total	(debt) 220,335 440,193	(debt) 186,277 465,181	(debt)-34,058 24,988	105.7

(Prepared in Aug 88, Unit: 1 million yen, (debt): national treasury debt)

Major Budgetary Appropriations

Item	FY88 budget (A)	Proposed FY89 budget (B)	Difference (B - A)	Comments
1. Contributions to advancement of world science	(debt) 42,431 32,377	(debt) 42,732 47,049	(debt) 301 14,672	145.3%
(1) Human frontier science program	0	1,586	1,586	Funds provided to research foundations, both domestic and foreign: Projects: financial assistance to international joint research activities 1,582
(2) Establishment of Organization for S&T International Cooperation	0	(debt) 783 527	(debt) 783 527	Regarded as a special status corporation Projects: accommodations for foreign guest researchers will be provided

Item	FY88 budget	Proposed FY89 budget	Difference	Comments
(3) International S&T Cooperation	/(debt)42,431\ \ 32,377/	/(debt)41,949\ \ 44,936/	/(debt) -482\ \ 12,559/	(including amounts appropriated from other categories) Participation in Space Station Program; nuclear fusion research projects; exchange of research personnel and data (debt) 41,853
General account	(debt) 42,431 31,891	(debt) 41,949 44,451	(debt) -482 12,560	
Special account for industrial investment	486	485	1	
2. Advancement of creative, basic research	5,331	(debt) 797 6,444	(debt) 797 1,113	120.9%
(1) Establishment of special fellowship program	0	105	105	Research environment conducive to innovative research by independent-minded young researchers will be provided
(2) Funding for Program for Advancement of Creative Studies in S&T	3,816	4,546	730	3 new projects: phase information, atomic-level control of surface, genome dynamism (all provisional designations)
(3) Funding for International Frontier Research System	1,515	(debt) 797 1,793	(debt) -797 -278	3 research topics: physiological homostasis, frontier materials technology, and cognition processes
3. Modernization of R&D facilities	9,972	12,010	2,038	120.4%
(1) Construction of large SOR	[612]	[2,051]	[1,439]	(including amounts appropriated from other categories) Basic design work and R&D for the facility
(2) Promotion of regional research	[132]	[347]	[215]	(including amounts appropriated from other categories) Funds for advancement of regional R&D activities

Item	FY88 budget	Proposed FY89 budget	Difference	Comments
(3) Advancement of research exchange between industry, academia & government	2,530	2,652	122	Specially designated government & private joint research programs: 151 High tech Consortium System: 257 New Technology Development Corp.: 1,585 /Total, covering creative science \ and high tech research: \ 6,389/ Limit of contract awards for entrusted development contracts: 5.4 billion yen
(4) Advancement of S&T information exchange	6,769	7,195	426	Funds for Japan S&T Information Center: 7,188 Allocations:
/ General account	2,069	1,995	-74	Database services: 5,127 Online services: 3,523 Development of the new online service system (JOIS-III): 396
\ Special account industrial investment	4,700	5,200	500	Operation and management of International S&T Information Network (STN) 1,136 Development of computer translation system: 227
4. S&T management and administration	9,653	10,718	1,065	111.0%
(1) Fulfillment of S&T advancement fund	9,200	10,100	900	Advancement of basic research with short-term international personnel recruitment
(2) Establishment of S&T Policy Research Institute	252	418	166	Fact-finding studies for S&T policy research
(3) Others	201	200	-1	Public relation works for promoting S&T policies
5. R&D of leading-edge, vital S&T areas	(debt)220,334 417,415	(debt)185,493 438,580	(debt)-34,841 -21,165	105.1%
(1) Development & utilization of nuclear energy & plans for safety issues	(debt)113,304 271,490	(debt) 91,510 279,962	(debt)-21,794 -8,372	103.1%

Item	FY88 budget	Proposed FY89 budget	Difference	Comments		
[General account]	(debt) 33,894	(debt) 55,285	(debt)-21,391			
	176,407	173,738	-2,669	98.5%		
a. Strengthening of safety measures & compliance with nuclear non-proliferation	1,944	1,973	29	Enforcement of reactor regulations:		109
				Security measures, and measures to protect against nuclear theft:		606
b. Japan Atomic Energy Research Institute	(debt) 22,309	(debt) 38,724	(debt)-16,415		(debt)	7,937
	97,310	94,011	-3,299			12,640
				Research of safety measures:	(debt)	13,185
				Nuclear fusion R&D:		22,263
				Allocations:		
				Upgrading of JT-60:	(debt)	12,013
						4,884
				Participation in ITER program:		1,679
				Construction of high temperature engineering test reactor:	(debt)	10,324
						2,044
				Advanced radiation technology:	(debt)	3,607
						4,526
				R&D of nuclear powered vessels:		4,630
c. Reactor & Nuclear Fuel Development Corp.	(debt) 5,431	(debt) 7,580	(debt) -2,149	/Special account for advancement of nulcear power development:	(debt)	43,805
	62,279	61,567	-712	\ Total including above:		143,528
				Development of reactors:	(debt)	5,688
						30,974
				Allocations:		
				Development of fast breeder reactor:	(debt)	3,228
						16,146
				Development of spent fuel processing technology:	(debt)	856
						9,177
				Allocations:		
				Development of highly radioactive waste disposal technology:	(debt)	856
						4,610
				Surveys of uranium mines abroad:		2,406
				Development of uranium enrichment technology:	(debt)	1,036
						2,434
d. National Institute of Radiological Sciences	(debt) 5,704	(debt) 8,545	(debt) 2,841	Production of a heavy particle beam instrument for cancer treatment:	(debt)	8,545
	8,118	9,866	1,748			4,295

Item	FY88 budget	Proposed FY89 budget	Difference	Comments	
e. Nuclear energy research by Institute of Physical & Chemical Research [RIKEN]	(debt) 450 4,283	(debt) 435 3,596	(debt) -15 -687	Heavy ion research: R&D for uranium enrichment technology through use of the laser:	(debt) 435 2,249 419
f. Nuclear energy research at national research institutions	1,815	2,065	250	Aggregated amounts allocated by all governmental agencies for experimental nuclear energy experimental research	
[Special account for measures to develop power resources]	(debt) 79,410 95,083	(debt) 36,225 106,124	(debt)-43,185 11,041	111.6%	
a. Assistance funds for construction of electric power facilities	15,032	19,135	4,103	127.3% Entrusted fund for safety measures for nuclear power generation: Subsidy for developing safety measures for nuclear power generation: Compensation fund for reactor site selection: Special grant for reactor site selection: Grant for developing safety measures for nuclear power generation: Assistance to international institutions:	9,057 289 4,024 2,142 3,432 50
b. Funds for power source diversification programs	(debt) 79,410 80,051	(debt) 36,225 86,989	(debt)-43,185 -6,938	108.7%	
A) Reactor & Nuclear Fuel Development Corp.	(debt) 79,410 75,806	(debt) 36,225 81,961	(debt)-43,185 -6,155	Construction of fast breeder reactor "Monju": R&D in spent fuel reprocessing:	(debt) 33,106 55,207 6,603
B) Miscellaneous	4,245	5,028	-783	Entrusted projects for R&D in nuclear reactor decommissioning technology: Entrusted projects for R&D in uranium enrichment laser technology: Assistance funds for development of radioactive waste disposal technology	2,163 898 630

Item	FY88 budget	Proposed FY89 budget	Difference	Comments		
(2) Advancement of space exploration	(debt)102,604 98,470	(debt) 91,823 108,892	(debt)-10,781 10,422	110.6%		
a. National Space Development Agency	(debt)102,457 96,534	(debt) 91,054 106,627	(debt)-11,403 10,093	Development of H-II rocket:	(debt)	37,372 34,394
				Development of Geostationary Meteorological Satellite 4:		2,099
				Development of Marine Observation Satellite 1b:		7,426
				Development of Broadcasting Satellite 3:	(debt)	160 4,707
				Development of Earth Resource Satellite 1:	(debt)	14,793 8,293
				Development of Engineering Test Satellite Type VI:	(debt)	10,138 6,247
				Development of Geostationary Meteorological Satellite 5:	(debt)	398 182
				Development of Advanced Earth Observation (Platform) Engineering Satellite:	(debt)	2,902 520
				Development of First Materials Production Test System	(debt)	1,570 2,219
				Participation in Space Station Program:	(debt)	10,311 3,165
b. Space engineering related R&D by National Aerospace Laboratory [NAL]	(debt) 147 1,400	(debt) 769 1,722	(debt) 622 322	R&D in rocket engine fuel technology for liquid oxygen & liquid hydrogen fuels for H-II:		199
				R&D in innovative aerospace transport support technology (space related):	(debt)	769 530
				/Total including air transportation related allocations:	(debt)	1,023| 1,533/

Item	FY88 budget	Proposed FY89 budget	Difference	Comments	
(3) Ocean development	9,277	10,536	1,049	111.1%	
a. Japan Marine S&T Center	7,277	10,324	1,047	Deep water survey & research:	7,209
				Allocations:	
				Construction of 6,000-meter survey submarine:	3,785
				Construction of mother ship:	1,987
				R&D in underwater technology:	1,390
				Allocations:	
				Operation of underwater experiment vessel:	1,108
b. Miscellaneous	210	212	2	Joint regional R&D:	100
				Survey & utilization of the Kuroshio Current:	115
(4) Advancement of R&D in earth science	(debt) 8,371 17,651	(debt) 18,093 30,359	(debt) -9,722 -12,708	172.0%	
a. Studies in Global Geological Effects	0	174	174	Research nn Asian monsoons:	105
				Research of the deep crust of the earth:	69
b. R&D in earth observation technology	/(debt) 8,371\ \ 15,083/	/(debt)18,093\ \ 27,623/	/(debt) 9,722\ \ 12,540/	(including allocations from other categories)	
				Development of Geostationary Meteorological Satellite 4:	2,099
				Development of Marine Observation Satellite 1b:	7,426
				Development of Earth Resource Satellite 1: (debt)	14,793 8,293
				Development of Geostationary Meteorological Satellite 5: (debt)	398 182
				Development of Advanced Earth Observation (Platform) Engineering Satellite: (debt)	2,902 520
				Deep sea surveys:	7,209
c. R&D in disaster preventive technology	2,568	2,562	-6	National Research Center for Disaster Prevention:	2,556
				Allocations:	
				Research on earth-quake prediction:	1,046
				Research on disaster assistance measures after an earthquake:	353
				Research on measures for snow related hazards:	82

Item	FY88 budget	Proposed FY89 budget	Difference	Comments
(5) Advancement of R&D in materials science	/(debt) 2,442\ \ 11,171/	/(debt) 1,110\ \ 12,895/	/(debt) 1,332\ \ 1,724/	115.4% (including appropriations from other categories)
a. Superconductor research	/(debt) 2,442\ \ 3,192/	/(debt) 930\ \ 3,899/	/(debt) 1,512\ \ 707/	National Research Institute for Metals: (debt) 930 5,600 /Aside from the above, the proposal for the special account includes Y5.738 billion for expenses to relocate the NRIM facilities to Tsukuba, prescribed by the "act for relocation of national institutions" \ /
/ New superconductor research \	(debt) 2,442 2,044	(debt) 930 3,082	(debt) -1,512 1,038	Allocations: R&D in 40T hybrid magnet: (debt) 930 National Institute for Research in Inorganic Materials: (debt) 180 2,756
				Allocations: Completion of ultra high resolution ultra high voltage electron microscope: 630 Estimated amount of funds allocated from S&T Advancement Fund: 2,200 Program for Advancement of Creative Studies in S&T: (Phase information, etc.) 1,458 International Frontier Research: 301 (Frontier materials)
(5) Advancement of life science	/(debt) 6,792\ \ 12,809/	/(debt) 5,516\ \ 14,928/	/(debt) 1,276\ \ 2,119/	116.5% (including appropriations from other categories)
Cancer research	/(debt) 5,704\ \ 6,253/	/(debt) 4,719\ \ 7,369/	/(debt) -985\ \ 1,116/	RIKEN: (debt) 797 3,257
Cancer research	/(debt) 3,639\ \ 5,545/	/(debt) 5,704\ \ 6,253/	/(debt) 2,065\ \ 708/	Allocations: International Frontier Research: 831 (Bio-homostasis, cognitive processes) Research for neurological & immunological technology: 309 Preservation of cells & genes: 214 Estimated amount of funds allocated from S&T Advancement Fund: 1,463 Program for Advancement of Creative Studies in S&T: 1,625 (Genome dynamism, etc.)

Item	FY88 budget	Proposed FY89 budget	Difference	Comments		
				National Institute of Radiological Sciences:	(debt)	4,719
				Allocations:		6,096
				Research on medical applications of heavy particle beams:	(debt)	4,719
						4,465
(7) Other vital research areas	(debt) 1,985 19,097	(debt) 254 18,285	(debt) -1,731 -812	95.7%		
a. Aerospace technology related research of NAL	(debt) 897 8,710	(debt) 254 7,842	(debt) 643 -868	R&D of fan jet STOL:		
				/Total of funds for NAL including space related		1,032 \
				\ appropriations:	(debt)	1,023 /
						9,564 /
b. Miscellaneous	(debt) 1,088 10,387	10,443	(debt) -1,088 56	RIKEN:		
				Allocations:		10,379
				Laser technology research:		198
				/Total of funds for RIKEN	(debt)	1,232 \
				\including all other appropriations:		15,871 /
				Comprehensive utilization of natural resources:		64

- END -

10

22161
45

NTIS
ATTN: PROCESS 103
5285 PORT ROYAL RD
SPRINGFIELD, VA 22161

Foreign Broadcast Information Service (FBIS) and Joint Publications Research Service (JPRS) publications contain political, economic, military, and sociological news, commentary, and other information, as well as scientific and technical data and reports. All information has been obtained from foreign radio and television broadcasts, news agency transmissions, newspapers, books, and periodicals. Items generally are processed from the first or best available source; it should not be inferred that they have been disseminated only in the medium, in the language, or to the area indicated. Items from foreign language sources are translated; those from English-language sources are transcribed, with personal and place names rendered in accordance with FBIS transliteration style.

Headlines, editorial reports, and material enclosed in brackets [ ] are supplied by FBIS/JPRS. Processing indicators such as [Text] or [Excerpts] in the first line of each item indicate how the information was processed from the original. Unfamiliar names rendered phonetically are enclosed in parentheses. Words or names preceded by a question mark and enclosed in parentheses were not clear from the original source but have been supplied as appropriate to the context. Other unattributed parenthetical notes within the body of an item originate with the source. Times within items are as given by the source. Passages in boldface or italics are as published.

SUBSCRIPTION/PROCUREMENT INFORMATION

The FBIS DAILY REPORT contains current news and information and is published Monday through Friday in eight volumes: China, East Europe, Soviet Union, East Asia, Near East & South Asia, Sub-Saharan Africa, Latin America, and West Europe. Supplements to the DAILY REPORTs may also be available periodically and will be distributed to regular DAILY REPORT subscribers. JPRS publications, which include approximately 50 regional, worldwide, and topical reports, generally contain less time-sensitive information and are published periodically.

Current DAILY REPORTs and JPRS publications are listed in *Government Reports Announcements* issued semimonthly by the National Technical Information Service (NTIS), 5285 Port Royal Road, Springfield, Virginia 22161 and the *Monthly Catalog of U.S. Government Publications* issued by the Superintendent of Documents, U.S. Government Printing Office, Washington, D.C. 20402.

The public may subscribe to either hardcover or microfiche versions of the DAILY REPORTs and JPRS publications through NTIS at the above address or by calling (703) 487-4630. Subscription rates will be provided by NTIS upon request. Subscriptions are available outside the United States from NTIS or appointed foreign dealers. New subscribers should expect a 30-day delay in receipt of the first issue.

U.S. Government offices may obtain subscriptions to the DAILY REPORTs or JPRS publications (hardcover or microfiche) at no charge through their sponsoring organizations. For additional information or assistance, call FBIS, (202) 338-6735,or write to P.O. Box 2604, Washington, D.C. 20013. Department of Defense consumers are required to submit requests through appropriate command validation channels to DIA, RTS-2C, Washington, D.C. 20301. (Telephone: (202) 373-3771, Autovon: 243-3771.)

Back issues or single copies of the DAILY REPORTs and JPRS publications are not available. Both the DAILY REPORTs and the JPRS publications are on file for public reference at the Library of Congress and at many Federal Depository Libraries. Reference copies may also be seen at many public and university libraries throughout the United States.